CAVS REPORT
MSU.CAVS.CMD.2009-R0010
June 2009

MSU Internal State Variable Plasticity-Damage Model 1.0 Calibration, DMGfit Production Version
Users Manual

M.F. Horstemeyer, R. Cariño, Y. Hammi, and K.N. Solanki

Prepared by
Center for Advanced Vehicular Systems
Mississippi State University
Mississippi State, MS 39762

Web site: http://www.cavs.msstate.edu

Not for public release.

Summary

The Mississippi State University internal state variable (ISV) plasticity-damage model (DMG) production version 1.0 is being released along with its model calibration tool (DMGfit). The model equations are explained in Appendix A, while material model fits to sixty one (61) metals and alloys are illustrated in Appendix B. The fits were obtained by the model calibration tool DMGfit described by this document.

The DMG model is implemented as an ABAQUS user material (UMAT) subroutine for production run finite element simulations. For consistency, the same UMAT is utilized for model calibration by the DMGfit tool. The calibrated model constants can be directly merged by DMGfit into the "USER MATERIAL, CONSTANTS" section an existing ABAQUS input deck.

The DMG model UMAT and a stand-alone DMGfit tool are available, upon request, from Mark Horstemeyer <mfhorst@cavs.msstate.edu>. An online version of the DMGfit tool, along with sample experimental data, is available on the Web at http://ccg.hpc.msstate.edu/cmd.

Software Application License Agreement
Version 3.23.09b

This License Agreement ("Agreement") is a legal agreement between LICENSEE and Mississippi State University ("MSU") for online access to the software application for material modeling ("Software Application"). By using the Software Application, LICENSEE is agreeing to be bound by the terms of this Agreement. LICENSEE agrees that LICENSEE's use of the Software Application acknowledges that LICENSEE has read this Agreement, understands it, and agrees to be bound by its terms and conditions.

1. **Grant of License**. Subject to the terms and conditions of this Agreement, MSU hereby grants to LICENSEE a non-exclusive license to use the Software Application. LICENSEE may use the Software on a single computer and make one copy of the Software in machine-readable form for backup purposes only. LICENSEE must reproduce on such copy MSU's copyright notice and any other proprietary legends that were on the original copy of the Software.

2. **Restrictions.** The Software Application contains copyrighted material, trade secrets and other proprietary material. In order to protect them, and except as permitted by applicable legislation, LICENSEE may not decompile, reverse engineer, disassemble, or otherwise reduce the Software Application to a human-perceivable form, or otherwise attempt to discover the source code of any Software Application provided in compiled form; modify, network, rent, lend, loan, distribute or create derivative works based upon the Software Application in whole or in part; electronically transmit the Software Application from one computer to another or over a network; copy the Software Application; or, transfer LICENSEE's license rights to use the Software Application, the related documentation, or this Agreement to another party.

3**.** **Copyright and Trademark.** The Software Application and Documentation are owned by MSU. All title, ownership, rights, and intellectual property rights in and to the Software Application and Documentation shall remain with and in MSU. The Software Application and the Documentation are protected by the copyright laws of the United States and international copyright treaties. LICENSEE shall not use the names, logos, trademarks or any other mark or image considered by MSU to be identified with or protected by MSU, or those of any of its employees or former employees, or any adaptation thereof, in any advertising, promotional or sales literature without prior written consent being obtained from MSU in each case, except that LICENSEE may state that it is licensed by MSU under this Agreement.

4. **Export Law Assurance**. LICENSEE hereby agrees that it shall not sell, transfer, export or re-export any Software Application or related information in any form, or any direct products of such information, except in compliance with all applicable laws, including the export laws of any U.S. Government agency and any regulations there under, and will not sell, transfer, export or re-export any such Software Application or information to any persons or any entities with regard to which there exist grounds to suspect or believe that they are violating such laws. LICENSEE shall be solely responsible for obtaining all licenses, permits or authorizations required from the U.S. and any other government for any such export or re-export. To the extent not inconsistent with this Agreement, MSU agrees to provide LICENSEE with such assistance as it may reasonably request in obtaining such licenses, permits or authorizations.

5. **Disclaimer of Warranty**. MSU MAKES NO REPRESENTATIONS AND EXTENDS NO WARRANTIES OF ANY KIND, EITHER EXPRESS OR IMPLIED, INCLUDING, BUT NOT LIMITED, TO WARRANTIES OF MERCHANTABILITY, FITNESS FOR A PARTICULAR PURPOSE, VALIDITY OF COPYRIGHT OR PATENT, ISSUED OR PENDING, OR FOR THE ABSENCE OF LATENT OR OTHER DEFECTS, WHETHER DISCOVERABLE OR NOT DISCOVERABLE. NOTHING IN THIS LICENSE AGREEMENT SHALL BE CONSTRUED AS A REPRESENTATION MADE OR WARRANTY GIVEN BY MSU THAT THE PRACTICE BY LICENSEE OR SUBLICENSEES OF THE LICENSE GRANTED HEREUNDER SHALL NOT INFRINGE THE COPYRIGHT OR PATENT OF THIRD PARTIES. IN NO EVENT SHALL THE MISSISSIPPI BOARD OF TRUSTEES OF STATE INSTITUTIONS OF HIGHER LEARNING, MSU THE TRUSTEES, OR ANY OFFICERS, AGENTS OR EMPLOYEES THEREOF BE LIABLE FOR INCIDENTAL OR CONSEQUENTIAL DAMAGES OF ANY KIND, INCLUDING ECONOMIC DAMAGE OR INJURY TO PROPERTY AND LOSS OF PROFITS, REGARDLESS OF WHETHER MSU SHALL BE ADVISED OF, SHALL OTHERWISE HAVE REASON TO KNOW, OR IN FACT SHALL KNOW OF THE POSSIBILITY THEREOF.

6. **MISCELLANEOUS PROVISIONS**

A. **Governing Laws**. This Agreement shall be construed, governed, interpreted and applied in accordance with the laws of the State of Mississippi, U.S.A without regard to its choice of law or conflicts of law rules or principles.

B. **Severability.** The provisions of this Agreement are severable, and in the event that any provisions of this Agreement shall be determined to be invalid or unenforceable, such invalidity or unenforceability shall not in any way affect the validity or enforceability of the remaining provisions hereof.

C. **No Waiver.** The failure of either party to assert a right hereunder or to insist upon compliance with any term or condition of this Agreement shall not constitute a waiver of that right or excuse a similar subsequent failure to perform any such term or condition by the other party.

D. **Lawful Use**. LICENSEE shall not use Software Application for any unlawful purpose, including infringement of copyrights or proprietary rights of others, or in any illegal manner or for the creation or distribution of illegal content.

E. **Entire Agreement.** The parties hereto acknowledge that this Agreement and any Appendices thereto, sets forth the entire Agreement and understanding of the parties hereto as to the subject matter hereof, and shall not be subject to any change or modification except by the execution of a written instrument subscribed to by the parties hereto.

TABLE OF CONTENTS

Quickstart Guide 6
Introduction 7
Input-Process-Output 8
Graphical User Interface 9
Menu Items 10
Data Set Controls 12
Loading Parameters 14
Fixed Constants 15
Single Parameter Study Controls 16
Parameter Set Controls 17
Fitted Constants 18
Stress-strain Data 20
References 21
Appendix A. MSU DMG 1.0 Production Model Equations 22
Appendix B. Material Model Fits 26

Quickstart Guide

On the Web, point your browser to **http://ccg.msstate.edu/cmd**, login with your credentials, select **Tools**, and then **DMGfit**. Online documentation is available by selecting **Help**. Login credentials may be requested from Tomasz Haupt <haupt@cavs.msstate.edu>. A demonstration video is available at **http://ccg.hpc.msstate.edu/cmd/files/MaterialDBDemoVideo.avi**.

To install DMGfit on a PC running Windows XP, request the following files from Mark Horstemeyer <mfhorst@cavs.msstate.edu>:

1. DMG.exe and DMG.chm – the executable and user guide.
2. MCRinstaller.exe - installer for the required runtime library.

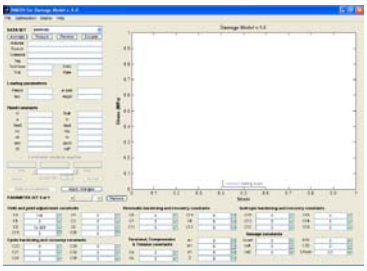

Copy the files to, say, C:\DMG\. Run the MCRinstaller.exe, once, as a computer administrator, to install the library. Then run DMG.exe; the DMGfit GUI (see figure on the right) should appear. Select the menu item Help to display the user guide. For technical support, contact Ric Carino <rlc@cavs.msstate.edu>.

To fit the damage model to experimental data, the general strategy is to work the GUI regions in the following order: Datasets; Loading parameters; Fixed constants; Yield and yield adjustment constants; Kinematic hardening and recovery constants; Isotropic hardening and recovery constants; Cyclic range hardening and recovery constants; Torsional, Compression and Tension constants; then Damage constants. The following sequence of steps is typical:

1. Load all experimental datasets. For each dataset, establish the experiment settings (initial temperature, strain rate, stress units, etc), loading parameters, and fixed constants.
2. Start by fitting the experimental dataset with the lowest temperature and lowest rate. Temporarily exclude the rest of the datasets. If there are different tests, fit the compression datasets first, followed by tension datasets, then torsion datasets.
3. For the first dataset, adjust the constants as follows: yield C3; kinematic hardening C9 and recovery C7; isotropic hardening C15 and recovery C13.
4. Restore second dataset. If it has a different temperature than the first, adjust the constants as follows: {C3, C4} if yield is temperature dependent; then {C10, C8, C16, C14}. If the dataset has a different strain rate, adjust C1 and C5 if yield is strain rate dependent, then {C9, C7, C11} and {C15, C13, C17}.
5. Repeat step 4 for the rest of the datasets. If adjusting the temperature dependence constants (even Cs) does not produce good models for high temperature data, adjust C19 and C20. Adjust torsion, compression and tension differentiation constants, if adding stress state dependent experimental data.
6. Adjust damage constants. To track the evolution of the damage state variable, select *Display* | *Plot a state variable* | *Damage*. Readjust constants in other boxes as necessary.
7. Record your results. Select *File* | *Write* | *A binary restart file* to create a record of your session, to resume it later. Select *File* | *Write* | *A "USER MATERIAL, CONSTANTS" for ABAQUS* to create a text file containing the properties, suitable for inclusion in an ABAQUS input deck. Select *File* | *Write* | *A "fitted constants+constrains" file* to create a text file record of the fitted constants, which may be used as starting values in future fitting sessions.

Introduction

The Mississippi State University internal state variable (ISV) plasticity-damage model (DMG) production version 1.0 is based from the ISV plasticity formulation of Bammann [1990] with the addition of porosity [Bammann et al., 1993] and the void nucleation, growth, and coalescence rate equations that admit heterogeneous microstructures [Horstemeyer et al, 2000]. The model is implemented as an ABAQUS user material subroutine (UMAT). The model calibration routine DMGfit was developed by Cariño [2007], which updated the original BFIT routine by Lathrop [1996]. The calibrated model constants can be directly merged into the "USER MATERIAL, CONSTANTS" section an existing ABAQUS input deck.

The pre-production release of DMGfit is based on a C translation of an earlier version of the DMG code (Research version 0.9 UMAT in Figure 1 below), instead of the state-of-the-art version used in production-run finite element simulations. Synchronizing DMGfit with the latest version of the ABAQUS UMAT implementation of the damage model by revising the C translation is a tedious process, a duplication of efforts and an error-prone procedure. Further, this revision has to be performed for future extensions to the damage model since these extensions are tested by MSU researchers on the UMAT implementation. In order to avoid these inefficiencies in the software maintenance process and to keep DMGfit always synchronized with the current version of the damage model, DMGfit has been modified to invoke the damage model UMAT.

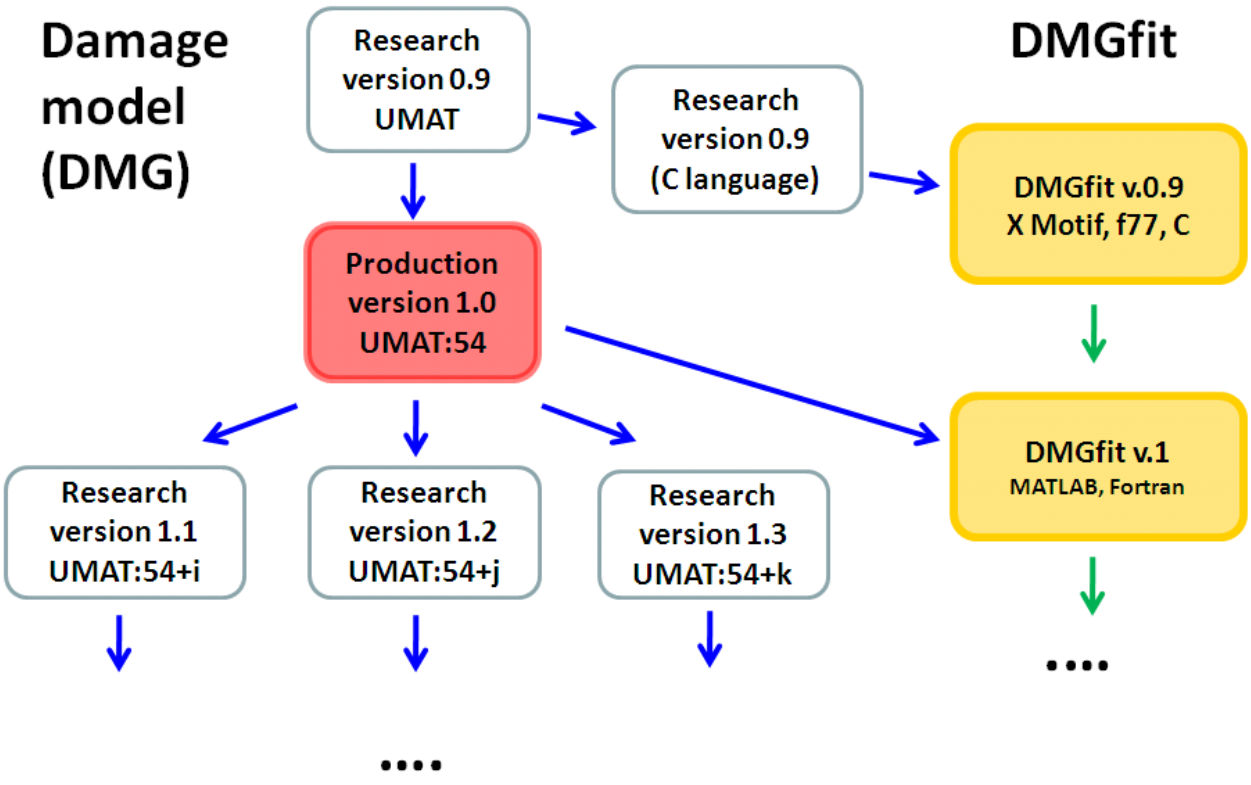

Figure 1. Development roadmap for DMG and DMGfit. The earlier DMGfit uses an outdated C-translation of DMG UMAT. DMGfit was upgraded to link with the production DMG UMAT.

Input-Process-Output

Production version 1.0 of the DMG model is specified by 54 constants or material properties. Some of these constants, like bulk modulus, shear modulus, and melting temperature, are fixed for a given material and are obtained from the literature. Microstructure constants, such as average radius of voids, average size of particles, and average grain size, are calculated from microscope images of samples of the material. The remaining constants are fitted, using DMGfit, from stress-strain experiments on the samples.

DMGfit expects the measurements associated with a sample of the material to be recorded in a "DMGfit data set". This data set contains experimental stress-strain data, fixed constants for the material, fixed constants for the specific sample, and the loading parameters to simulate the experiment. DMGfit solves an optimization problem to calculate the model constants that are not included in a data set.

Figure 2 is a high-level description of the process to calibrate the damage model using DMGfit. Three codes are involved: an optimization routine (in MATLAB), a material point simulator (in Fortran), and the damage model UMAT (in Fortran). Collaborators may request these codes from Mark Horstemeyer <mfhorst@cavs.msstate.edu>. The inputs to the process are estimated initial values for the constants and experimental stress-strain data. Candidate model constants are generated by the optimization routine. These constants are passed as material properties to the Material Point Simulator. The simulator invokes the damage model UMAT with the properties to produce a model stress-strain curve. The process successfully terminates when the model curve gives a good correlation to the experimental data.

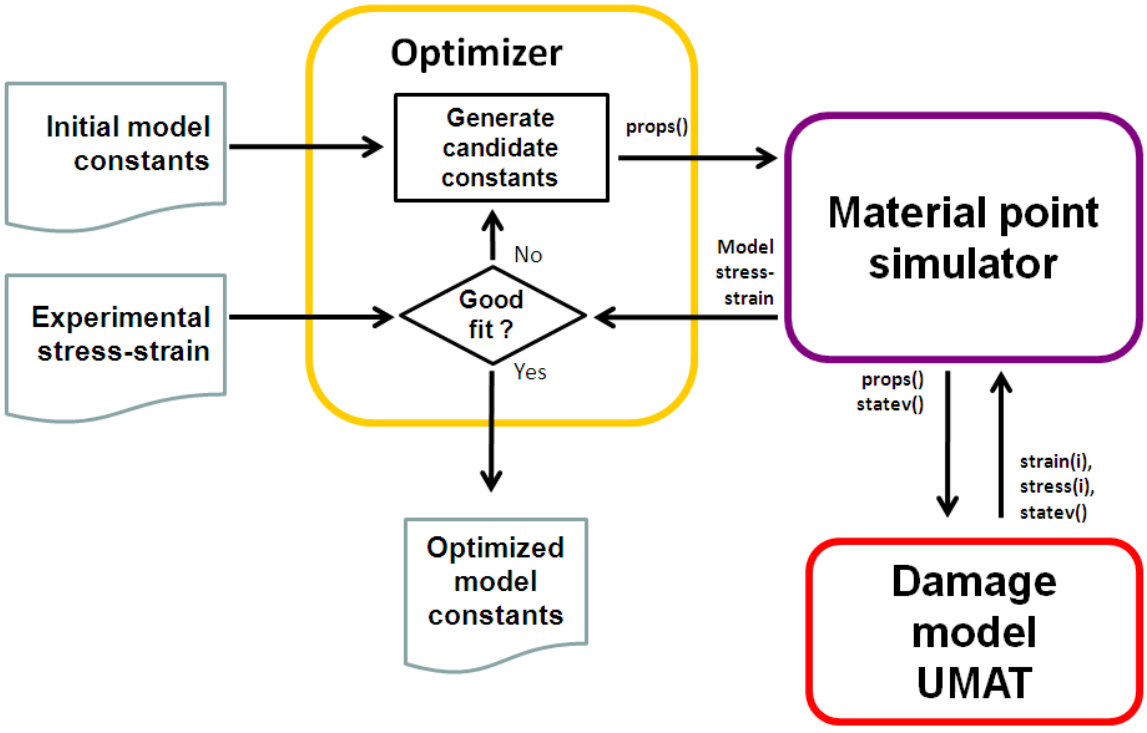

Figure 2. Overview of model calibration process using DMGfit.

Graphical User Interface

The remainder of this report describes the user interface of the stand-alone version of DMGfit. The documentation for the Web version of DMGfit is online at **http://ccg.hpc.msstate.edu/ccgportlets/apps/cmd/html/help/Help.htm**.

A snapshot of the DMGfit GUI in operation, annotated to highlight the logical groupings of the controls, is shown by Figure 3.

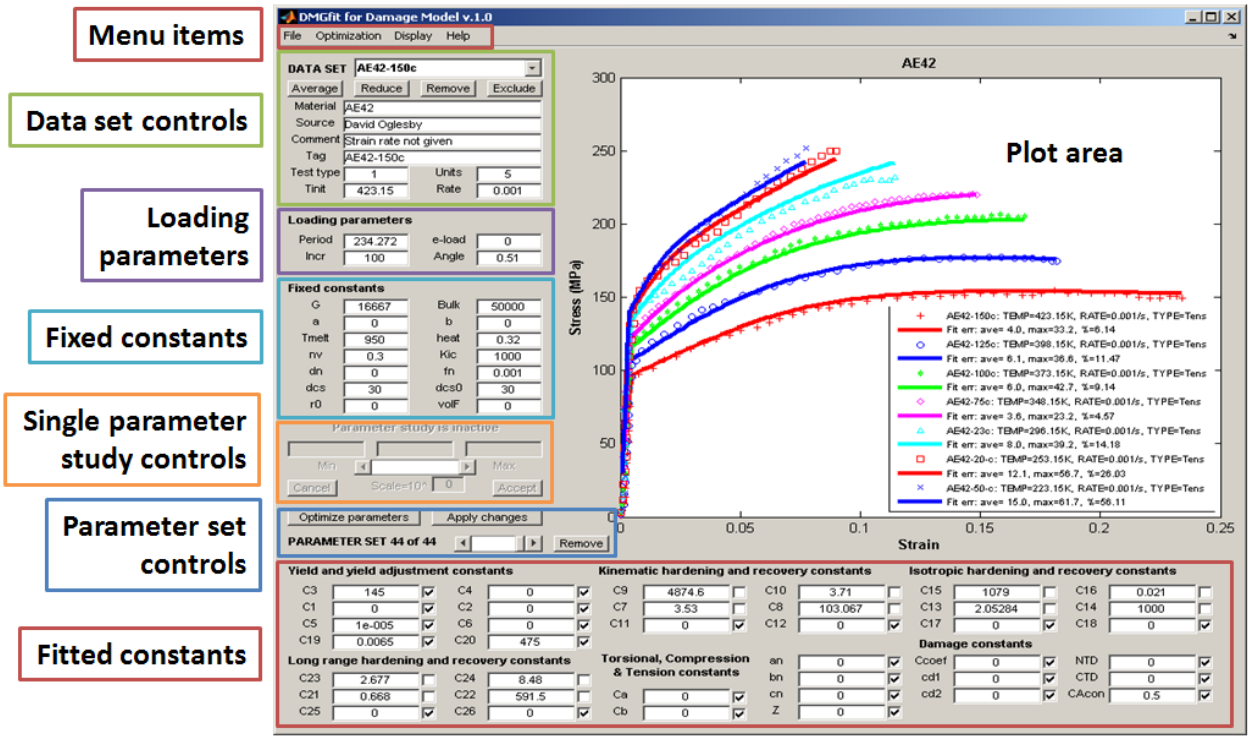

Figure 3. The logical groupings of controls in the DMGfit GUI.

Brief descriptions of the controls are:

Menu items - file operations, optimization options, plot appearance settings, and help links.

Data set controls - describes the experimental stress-strain data measured from a sample of the material under consideration.

Loading parameters - parameters for the material point simulator to model the experiment.

Fixed constants - damage model constants that are fixed, from the literature, or measured from microscope images of the sample represented by the data set.

Single parameter study controls - activated by a right-click on a fitted constant, to investigate the *solitary* effect of the constant on the model.

Parameter set controls - operations that apply to the current *set* of fitted constants.

Fitted constants - damage model constants to be calibrated.

The controls are further described in the sections that follow.

Menu Items

File

Load

A data file - load a DMGfit data set file (see **Data set controls**).

A "fixed constants" file - load a text file containing lines with the format "name=value", where "name" is a fixed constant in the damage model

Stress-strain from Excel file - load stress-strain data from an Excel file (see **Stress-strain data**).

A "fitted constants+constraints" file - load a text file containing lines with the format "name=value fix min max", where "name" is a fitted constant in the damage model, fix is 0 or 1 to indicate that the value is to be fixed during optimization, and [min, max] is the range of permissible values for the constant if fix=0.

A "fitted constants only" file - load a text file containing lines with the format "name=value", where "name" is a fitted constant in the damage model

A binary restart file - a record of a previous fitting session.

Write

A post-processing info text file - create a text file containing the model constants, data points and model points for post-processing, most likely to produce publication-quality plots. This file can be imported as comma-separated-values (CSV) into a spreadsheet program like MS Excel.

A Gnuplot script for the plots - create a Gnuplot script for the plots and the parameter set on focus.

A binary restart file - create a record of the state of a fitting session. Loading the file with **Load | Binary restart file** continues the session from the point the file was saved.

A data file - create a template for a data file from a loaded data set.

A "fitted constants+constraints" file - create a file for the fitted constants and their constraints, from the parameter set on focus.

A "USER MATERIAL, CONSTANTS" for ABAQUS - write the fixed constants and fitted constants into an existing ABAQUS input deck, or create such a section if the deck does not exist yet.

Utilities

Extract constants from ABAQUS input - extract the "USER MATERIAL, CONSTANTS=54" section of an ABAQUS input deck, then write the constants into a text file that can be retrieved using **Load | A "fitted constants only" file** or **Load | A "fixed constants" file**

Extract constants from legacy param file - extract the constants from a BFIT param file, then write the constants into a text file that can be retrieved using **Load | A "fitted constants only" file**

Extract constants from 1-column props file - read a text file with a single column of 54 numbers, then write the numbers as damage model constants into a text file that can be retrieved using **Load | A "fitted constants only" file** or **Load | A "fixed constants" file**

Print - open a print preview of the DMGfit window.
Reset - re-initialize DMGfit.
Replay - execute a replay file, which is a text record of the actions in a previous DMGfit session.
Quit - write a replay file for the session if wanted; then quit DMGfit.

Optimization

Use fmincon - use MATLAB's fmincon(), after setting some options.
Use fminsearch - use MATLAB's fminsearch(), after setting some options (the default).
Use lsqnonlin - use MATLAB's lsqnonlin(), after setting some options.
Use patternsearch - use MATLAB's patternsearch(), after setting some options.
Use genetic algorithm - use MATLAB's ga(), after setting some options.
Estimate C3 and C4 - calculate C3 and C4 from two datasets with different temperatures.

Display

Plot settings - open a dialog to modify the appearance of the plot area.
Plot a state variable - open a dialog to select the state variable to plot.
Toggle Hide|Show model plots - enable or disable plotting of the model curves.
Font size - set the font size; fonts in the plot area will be changed when the plot is updated.
Font name - set the font style; fonts in the plot area will be changed when the plot is updated.

Help

Help topics - display the help file.
About - display the current version of DMGfit and the contact information of the developer/maintainer .

Data Set Controls

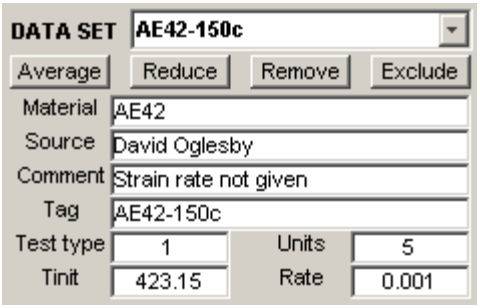

A DMGfit data set is a file that contains experimental stress-strain data, descriptive elements of the experimental sample, the loading parameters to model the stress-strain data, and the fixed constants associated with the sample. A data set file is retrieved from disk using **File | Load | A data file**. The information contained in the file are automatically displayed when the data set is selected using the **DATA SET** popup.

Hovering the mouse pointer over a control causes a pop-up to appear. For examples, Average experiments on Average; and Stress units: 1=psi 2=Ksi 3=Pa 4=KPa 5=MPa 6=GPa on Units 5.

The stress-strain data is described by the following elements:

Material - a descriptive name for the material.
Source - who provided the experimental data.
Comment - any remarks about the data or the experiment.
Tag - a tag to differentiate data sets.
Test type - 1=Tension, 2=Compression, 3=Torsion, 4=Tension+Compression, 5=Compression+Tension
Units - stress units: 1=psi 2=Ksi 3=Pa 4=KPa 5=MPa 6=GPa
Tinit - initial temperature.
Rate - strain rate.

Except for the stress-strain data which are plotted, the above elements may be edited directly. Changes will take effect after clicking Apply changes (see **Parameter set controls**).

Operations on a data set are:

Average starts a dialog to average two or more experiments with the same Test type, Tinit and Rate. A dialog ensues to select the data sets to be averaged, the number of strain values (say, *npoints*) to be generated, and a file name for the differences between the average stress and experimental stresses. A "new" data set will be created from the selected experiments and given an "Averaged" Tag. The stress values will be the average of the interpolated stress at *npoints* equally-spaced values between the minimum and maximum experimental strain values. The descriptive elements, loading parameters and fixed constants are derived from the first data set that was selected. If a file name was specified, the file will be created with the following columns: the strain values, the averaged interpolated stress, the differences between the average stress and experimental stresses, and the minimum and maximum differences

Reduce disables all controls and makes visible controls for reducing the number of stress-strain pairs in the data set. Thousands of data points translate into long running times for the fitting procedure since an estimate of the error at each point has to be calculated.

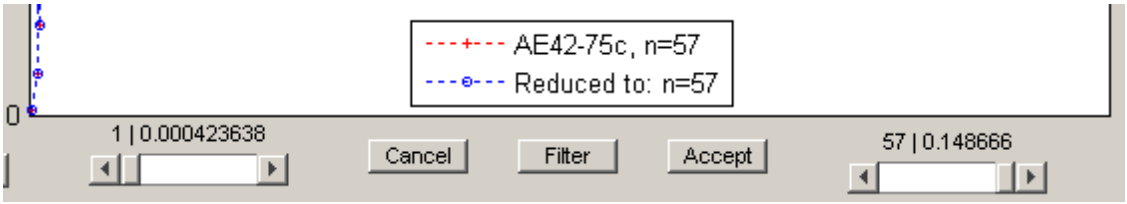

The **left slider** moves the left endpoint, while the **right slider** moves the right endpoint. The Filter button invokes a filtering routine to find points such that a line drawn between the points approximates the data between those points to a relative error not exceeding the filter tolerance. For comparison, the points found are superimposed on the original dataset. Cancel discards changes to the data set, deactivates the reduction controls, and enables the rest of the controls. Accept creates a new data set from the filtered/reduced stress-strain data points of the data set on focus, prefixing "reduced-" to the tag. The data set on focus is automatically excluded, and the reduced data set becomes the focus.

Remove deletes the data set on focus from memory.

Exclude inhibits the data set from being plotted and fitted. The data set Tag is annotated with "(excl)". If an excluded data set is selected for focus, this button changes to Restore, for the opposite effect.

Tips:

1. If the data set on focus has Test type=2 (compression) and the stress-strain data are negative, it is necessary to "flip" the data so that the strain and stress values become positive. A right-click on Average exposes the context menu

   for this purpose.
2. A right-click on Remove exposes the context menu

   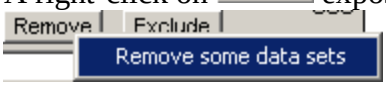

   to remove two or more data sets. A dialog ensues, to select the data sets to be removed.
3. A right-click on Exclude exposes the context menu

   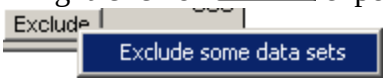

   to exclude two or more data sets. A dialog ensues, to select the data sets to be excluded or restored.
4. A right-click on the value of Tinit exposes the context menu

   to enter the initial temperature in Celsius or Fahrenheit.

Loading Parameters

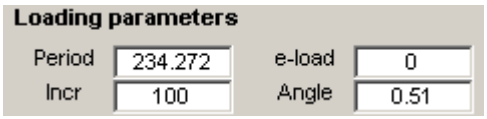

A set of loading parameters is associated with each experimental data. These parameters are used by the material point simulator to model the data. The values of these parameters are automatically displayed upon selection of a data set. Hovering the mouse pointer over a value causes a pop-up describing the parameter to appear. These values may be edited directly. Changes will take effect after clicking Apply changes (see **Parameter set controls**).

Descriptions of the loading parameters:

Period - simulation time period; the final simulated strain value will be (Period*Rate)
e-load - for Test type=4 or 5; the strain value where the load direction changes; otherwise 0.
Incr - number of strain increments (up to 1000) for the simulation; the execution time of the simulation is directly proportional to this value.
Angle - the bi-axial loading ratio.

Tips:

1. If Period is 0, a model will not be generated for the data set.
2. If a model curve is a "zigzag" or is "wavy", increase the corresponding Incr parameter.
3. A right-click on Period exposes the context menu

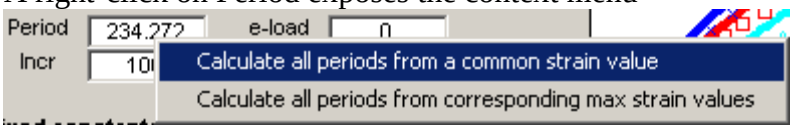

to automatically calculate all periods so that all data models will end at a common strain value, or at the respective final strain values. For example, in the figure below, the Periods were automatically computed to model up to strain=0.02.

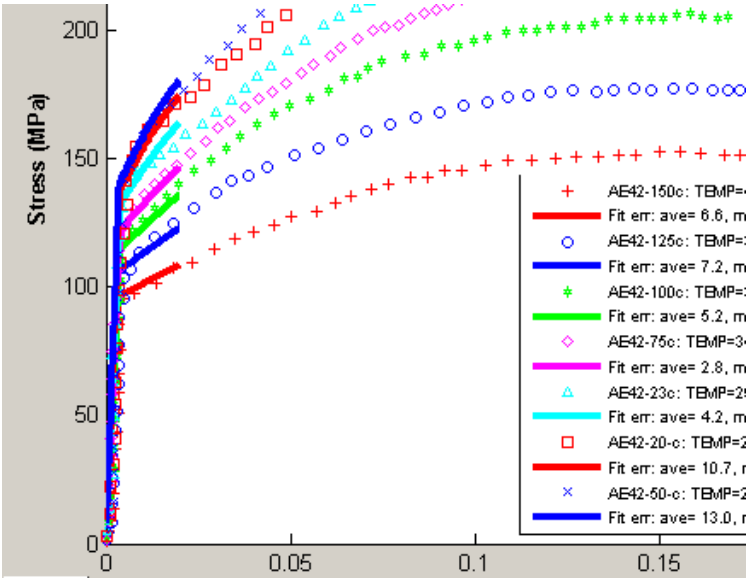

Fixed Constants

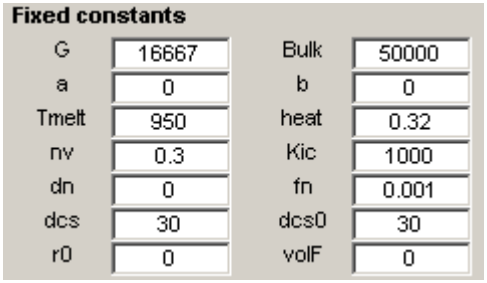

Some constants in the damage model are fixed for the material. These are obtained from the literature or measured from microscope images of the sample used in the experiment. The **Fixed constants** associated with a sample are automatically displayed upon selection of the data set. These values may be edited directly. Changes will take effect after clicking 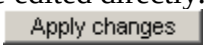

(see **Parameter set controls**). Hovering the mouse pointer over a value causes a pop-up describing the constant to appear.

Descriptions of the fixed constants:

G - Shear modulus (default: 0)
Bulk - Bulk modulus (default: 0)
a - Constant to adjust shear modulus due to variation of temperature from initial (default: 0)
b - Constant to adjust bulk modulus due to variation of temperature from initial (default: 0)
Tmelt - Melt temperature (K) (default: 3000)
heat - Heat generation term (default: 0.34)
Kic - Particle fracture toughness (default: 1000)
nv - Particle McClintock damage constant (default: 0.3)
dn - Particle average size (default: 0)
fn - Particles volume fraction, must be greater than 0 (default: 1e-3)
dcs0 - Reference grain size or dendrite cell size, must be greater than 0 (default: 30)
dcs - Grain size or dendrite cell size of experiment sample (default: 30)
r0 - Initial radius of a spherical void (default: 0)
volF - Initial void volume fraction (default: 0)

Tips:

1. The constants fn and dcs0 should not be zero; these are divisors inside the UMAT.
2. If r0 and volF are zero, the damage constants will have no effect on the model.
3. If G or Bulk is 0, a model will not be generated for the data set.
4. A right-click on G or Bulk exposes a context menu

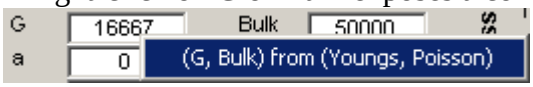

to calculate the bulk and shear moduli from the Young modulus and Poisson ratio if these are the known quantities.

Single Parameter Study Controls

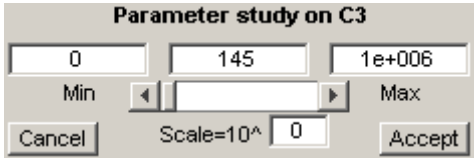

A right-click on the current value of a fitted constant activates the parameter study controls and disables the rest of the DMGfit controls. In the above example, the right-click was on 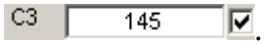

.

The range constraint for C3 is transferred to the **Min** and **Max** edit fields as well as to the slider limits. The current value is transferred to the **Current** edit field and is used to initially position the slider.

The **Min**, **Current** and **Max** values may be edited directly. Changes will take effect after clicking anywhere in the window outside of the edit boxes.

Operating the slider decreases or increases the **Current** value, depending on where the slider bar is positioned. The model plots are updated automatically with each change of the current value.

If the **Min** value is close to the **Max** value, the slider may not work properly due to the resulting low resolution of the slider steps. In this case, setting the scale (Scale=**10^** edit box) to a negative integer may restore the expected functionality. Similarly, for a large range of values, setting the scale to a positive integer may prevent huge jumps in **Current** when the slider is operated.

Accept creates a new parameter set from the set currently on focus, with the current value and constraint for the selected constant coming from the parameter study controls. This also exits the parameter study. **Cancel** exits the parameter study without any changes to the constant.

Parameter Set Controls

DMGfit keeps track of the sets of fitted constants (i.e., parameter sets) attempted during a session. The **PARAMETER SET slider** selects the set which will be used to generate the model plots.

Remove discards the current parameter set. The next available parameter set becomes the focus.

Optimize parameters invokes the optimization routine to automatically update the values in the parameter set.

Apply changes commits changes to any displayed value (experiment descriptions, loading parameters, fixed constants, fitted constants) or check box in the GUI. If fitted constants are changed, a new parameter set is created from the displayed values. The new set automatically becomes the parameter set on focus.

Fitted Constants

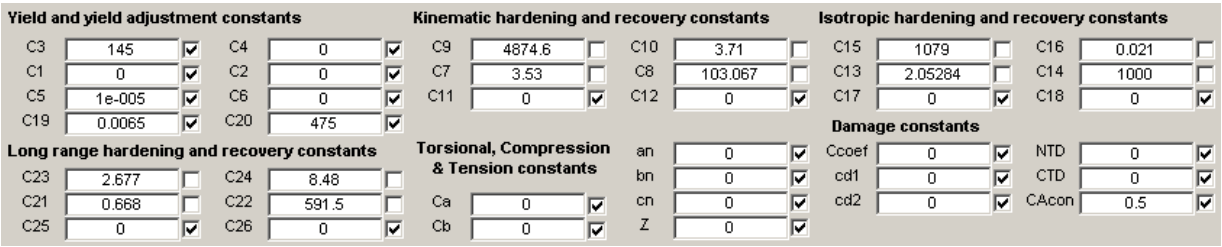

For each fitted constant, there are three controls: the **label** static text, the current **value** edit box, and the **fix** check box.

For example, consider 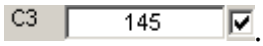

. Hovering the mouse pointer on the edit box will activate a popup that displays a description and current range constraint for the constant.

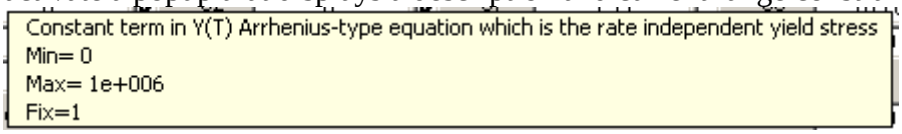

The current value can be changed directly. The change will take effect when

is clicked.

A right-click on the current value activates the **Single parameter study controls** and disables the rest of the DMGfit controls.

If the check box is unchecked, the constant may be updated when

is clicked. If checked, the constant will be fixed (not changed) by the optimization routine.

Tips:

1. Leave C5 to the default nonzero value if yield is NOT strain rate dependent. C5=0 does not produce a good model.
2. Several values can be modified and/or fixed before

is clicked. A new parameter set is created from the set on focus, using the updated values. The new set automatically becomes the focus.
3. Depending on the optimization routine, a constant set to zero may be respected, and may remain zero *even if it is not fixed*. For the constant to participate in fitting, set it initially to a "small" non-zero value.
4. The group ordering of the fitted constants in the GUI suggests the fitting strategy. After establishing the fixed constants, the suggested order for the constants to be fitted is:
    1. Yield and yield adjustment constants,
    2. Kinematic hardening and recovery constants,
    3. Isotropic hardening and recovery constants,
    4. Long range hardening and recovery constants,
    5. Torsional, Compression & Tension differentiation constants, and
    6. Damage constants.

Descriptions of the constants:

C1 - Constant term in V(T) Arrhenius-type equation which determines the magnitude of rate dependence on yielding (units=MPa)

C2 – Temperature dependent activation term in V(T) Arrhenius-type equation (units=Kelvin)

C3 - Constant term in Y(T) Arrhenius-type equation which is the rate independent yield stress (units=MPa)

C4 - Temperature dependent activation term in Y(T) Arrhenius-type equation (units=Kelvin)

C5 - Constant term in f(T) Arrhenius-type equation which determines the transition strain rate from rate independent to dependent yield (units=1/sec)

C6 - Temperature dependent activation term in f(T) Arrhenius-type equation (units=Kelvin)

C7 - Constant term in rd1 equation which describes the kinematic dynamic recovery (units=1/MPa)

C8 - Temperature dependent activation term in rd1 equation (units=Kelvin)

C9 - Constant term in h1 equation which describes the kinematic anisotropic hardening modulus (units=MPa)

C10 - v term in h1 equation (units=MPa/Kelvin)

C11 - Constant term in rs1 equation which describes the kinematic static recovery (units=1/(MPa sec))

C12 - Temperature dependent activation term in rs1 equation (units=Kelvin)

C13 - Constant term in rd2 equation which describes the isotropic dynamic recovery (units=1/MPa)

C14 - Temperature dependent activation term in rd2 equation (units=Kelvin)

C15 - Constant term in h2 equation which describes the isotropic hardening modulus (units=MPa)

C16 - Temperature dependent activation term in h2 equation (units=MPa/Kelvin)

C17 - Constant term in rs2 equation which describes the isotropic static recovery (units=MPa/sec)

C18 - Temperature dependent activation term in rs2 equation (units=Kelvin)

C19 - Multiplication term in equation 1 + tanh(c19(c20-T)), which is an adjustment to the yield strength over a large temperature range (units=1/Kelvin)

C20 - Used in yield strength adjustment equation (units=Kelvin)

C21 – Long range kinematic dynamic recovery rd3 (units=1/MPa)

C22 - Temperature dependent activation in rd3 dynamic recovery equation (units=Kelvin)

C23 – Long range kinematic hardening h3 (units=MPa)

C24 - Temperature dependent activation in h3 equation (units=MPa/Kelvin)

C25 – Long range kinematic static recovery rs3 (units=1/(MPa sec))

C26 - Temperature dependent activation in rs3 static recovery equation (units=Kelvin)

Ca – Torsional softening constant in kinematic and isotropic hardening and dynamic recovery equations

Cb – Tension/compression asymmetry constant in kinematic and isotropic hardening and dynamic recovery equations

an - Torsional constant a in void-crack nucleation model

bn - Tension/compression constant b in void-crack nucleation model

cn - Triaxiality constant c in void-crack nucleation model

Z - Grain size or dendrite cell size exponent

Ccoef - Coefficient constant in void-crack nucleation model

cd1 – Void impingement coalescence factor, D=nucleation*void volume*coal
cd2 – Void sheet coalescence factor, D=nucleation*void volume*coal
NTD – Void-crack nucleation Temperature Dependence
CTD – Void coalescence Temperature Dependence
CAcon - Cocks Ashby void growth constant

Stress-strain Data

For compatibility with the original BFIT, text files with the following formats for stress-strain data are recognized:

1. Two-column
```
<strain> <stress>
<strain> <stress>
...
```
2. Four-column
```
<stress> <strain> <rate> <temp>
<stress> <strain> <rate> <temp>
...
```

The other elements of the data set (Tag, Source, Comment, Initial temperature, Strain rate, etc) may be entered using the **Data set controls**.

DMGfit is able to load stress-strain data from Excel files. Use the menu item **File | Load data from Excel file** to open an MS Excel file and read a rectangular array of numbers. Column indices for the strain and stress values and other data set elements are specified in the subsequent dialog.

Use the menu item **File | Write a data file** to create a template for data files from a loaded data set. Data files so created may later be loaded using **File | Load a data file.**

References

Bammann, D. J., "Modeling Temperature and Strain Rate Dependent Large of Metals," *Applied Mechanics Reviews*, Vol. 43, No. 5, Part 2, May, 1990.

Bammann, D. J., Chiesa, M. L., Horstemeyer, M. F., Weingarten, L. I., "Failure in Ductile Materials Using Finite Element Methods," *Structural Crashworthiness and Failure*, eds. T. Wierzbicki and N. Jones, Elsevier Applied Science, The Universities Press (Belfast) Ltd, 1993.

Cariño, R., Horstemeyer, M., & Burton, C. (Dec 2007). Re-engineering DMGFIT – Fitting Material Constants to Internal State Variable Models. *MSU.CAVS.CMD.2007-R0040*.

Horstemeyer, M.F., Lathrop, J., Gokhale, A.M., and Dighe, M., "Modeling Stress State Dependent Damage Evolution in a Cast Al-Si-Mg Aluminum Alloy," *Theoretical and Applied Fracture Mechanics*, Vol. 33, pp. 31-47, 2000.

Lathrop, J.F., (Dec 1996). BFIT—A Program to Analyze and Fit the BCJ Model Parameters to Experimental Data Tutorial and User's Guide. *SANDIA REPORT SAND97-8218 . UC-405, Unlimited Release, Printed December 1996*.

Appendix A. MSU ISV DMG 1.0 Production Model Equations

The MSU ISV DMG 1.0 production material model is given by the following equations. The pertinent equations in this model are denoted by the rate of change of the observable and internal state variables. The equations used within the context of the finite element method are given by,

$$\overset{\circ}{\underline{\sigma}} = \dot{\underline{\sigma}} - \underline{W}^e\underline{\sigma} - \underline{\sigma}\underline{W}^e = \lambda(1-D)tr\left(\underline{D}^e\right)\underline{I} + 2\mu(1-D)\underline{D}^e - \frac{\dot{D}}{1-D}\underline{\sigma} \qquad \text{Equation A.1}$$

$$\underline{D}^e = \underline{D} - \underline{D}^{in} \qquad \text{Equation A.2}$$

$$\underline{D}^{in} = f(T)\sinh\left[\frac{\|\underline{\sigma}' - \underline{\alpha}\| - \{R + Y(T)\}\{1-D\}}{V(T)\{1-D\}}\right]\frac{\underline{\sigma}' - \underline{\alpha}}{\|\underline{\sigma}' - \underline{\alpha}\|} \qquad \text{Equation A.3}$$

$$\overset{o}{\underline{\alpha}} = \dot{\underline{\alpha}} - \underline{W}^e\underline{\alpha} + \underline{\alpha}\underline{W}^e = \left\{h(T)\underline{D}^{in} - \left[\sqrt{\frac{2}{3}}r_d(T)\left\|\underline{D}^{in}\right\| + r_s(T)\right]\|\underline{\alpha}\|\underline{\alpha}\right\}\left[\frac{DCS_0}{DCS}\right]^z \qquad \text{Equation A.4}$$

$$\dot{R} = \left\{H(T)\underline{D}^{in} - \left[\sqrt{\frac{2}{3}}R_d(T)\left\|\underline{D}^{in}\right\| + R_s(T)\right]R^2\right\}\left[\frac{DCS_0}{DCS}\right]^z \qquad \text{Equation A.5}$$

$$\dot{D} = \left[\dot{\phi}_{particles} + \dot{\phi}_{pores}\right]c + \left[\phi_{particles} + \phi_{pores}\right]\dot{c}\,, \qquad \text{Equation A.6}$$

$$\dot{\phi}_{particles} = \dot{\eta}v + \eta\dot{v} \qquad \text{Equation A.7}$$

$$\dot{\eta} = \left\|\underline{D}^{in}\right\|\frac{d^{1/2}}{K_{IC}f^{1/3}}\eta\left\{a\left[\frac{4}{27} - \frac{J_3^{\,2}}{J_2^{\,3}}\right] + b\frac{J_3}{J_2^{3/2}} + c\left\|\frac{I_1}{\sqrt{J_2}}\right\|\right\}\exp\left(-C_{\eta T}/T\right) \qquad \text{Equation A.8}$$

$$\dot{v} = \frac{3}{2}v\left[\frac{3}{2}\frac{V(T)}{Y(T)}\frac{\sigma_H}{\sigma_{vm}} + \left(1 - \frac{V(T)}{Y(T)}\right)(1 + 0.4319)\right]^{Y(T)/V(T)}\underline{D}^{in} \qquad \text{Equation A.9}$$

$$\dot{c} = C_{coal}\left[\eta\dot{v} + \dot{\eta}v\right]\exp(C_{CT}T)\left(DCS_0/DCS\right)^z \qquad \text{Equation A.10}$$

$$\dot{\phi}_{pores} = \left[\frac{1}{(1-\phi_{pores})^m} - (1-\phi_{pores})\right]\sinh\left\{\frac{2\left(2^{V(T)/Y(T)} - 1\right)}{\left(2^{V(T)/Y(T)} + 1\right)}\frac{\sigma_H}{\sigma_{vm}}\right\}\left\|\underline{D}^{in}\right\| \qquad \text{Equation A.11}$$

The rate equations are generally written as objective rates ($\overset{o}{\underline{\sigma}}, \overset{o}{\underline{\alpha}}$) with indifference to the continuum frame of reference assuming a Jaumann rate in which the continuum spin equals the elastic spin ($\underline{W} = \underline{W}^e$). The internal state variable (ISV) equations are functions of the observable variables (temperature, stress state, and rate of deformation). In general, the rate equations of generalized displacements, or thermodynamics fluxes, describing the rate of change may be written as independent equations for each ISV or as derivatives of a suitably chosen potential function arising from the hypothesis of generalized normality. An advantage of assuming generalized normality, although somewhat restrictive, is unconditional satisfaction of the Kelvin inequality of the second law of thermodynamics (nonnegative intrinsic dissipation), i.e.

$$\underline{\sigma} : \underline{D}^{in} - \underline{b} : \overset{\circ}{\underline{\alpha}} - \kappa \bullet \dot{R} - \phi \bullet \dot{D} \geq 0 . \qquad \text{Equation A.12}$$

The selection of the ISVs may, in principle, be somewhat arbitrary, but the kinematic hardening, isotropic hardening, and damage rate equations are physically motivated and strongly influence the history of the material. The ISV model accounts for deviatoric inelastic deformation resulting from the presence of dislocations in crystallographic material, dilatational deformation, and ensuing failure from damage progression. Damage will reduce the material strength, enhance the inelastic flow, and soften the elastic moduli.

In Equation A.1, the elastic Lame constants are denoted by λ and μ. The elastic rate of deformation ($\underline{D}^{e}$) results when the flow rule as shown in Equation A.2 is subtracted from the total deformation ($\underline{D}$), which is defined by the boundary conditions.

The independent variables for the inelastic rate of deformation are given in Equation A.3 as the stress, temperature, and internal state variables. This is similar to power law and Garofalo equations for creep except that the ISVs are now included. The deviatoric inelastic flow rule, $\underline{D}^{in}$, encompasses the regimes of creep and plasticity and is a function of the temperature, the kinematic hardening internal state variable ($\underline{\alpha}$), the isotropic hardening internal state variable (R), the volume fraction of damaged material (D), and the functions $f(T)$, $V(T)$, and $Y(T)$, which are related to yielding with Arrhenius-type temperature dependence. The function $Y(T)$ is the rate-independent yield stress. The function $f(T)$ determines when the rate-dependence affects initial yielding. The function $V(T)$ determines the magnitude of rate-dependence on yielding. These functions are determined from simple isothermal compression tests with different strain rates and temperatures,

$$V(T) = C_1 \exp\left(-C_2 \big/ T\right),\ Y(T) = C_3 \exp\left(C_4 \big/ T\right),\ f(T) = C_5 \exp\left(-C_6 \big/ T\right). \qquad \text{Equation A.13}$$

The kinematic hardening internal state variable, $\underline{\alpha}$, reflects the effect of anisotropic dislocation density, and the isotropic hardening internal state variable R, reflects the effect of the global dislocation density. As such, the hardenings are cast in a hardening-recovery format that includes dynamic and static recovery. The functions $r_s(T)$ and $R_s(T)$ are scalar in nature and describe the diffusion-controlled static or thermal recovery, while $r_d(T)$ and $R_d(T)$ are scalar functions describing dynamic recovery. Hence, the two main types of recovery that are exhibited by populations of dislocations within crystallographic materials are captured in the ISVs. The anisotropic hardening modulus is $h(T)$, and the isotropic hardening modulus is $H(T)$.

The hardening moduli and dynamic recovery functions account for deformation-induced anisotropy arising from texture and dislocation substructures by means of stress-dependent variables. Miller *et al.* (1995) showed that by using $J_3^{'}$ in the hardening equations the different hardening rates between axisymmetric compression and torsion (torsional softening) were accurately captured. Miller *et al*. (1995) and Horstemeyer *et al.* (1995) included this feature in

the Bammann ISV model as

$$r_d(T) = C_7\left(1+C_{19}\left\lceil\frac{4}{27}-\frac{J_3^{'2}}{J_2^{'3}}\right\rceil\right)\exp\left(-C_8/T\right), \quad \text{Equation A.14}$$

$$h(T)=\left\{C_9\left(1+C_{20}\left\lceil\frac{4}{27}-\frac{J_3^{'2}}{J_2^{'3}}\right\rceil\right)\right\}-C_{10}T, \quad \text{Equation A.15}$$

$$r_s(T)=C_{11}\exp\left(-C_{12}/T\right), \quad \text{Equation A.16}$$

$$R_d(T) = C_{13}\left(1+C_{21}\left\lceil\frac{4}{27}-\frac{J_3^{'2}}{J_2^{'3}}\right\rceil\right)\exp\left(-C_{14}/T\right), \quad \text{Equation A.17}$$

$$H=\left\{C_{15}\left(1+C_{22}\left\lceil\frac{4}{27}-\frac{J_3^{'2}}{J_2^{'3}}\right\rceil\right)\right\}-C_{16}T, \quad \text{Equation A.18}$$

$$R_s(T)=C_{17}\exp\left(-C_{18}/T\right), \quad \text{Equation A.19}$$

where $J_2^{'}=\frac{1}{2}(\underline{\sigma}'-\underline{\alpha})^2$ and $J_3^{'}=\frac{1}{3}(\underline{\sigma}'-\underline{\alpha})^3$. The deviatoric stress $\underline{\sigma}'$ is expressed in indicial notation as

$$\sigma_{ij}'=\sigma_{ij}-\frac{1}{3}\sigma_{ii}. \quad \text{Equation A.20}$$

The damage variable D represents the damage fraction of material within a continuum element. The mechanical properties of a material depend upon the amount and type of microdefects within its structure. Deformation changes these microdefects, and when the number of microdefects accumulates, damage is said to have grown. The notion of a damaged state in continuum field theory emerged when Kachanov (1958) introduced a damage variable to describe the microdefect density locally in a creeping material. The idea was that damage could be measured by the volume fraction of voids under creep conditions. Rabotnov (1969) furthered this notion with a rate equation of void density.

Equation A.6 introduces the void volume fraction (porosity) as damage. By including damage, D, as an ISV, different forms of damage rules can easily be incorporated into the constitutive framework. Bammann *et al*. (1993; 1996) and Horstemeyer (1992, 1993) have demonstrated the applicability of the Cocks and Ashby (1980) void growth rule used as the damage rate equation in the ISV model.

The generalized thermodynamic force conjugate, ϕ, is often referred to as the energy release rate for elastic brittle materials and the J-integral for inelasticity. In essence, an increment of damage will have associated energy released per unit damage extension as new damaged area (or volume) is developed.

The damage progression is divided into void nucleation and growth from silicon particles and

from pores. Coalescence is introduced to reflect pore-pore interactions and silicon-pore interactions as expressed in Equation A.10. The void nucleation evolution described by Equation A.8 is discussed in length by Horstemeyer and Gokhale (1999). The void growth related to silicon particles, Equation A.9, is that from Budiansky *et al*. (1982). Other forms can be used and evaluated (cf., Horstemeyer *et al*., 1999), but this equation allows for a strain rate sensitivity in relation the plasticity model ($m=V(T)/Y(T)$). For the porosity evolution, the Cocks and Ashby (1981) void growth rule is used as shown in Equation A.11.

Appendix B. MSU ISV DMG 1.0 Production Version: Material Model Fits

B1. Al A356-T6 alloy	B2. Al 99% pure alloy
B3. Al 1060-T0 alloy	B4. Al 1100 alloy
B5. Al 2024-T0 alloy	B6. Al 2024 T351 alloy
B7. Al 2024-T4 alloy	B8. Al 5083 alloy
B9. Al 5086-T6 alloy	B10. Al 6022 alloy
B11. Al 6061-T0 alloy	B12. Al 6061-T6 alloy
B13. Al 6061-T651 alloy	B14. Al 7039 alloy
B15. Al 7075-T0 alloy	B16. Al 7075-T6 alloy
B17. Al 7075-T65l alloy	B18. 300mmarsteel alloy
B19. 1006 steel alloy	B20. 1020 steel alloy
B21. 10b22 steel alloy	B22. 304L SS alloy
B23. 321 SS alloy	B24. 410 SS alloy
B25. 4140 steel alloy	B26. 4340 steel alloy
B27. A286 steel alloy	B28. AF steel alloy
B29. Armco Iron	B30. Armor Steel
B31. C1008 Steel	B32. Capeleciron
B33. FC0205 steel alloy	B34. HY80 steel alloy
B35. HY100 steel alloy	B36. HY130 steel alloy
B37. Mild Steel	B38. RHA Steel
B39. S7tool steel alloy	B40. AM30 Mg alloy
B41. AM50 Mg alloy	B42. AM60 Mg alloy
B43. AZ31 Mg alloy	B44. AZ91 Mg alloy
B45. AE42 Mg alloy	B46. AE44 Mg alloy
B47. Ti7Al4Mo alloy	B48. Ti8Al1Mo1V alloy
B49. Ti0Al6V4 alloy	B50. Ti6Al6V2Sn alloy
B51. D38 Uranium	B52. D380075Ti Uranium
B53. D38006 Nb Uranium	B54. 200 Nickel
B55. In718 alloy	B56. Copper
B57. OFHC Copper	B58. ETP Copper
B59. 99% Brass	B60. Lead
B61. Tantalum	

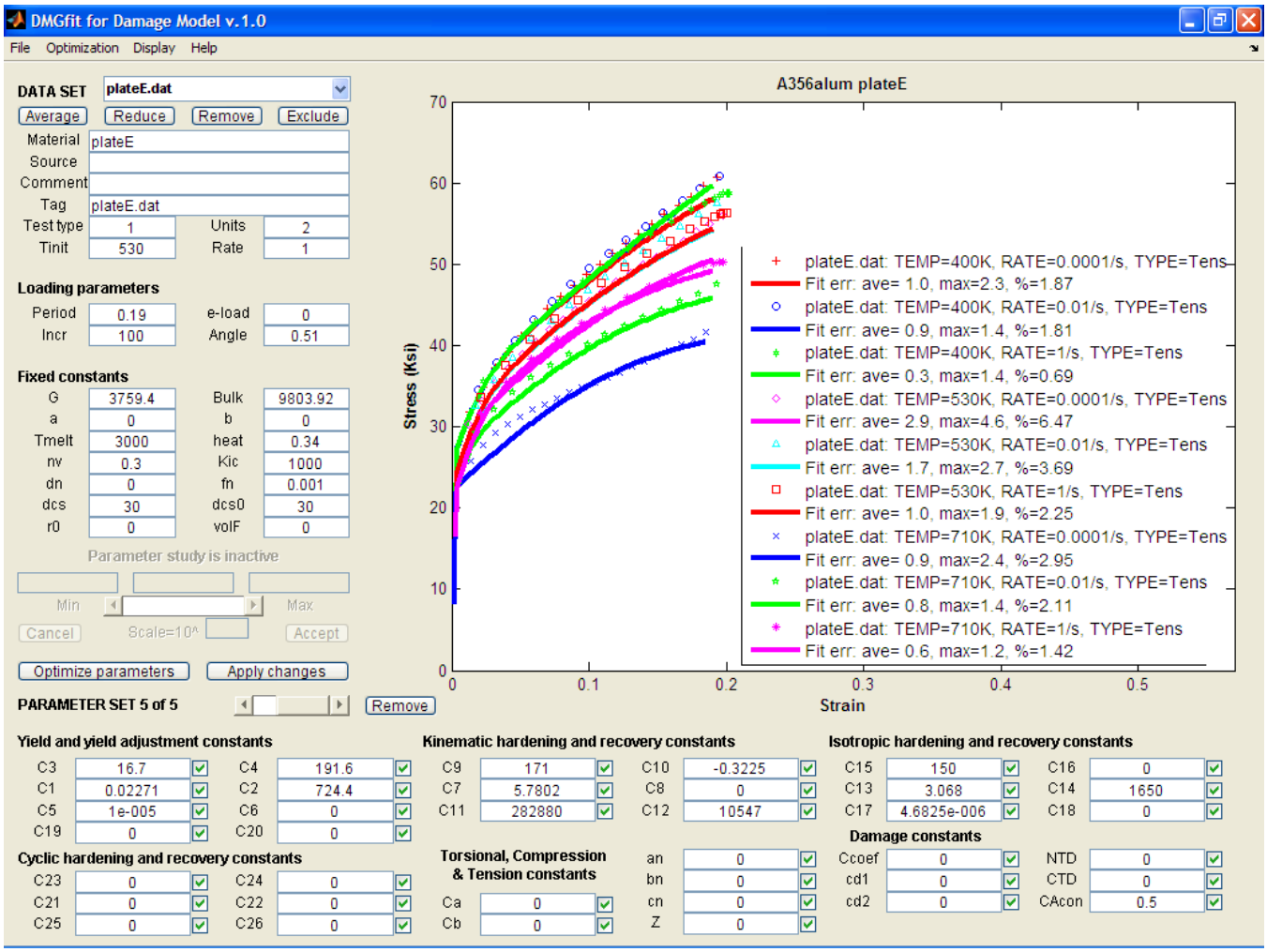

B1. Al A356-T6 alloy: model correlation with different temperatures and strain rates

Reference: Horstemeyer, M.F., Lathrop, J., Gokhale, A.M., and Dighe, M., "Modeling Stress State Dependent Damage Evolution in a Cast Al-Si-Mg Aluminum Alloy," *Theoretical and Applied Fracture Mechanics*, Vol. 33, pp. 31-47, 2000.

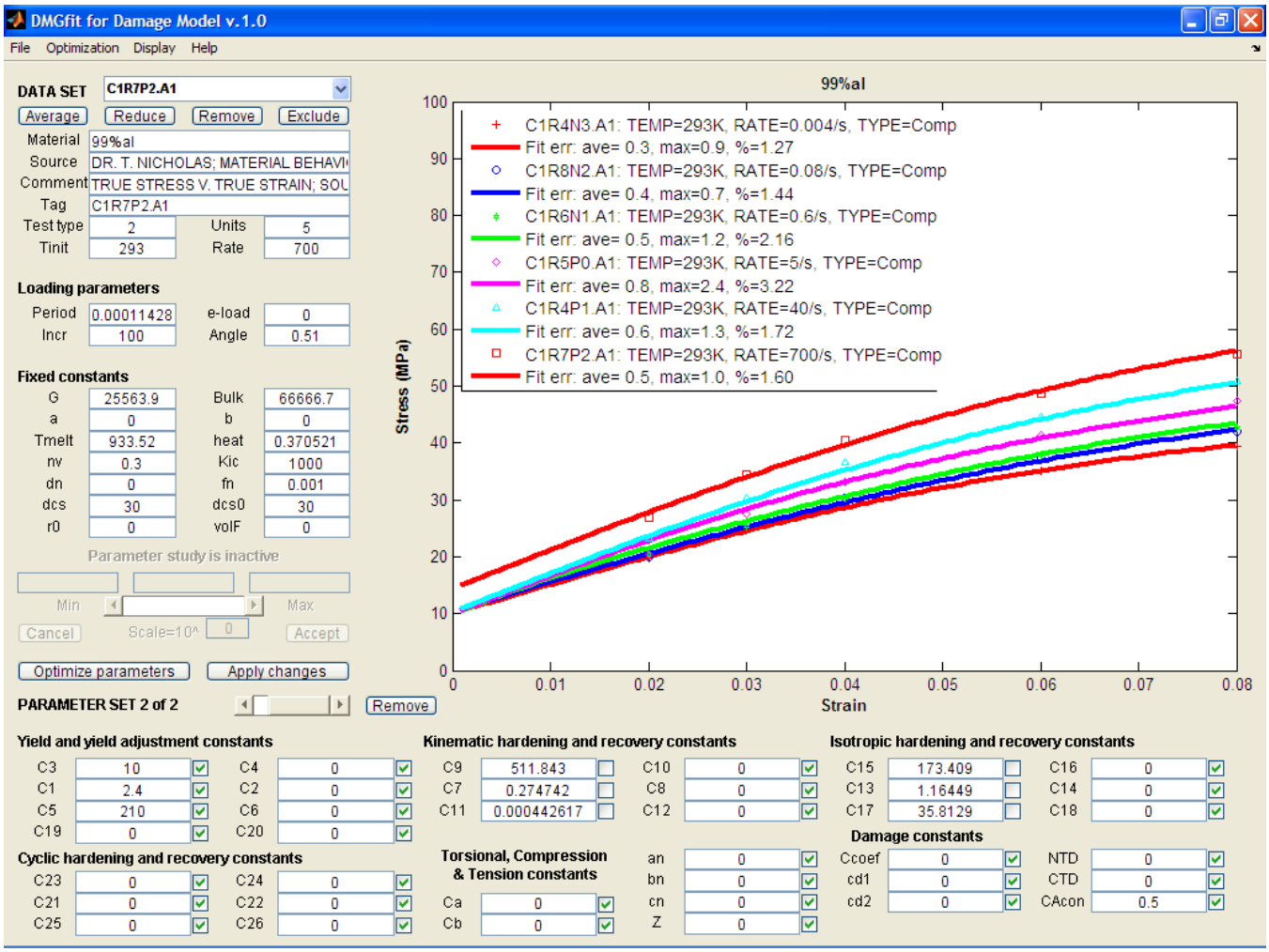

B2. Al 99% pure alloy: model correlation with different strain rates.

References:

1. Holt, D.L., Babcock, S.G. Green, S.J. and Maiden, C.J., The Strain Rate Dependence of the Flow Stress in Some Aluminum Alloys, General Motors Research Laboratories, TR66-75, 1996.

2. Nicholas, T., Material behavior at high strain rates, Report AFWAL-TR-80-4053, USAF Wright Aeronautical Laboratories, Wright-Patterson Air Force Base, OH, USA, 1980.

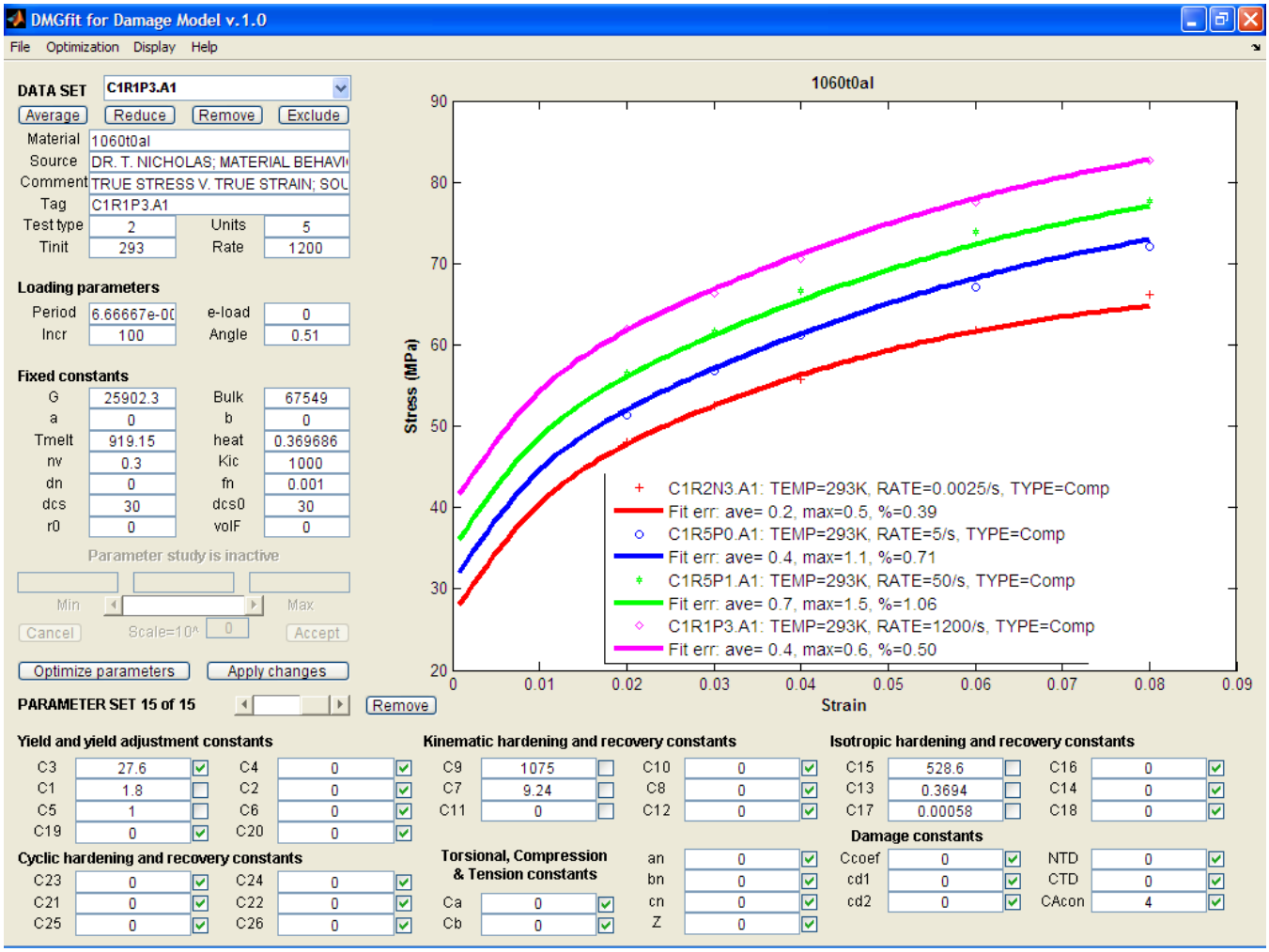

B3. Al 1060-T0 alloy: model correlation with different strain rates

References:

1. Holt, D.L., Babcock, S.G. Green, S.J. and Maiden, C.J., The Strain Rate Dependence of the Flow Stress in Some Aluminum Alloys, General Motors Research Laboratories, TR66-75, 1996.

2. Nicholas, T., Material behavior at high strain rates, Report AFWAL-TR-80-4053, USAF Wright Aeronautical Laboratories, Wright-Patterson Air Force Base, OH, USA, 1980.

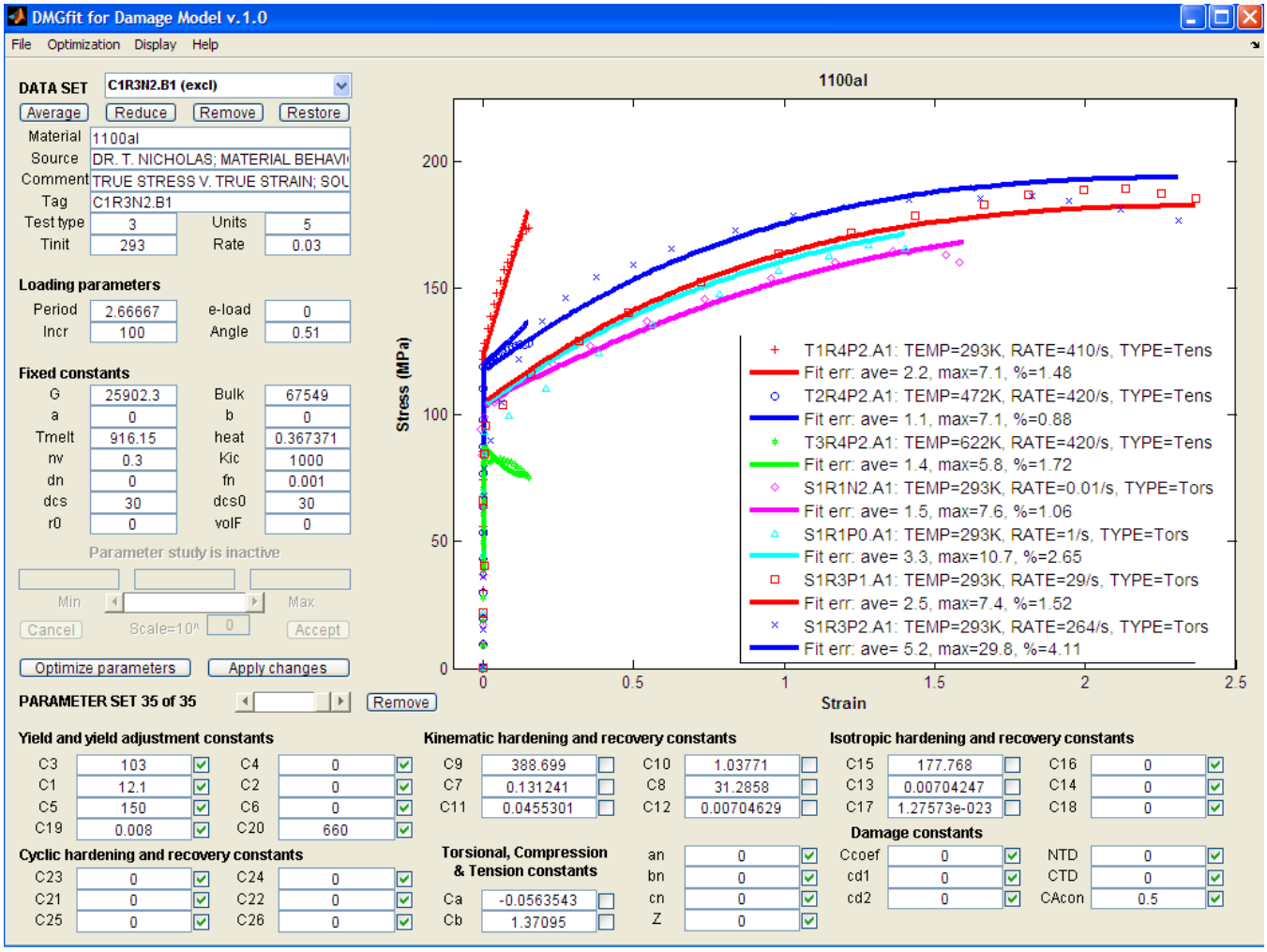

B4. Al 1100 alloy: model correlation with different strain rates

References:

1. Holt, D.L., Babcock, S.G. Green, S.J. and Maiden, C.J., The Strain Rate Dependence of the Flow Stress in Some Aluminum Alloys, General Motors Research Laboratories, TR66-75, 1996.

2. Horstemeyer, M.F. and Ramaswamy, S., "On Factors Affecting Localization and Void Growth in Ductile Metals: A Parametric Study," *Int. J. Damage Mech.*, Vol. 9, pp. 6-28, 2000.

3. Johnson, G.R. and Holmquist, T.J., Test data and computational strength and fracture model constants for 23 materials subjected to large strains, high strain rates, and high temperatures, LA-11463-MS, Los Alamos National Laboratory, 1989.

4. Nicholas, T., Material behavior at high strain rates, Report AFWAL-TR-80-4053, USAF Wright Aeronautical Laboratories, Wright-Patterson Air Force Base, OH, USA, 1980.

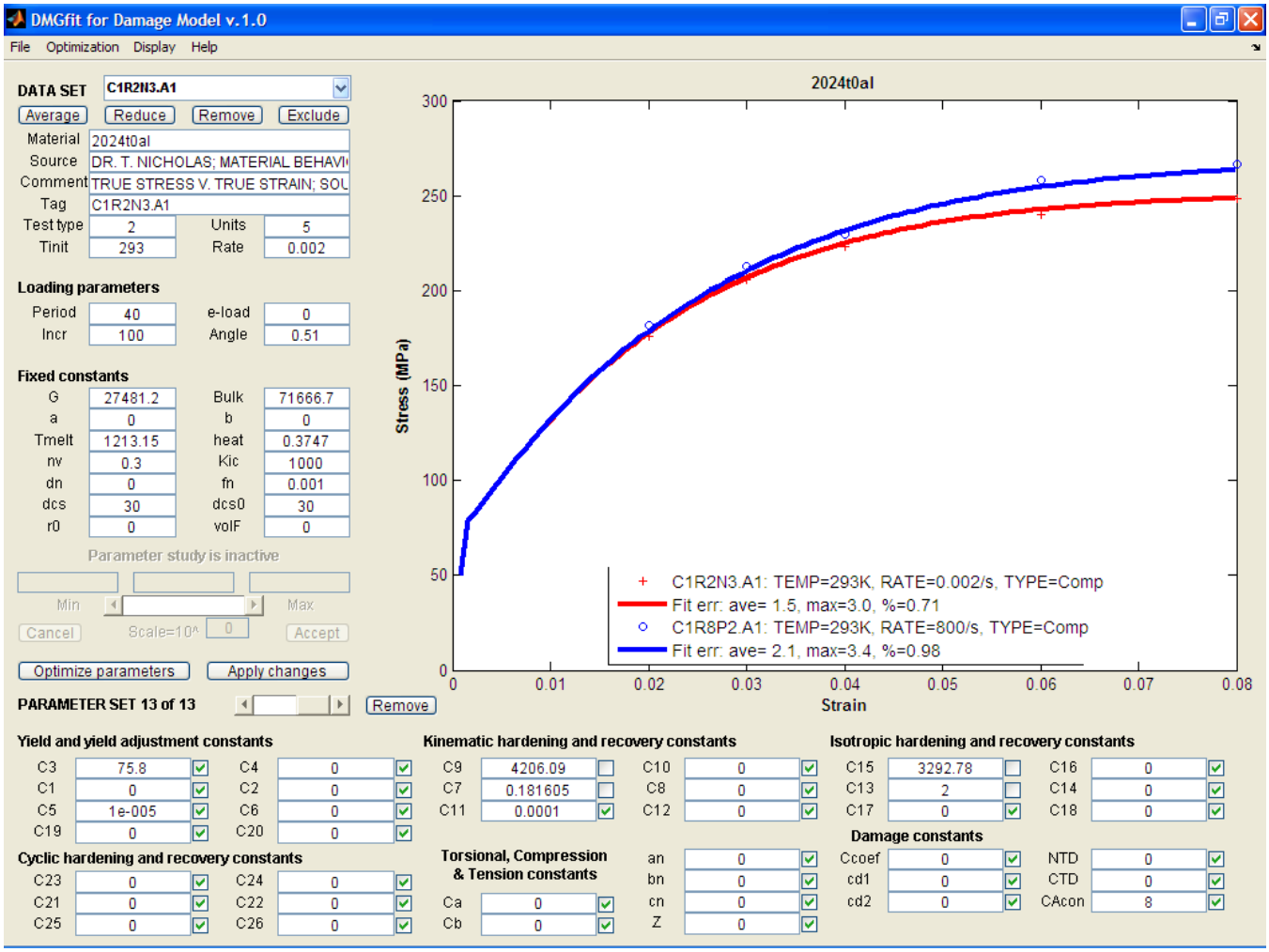

B5. Al 2024-T0 alloy: model correlation with different strain rates

References:

1. Holt, D.L., Babcock, S.G. Green, S.J. and Maiden, C.J., The Strain Rate Dependence of the Flow Stress in Some Aluminum Alloys, General Motors Research Laboratories, TR66-75, 1996.

2. Nicholas, T., Material behavior at high strain rates, Report AFWAL-TR-80-4053, USAF Wright Aeronautical Laboratories, Wright-Patterson Air Force Base, OH, USA, 1980.

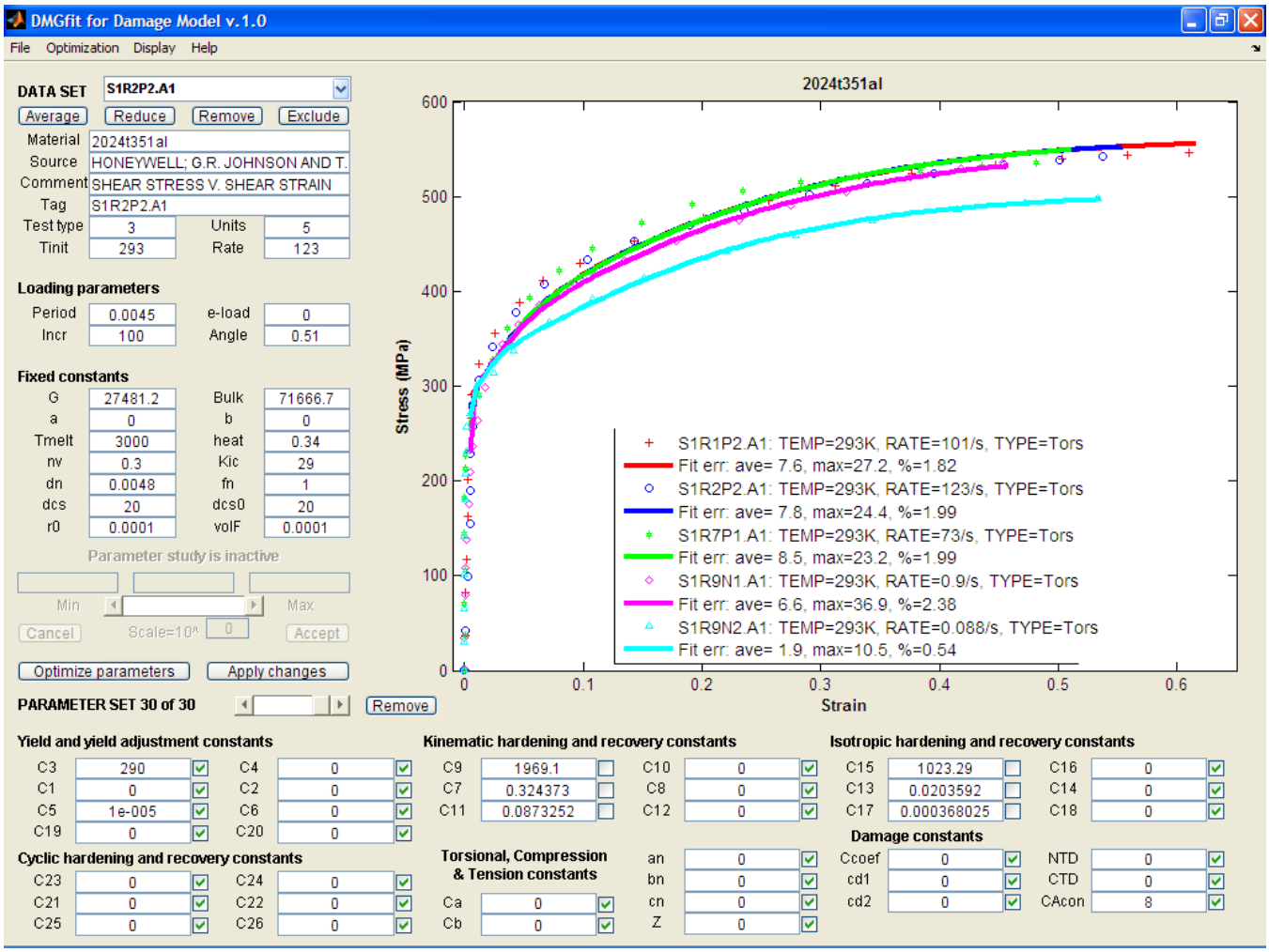

B6. Al 2024-T351 alloy: model correlation with different strain rates

Reference: Johnson, G.R. and Holmquist, T.J., Test data and computational strength and fracture model constants for 23 materials subjected to large strains, high strain rates, and high temperatures, LA-11463-MS, Los Alamos National Laboratory, 1989.

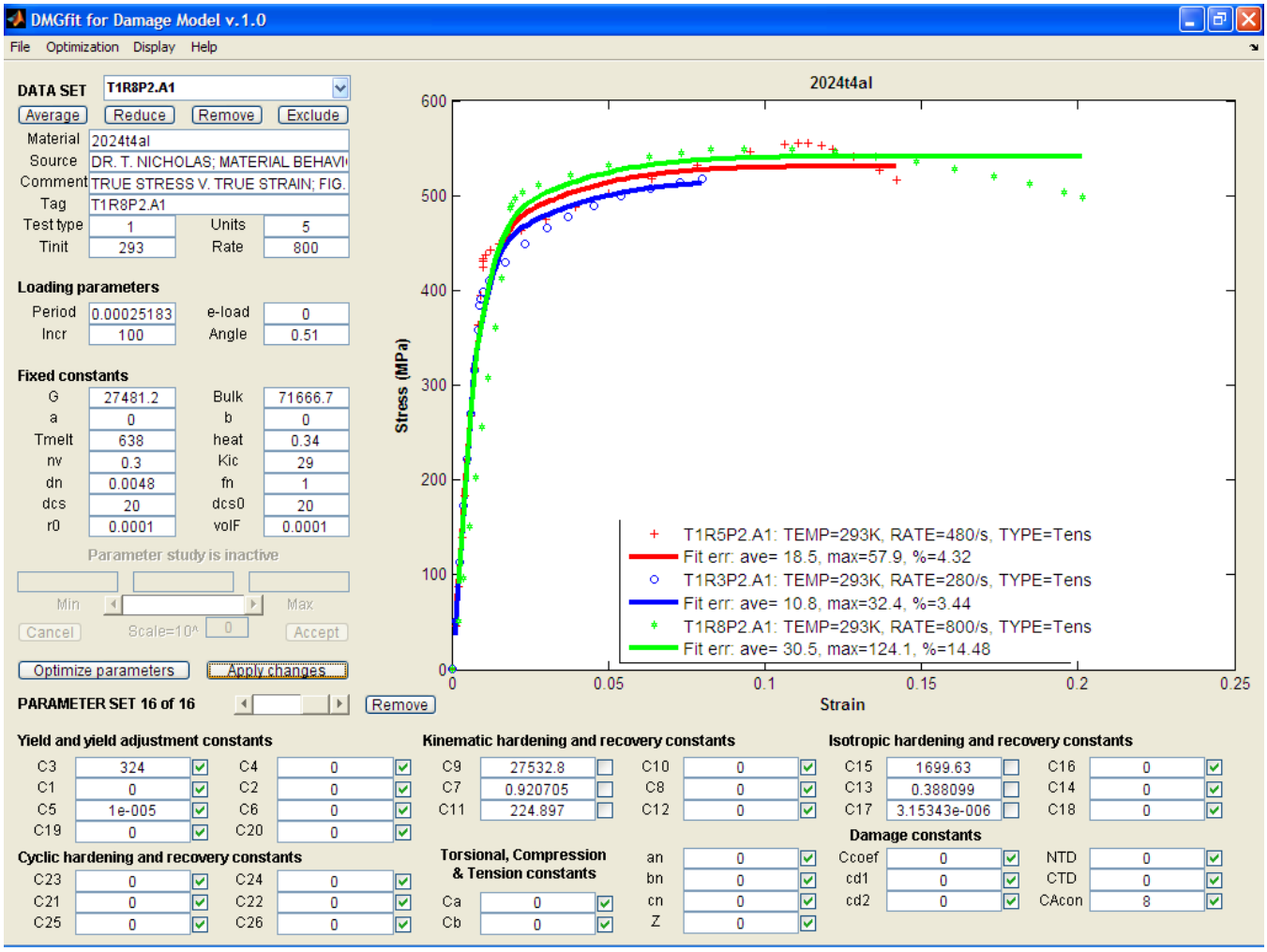

B7. Al 2024-T4 alloy: model correlation with different strain rates

Reference: Nicholas, T., Material behavior at high strain rates, Report AFWAL-TR-80-4053, USAF Wright Aeronautical Laboratories, Wright-Patterson Air Force Base, OH, USA, 1980.

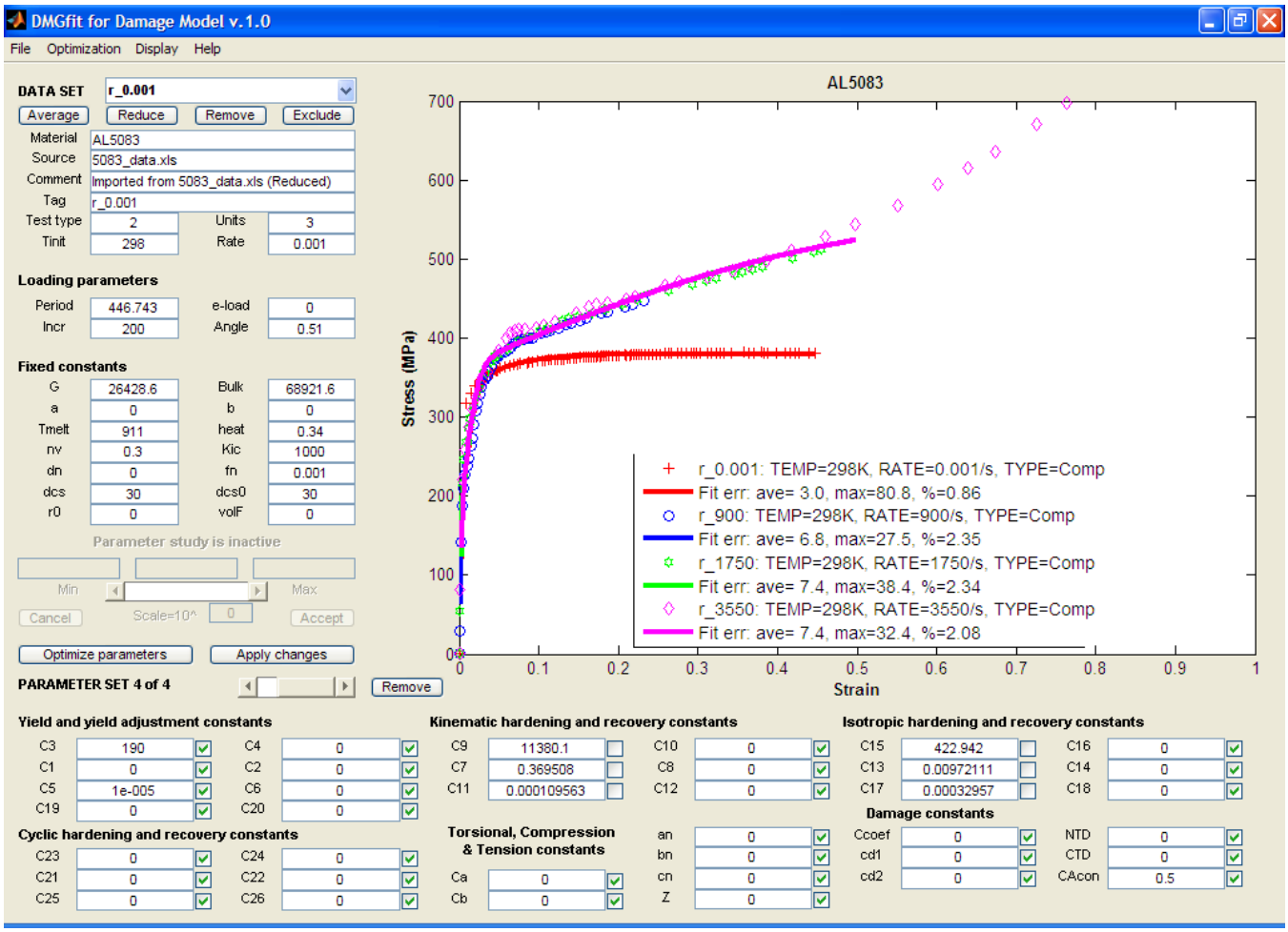

B8. Al 5083 alloy: model correlation with different strain rates

Reference: Tucker, M.T., Horstemeyer, M.F., Whittington, W.R., Solanki, K.N., Gary, G., and Gullett, P.M., The Effect of Varying Strain Rates and Stress States on the Plasticity, Damage, and Fracture of Aluminum Alloys, Mechanics of Materials, (submitted).

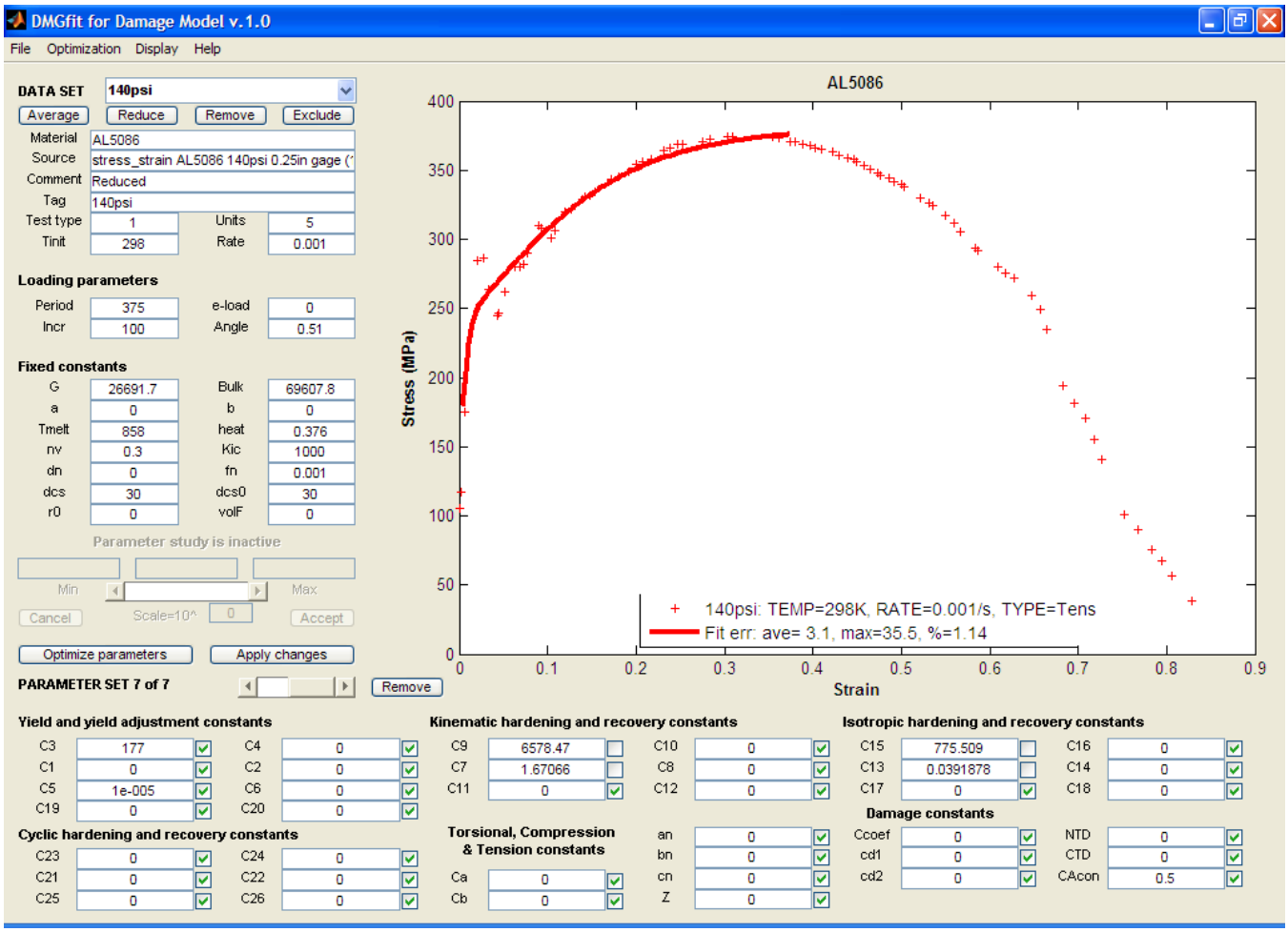

B9. Al 5086-T6 alloy model correlation

Reference: Balasundaram, A., Shan, Z., Gokhale, A.M., Graham, S., and Horstemeyer, M.F., "Particle Rotations During Plastic Deformation of 5086 (O) Aluminum Alloy", *Materials Characterization*, Vol. 48 (no. 5), PP. 363-369, 2002.

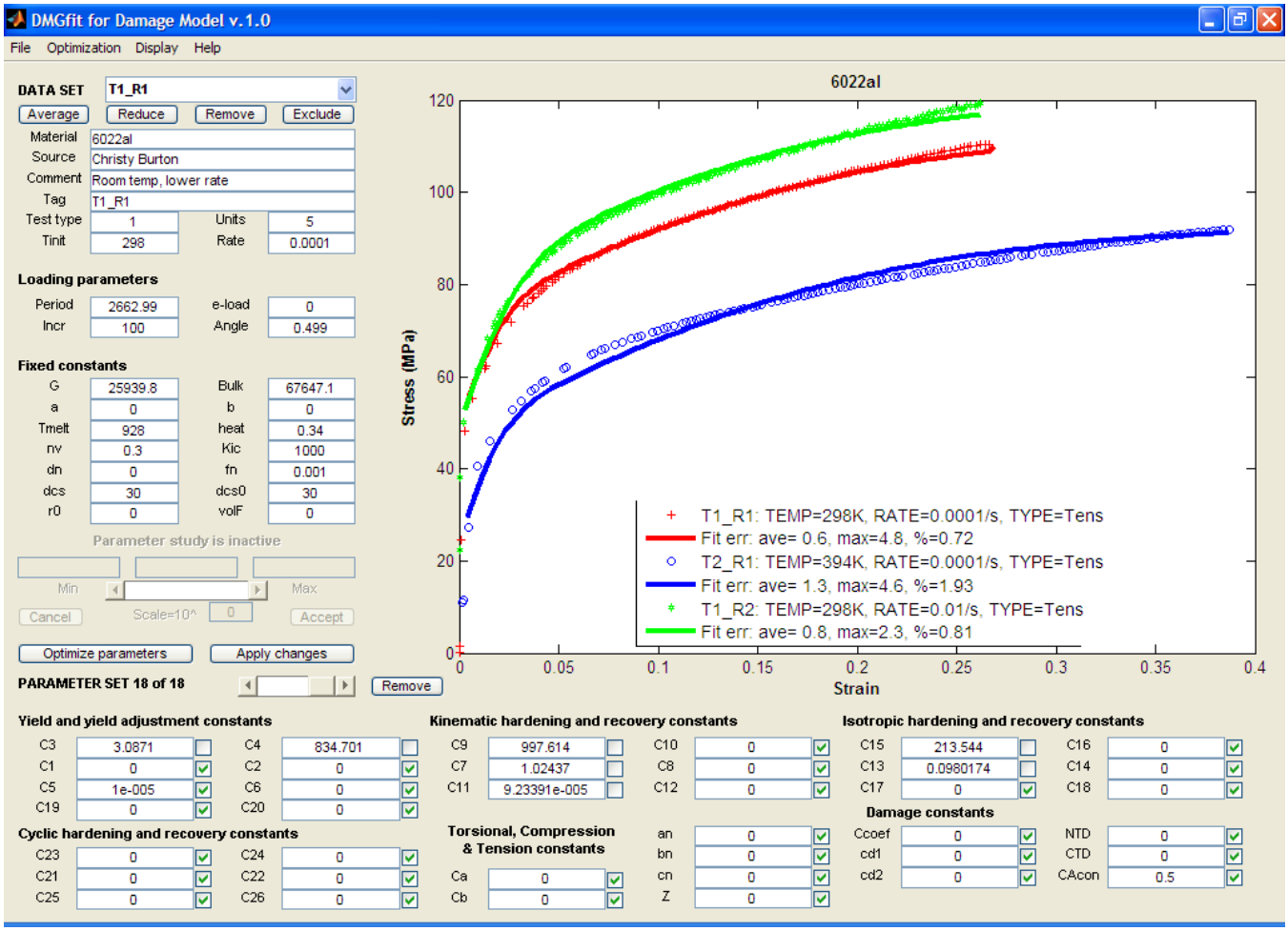

B10. Al 6022 alloy model correlation.

Reference: Burton, C., Horstemeyer, M., Wang, P., and Shahbazian-Yassar, R., Rolling history microstructural analysis of texture gradients for 6022 aluminum sheet, *136th TMS Annual Meeting*, Orlando, Fl, Feb. 2007.

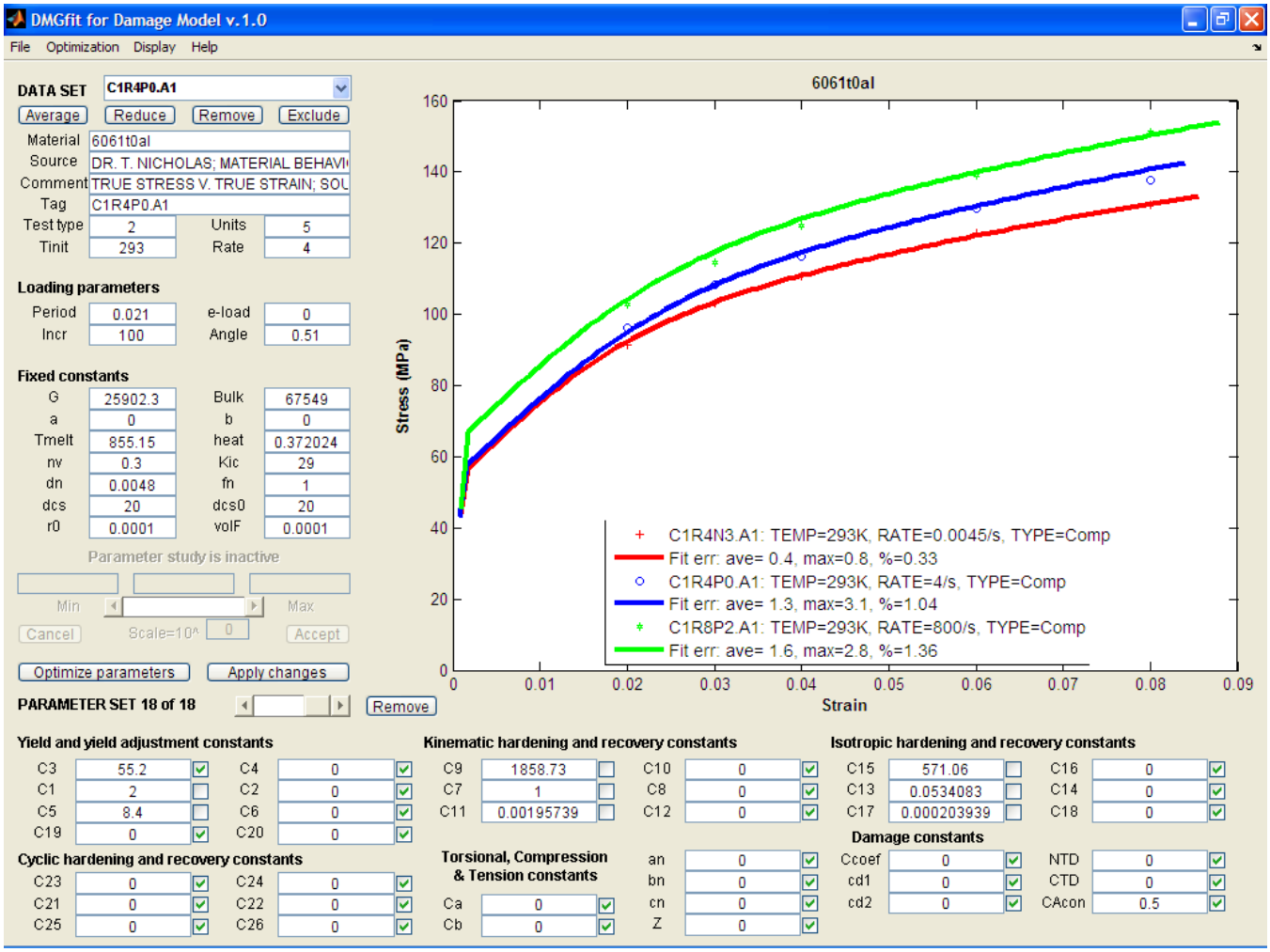

B11. Al 6061-T0 alloy: model correlation with different strain rates

References:

1. Holt, D.L., Babcock, S.G. Green, S.J. and Maiden, C.J., The Strain Rate Dependence of the Flow Stress in Some Aluminum Alloys, General Motors Research Laboratories, TR66-75, 1996.

2. Nicholas, T., Material behavior at high strain rates, Report AFWAL-TR-80-4053, USAF Wright Aeronautical Laboratories, Wright-Patterson Air Force Base, OH, USA, 1980.

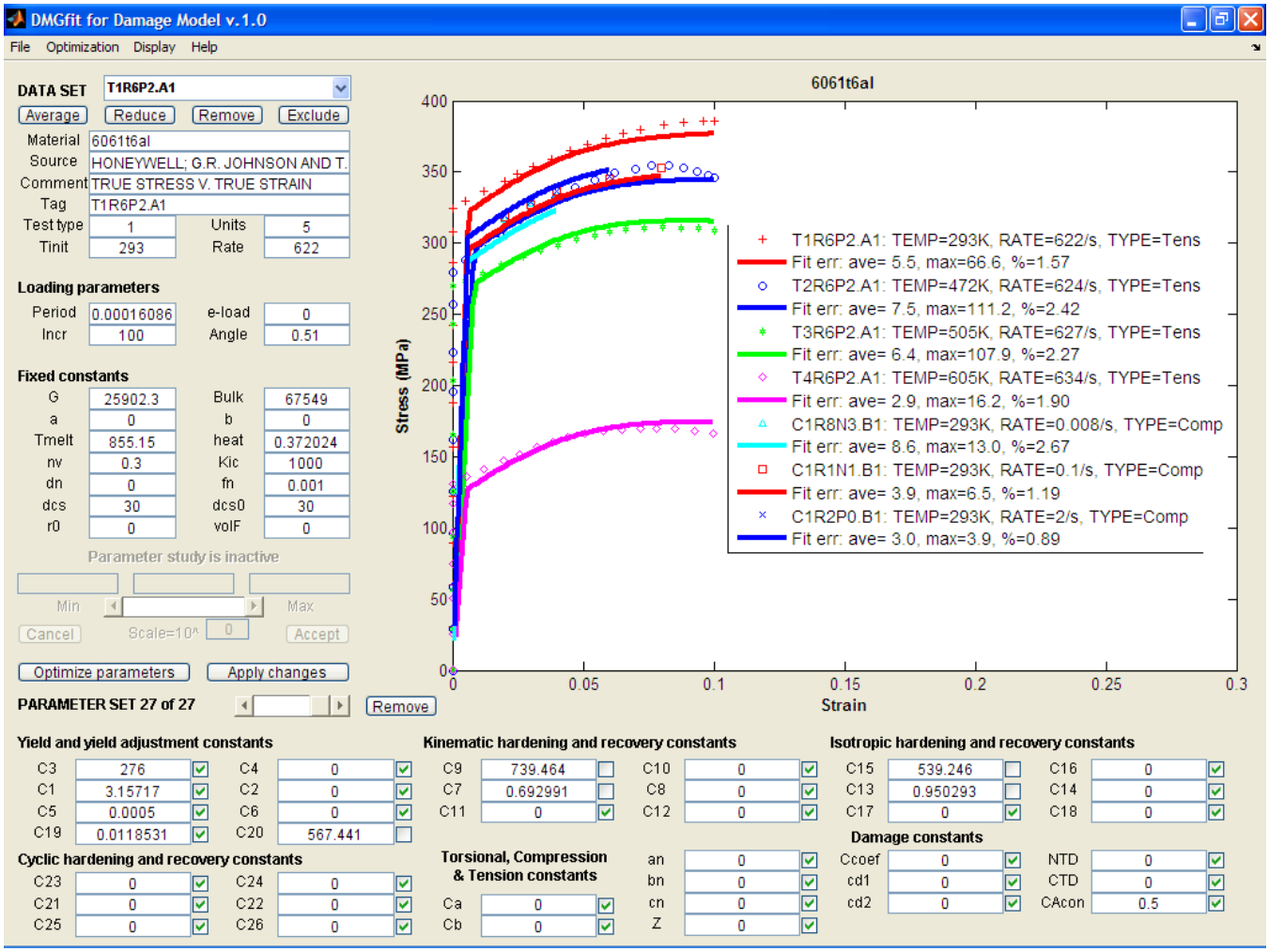

B12. Al 6061-T6 alloy: model correlation with different temperatures and strain rates

References:

1. Department of Defense. Aerospace Structural Metals Handbook, Volume 2. West Lafayette: CINDAS/Purdue, 1993.

2. Holt, D.L., Babcock, S.G. Green, S.J. and Maiden, C.J., The Strain Rate Dependence of the Flow Stress in Some Aluminum Alloys, General Motors Research Laboratories, TR66-75, 1996.1. Horstemeyer, M.F., "A Numerical Parametric Investigation of Localization and Forming Limits," Int. J. Damage Mech, Vol. 9, pp. 255-285, 2000.

3. Johnson, G.R. and Holmquist, T.J., Test data and computational strength and fracture model constants for 23 materials subjected to large strains, high strain rates, and high temperatures, LA-11463-MS, Los Alamos National Laboratory, 1989.

4. Nicholas, T., Material behavior at high strain rates, Report AFWAL-TR-80-4053, USAF Wright Aeronautical Laboratories, Wright-Patterson Air Force Base, OH, USA, 1980.

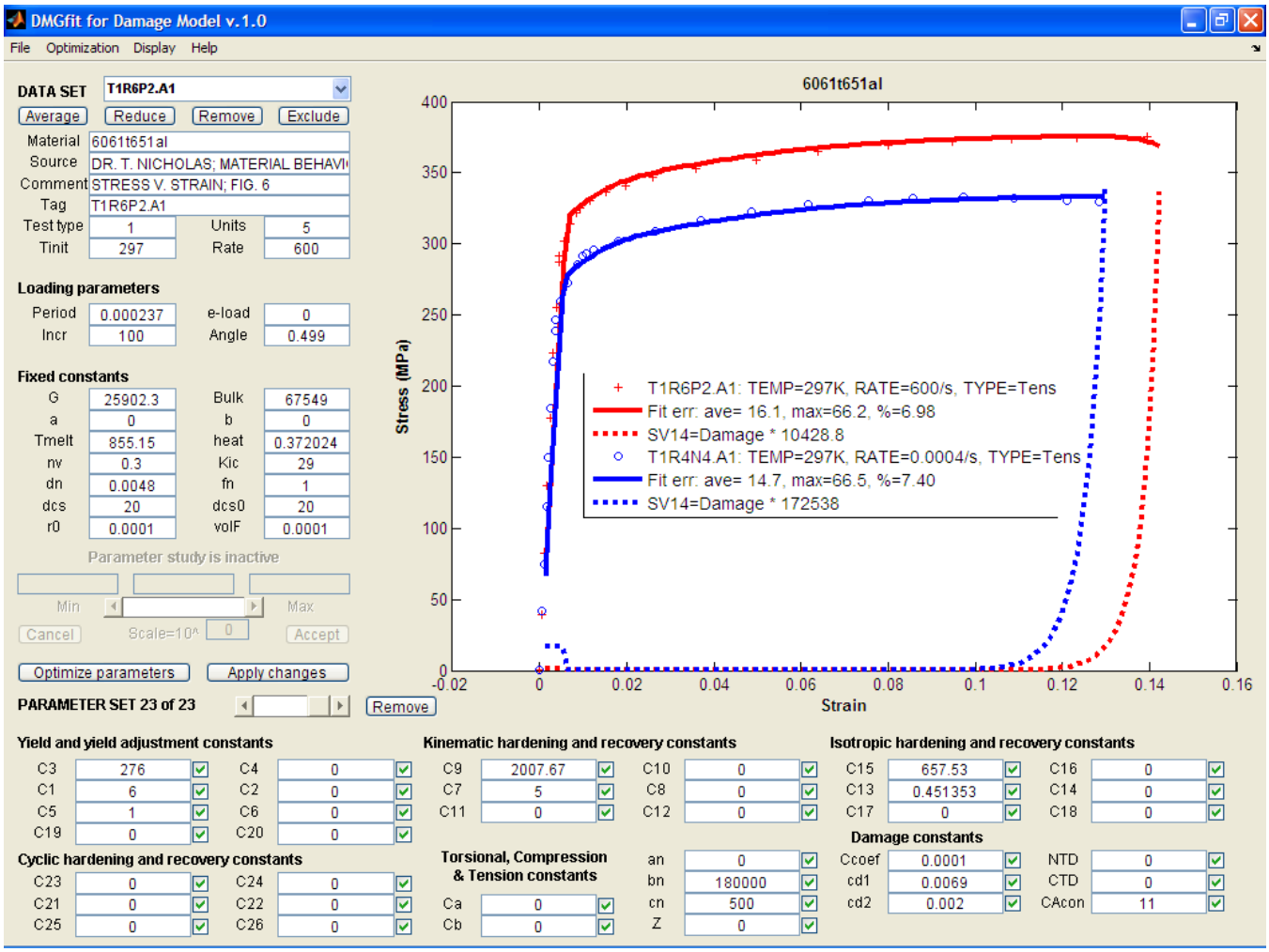

B13. Al 6061-T651 alloy: model correlation with different strain rates, damage state variable

References :

1. Horstemeyer, M.F., "A Numerical Parametric Investigation of Localization and Forming Limits," Int. J. Damage Mech, Vol. 9, pp. 255-285, 2000.

2. Nicholas, T., Material behavior at high strain rates, Report AFWAL-TR-80-4053, USAF Wright Aeronautical Laboratories, Wright-Patterson Air Force Base, OH, USA, 1980.

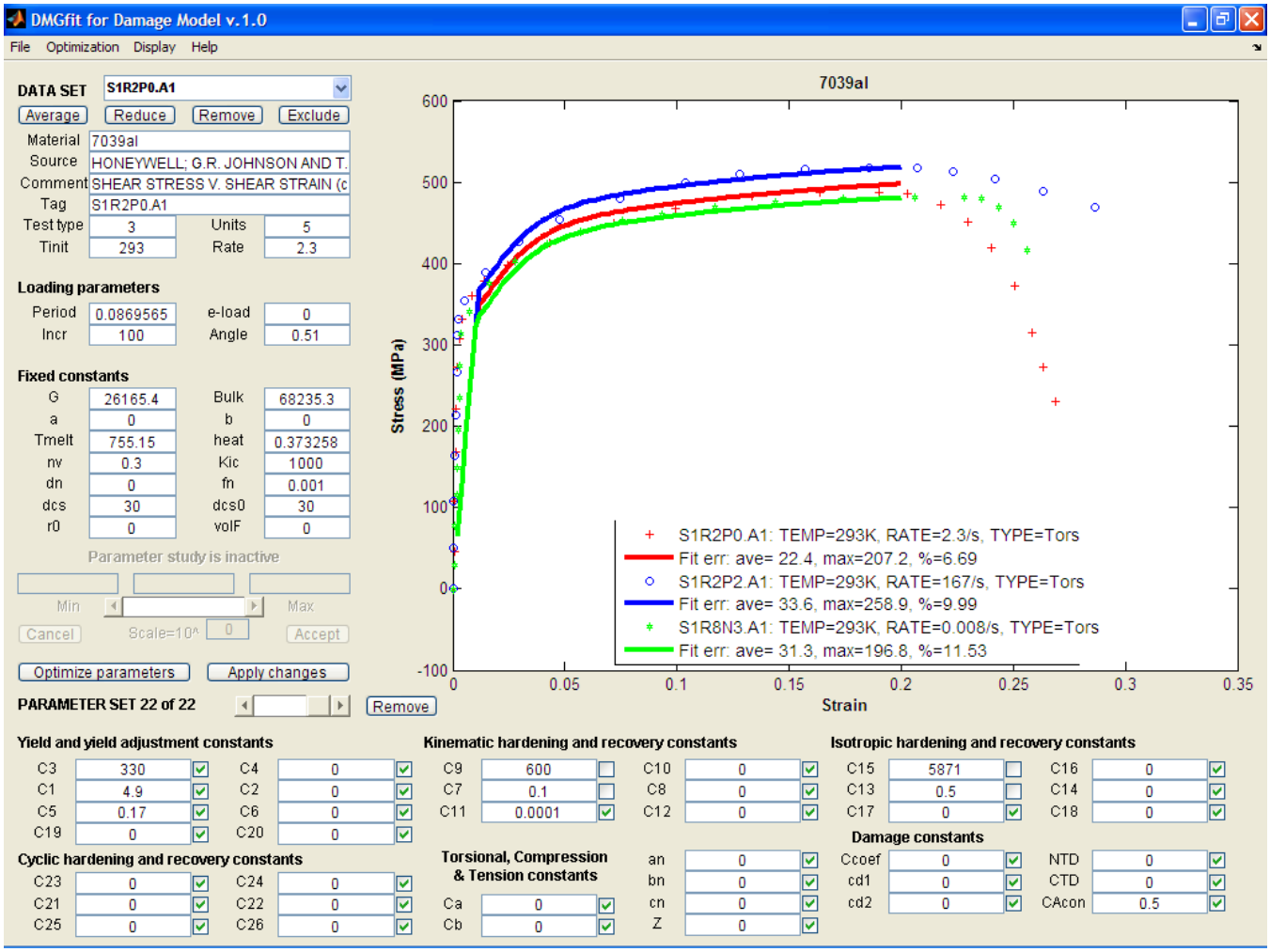

B14. Al 7039 alloy: model correlation with different strain rates

Reference: Johnson, G.R. and Holmquist, T.J., Test data and computational strength and fracture model constants for 23 materials subjected to large strains, high strain rates, and high temperatures, LA-11463-MS, Los Alamos National Laboratory, 1989.

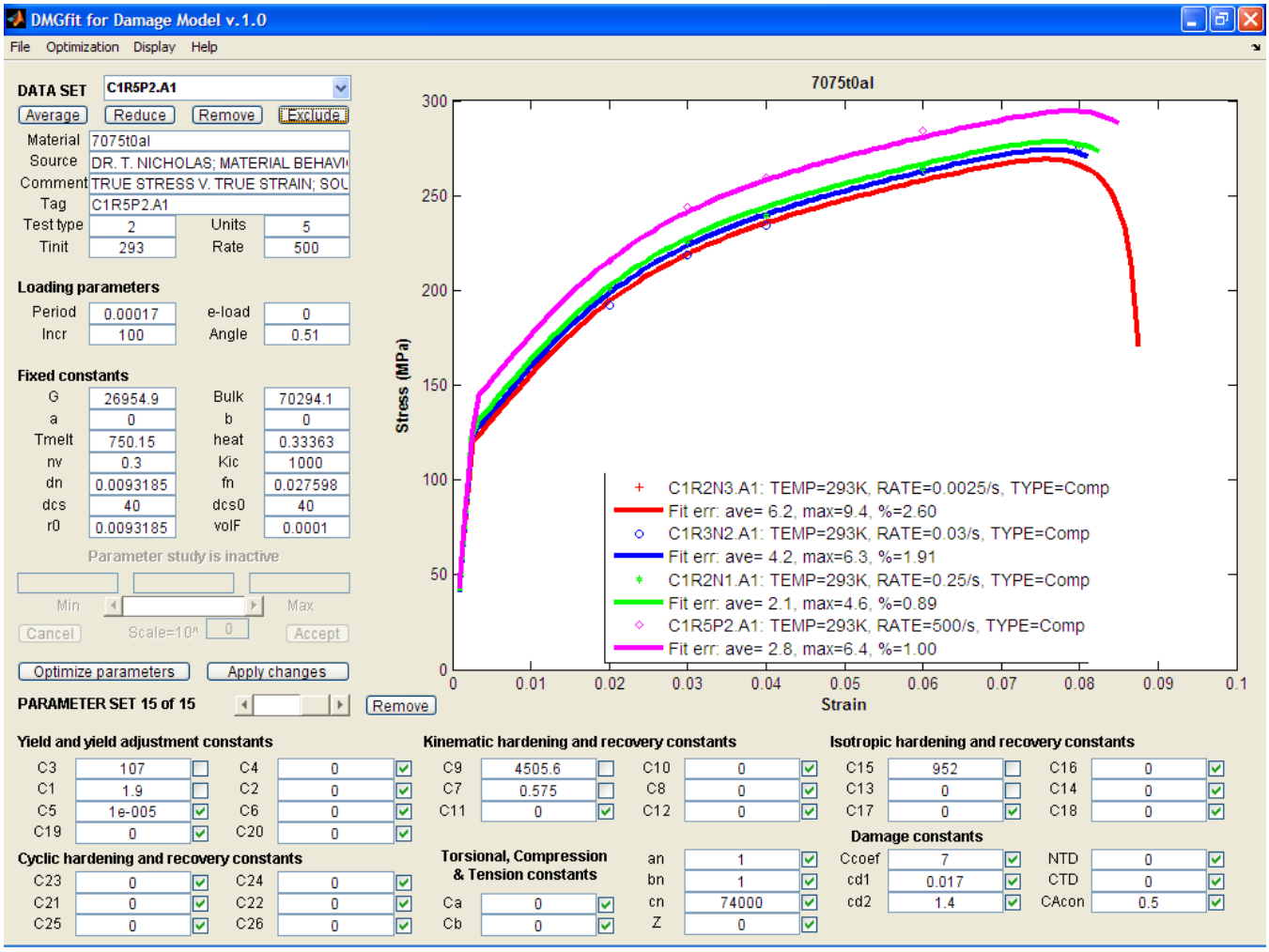

B15. Al 7075-T0 alloy: model correlation with different strain rates

References:

1. Holt, D.L., Babcock, S.G. Green, S.J. and Maiden, C.J., The Strain Rate Dependence of the Flow Stress in Some Aluminum Alloys, General Motors Research Laboratories, TR66-75, 1996.

2. Nicholas, T., Material behavior at high strain rates, Report AFWAL-TR-80-4053, USAF Wright Aeronautical Laboratories, Wright-Patterson Air Force Base, OH, USA, 1980.

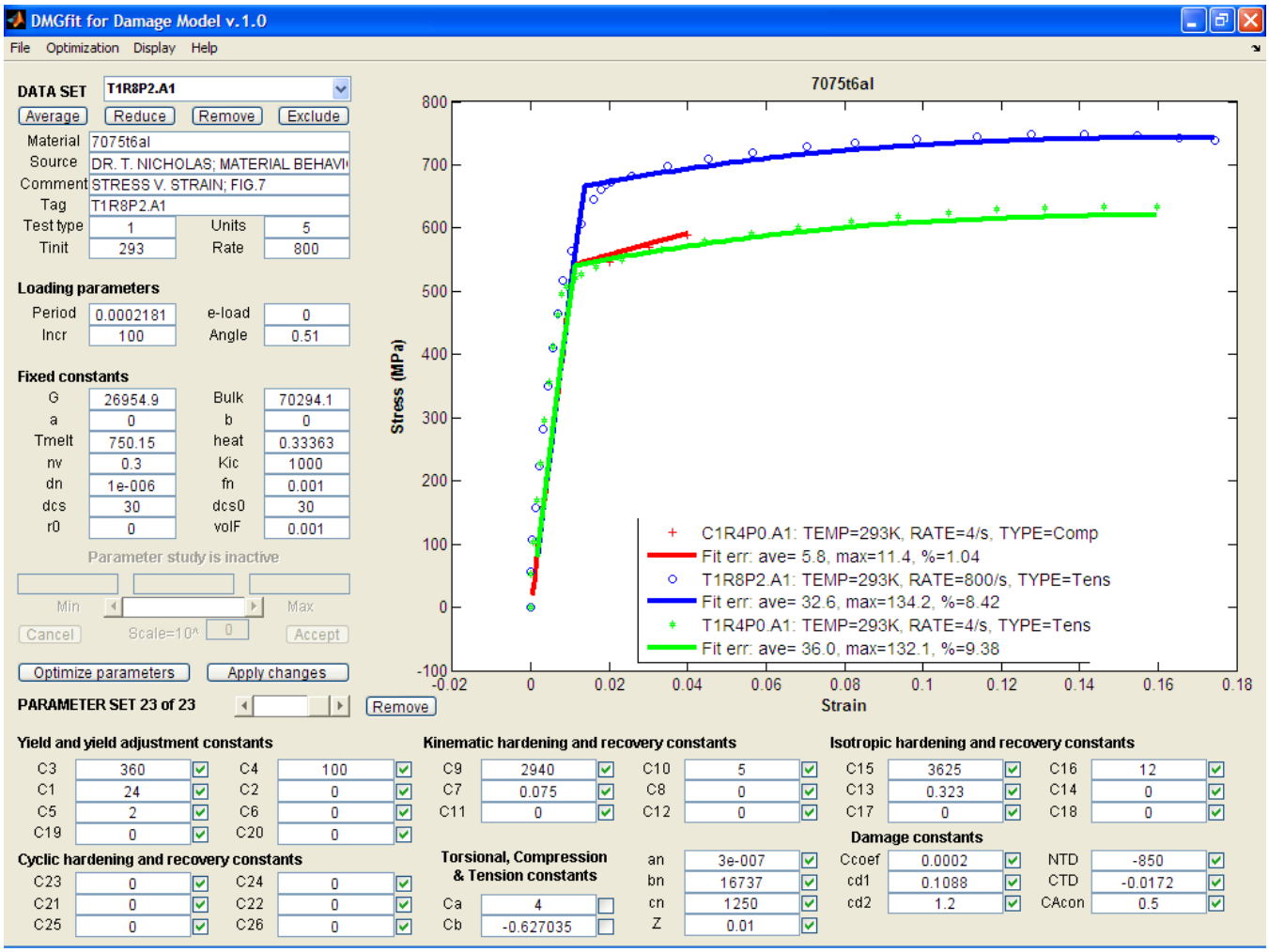

B16. Al 7075-T6 alloy: model correlation with different strain rates

References:

1. Holt, D.L., Babcock, S.G. Green, S.J. and Maiden, C.J., The Strain Rate Dependence of the Flow Stress in Some Aluminum Alloys, General Motors Research Laboratories, TR66-75, 1996.

2. Nicholas, T., Material behavior at high strain rates, Report AFWAL-TR-80-4053, USAF Wright Aeronautical Laboratories, Wright-Patterson Air Force Base, OH, USA, 1980.

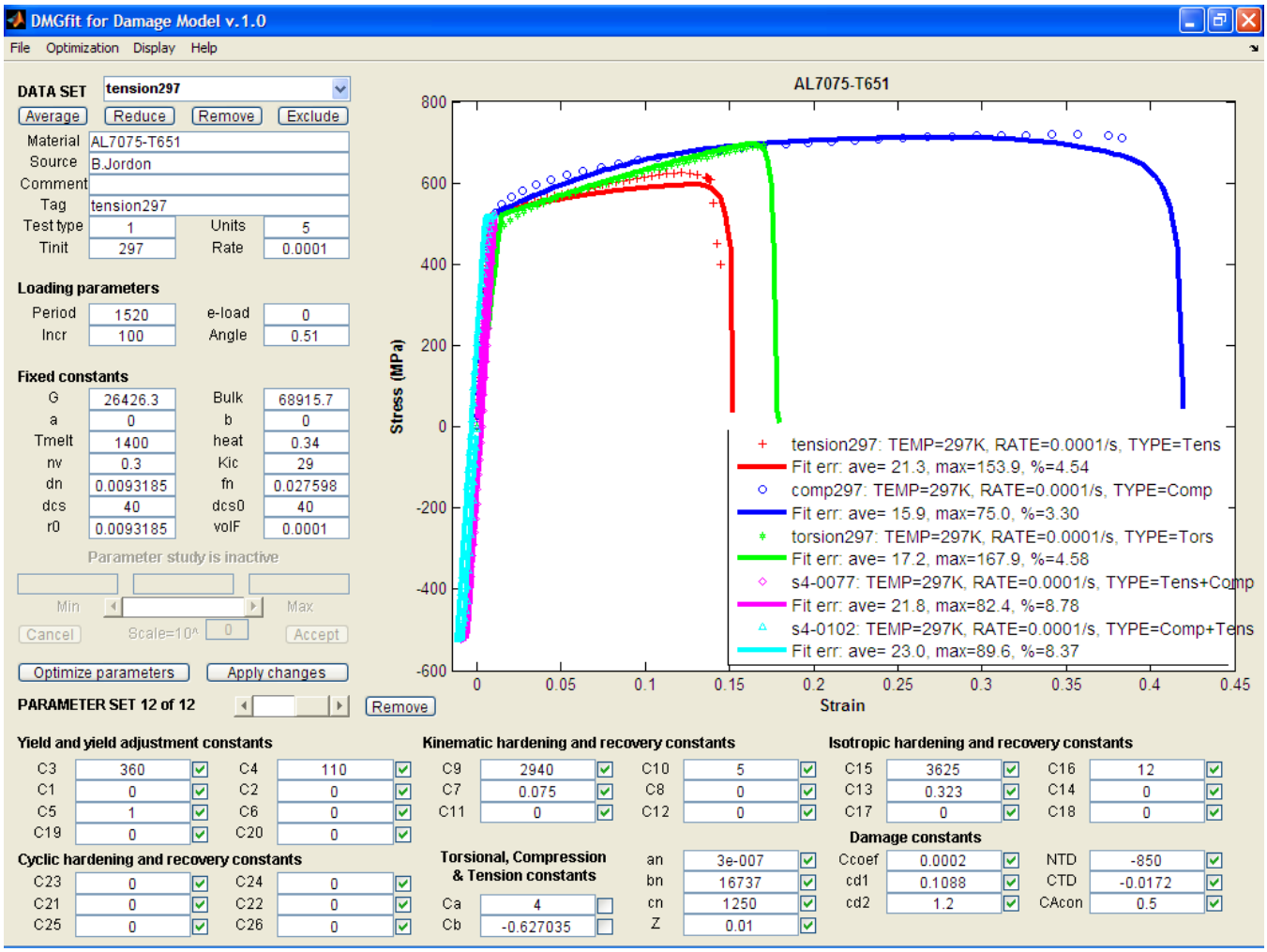

B17-a. Al 7075-T651 alloy: damage model correlation

Reference: Jordon, J.B., Horstemeyer, M.F., Solanki, K., Xue, Y., "Damage and stress state influence on the Bauschinger effect in aluminum alloys", *Mechanics of Material*, Vol. 39, pp. 920-931, 2007.

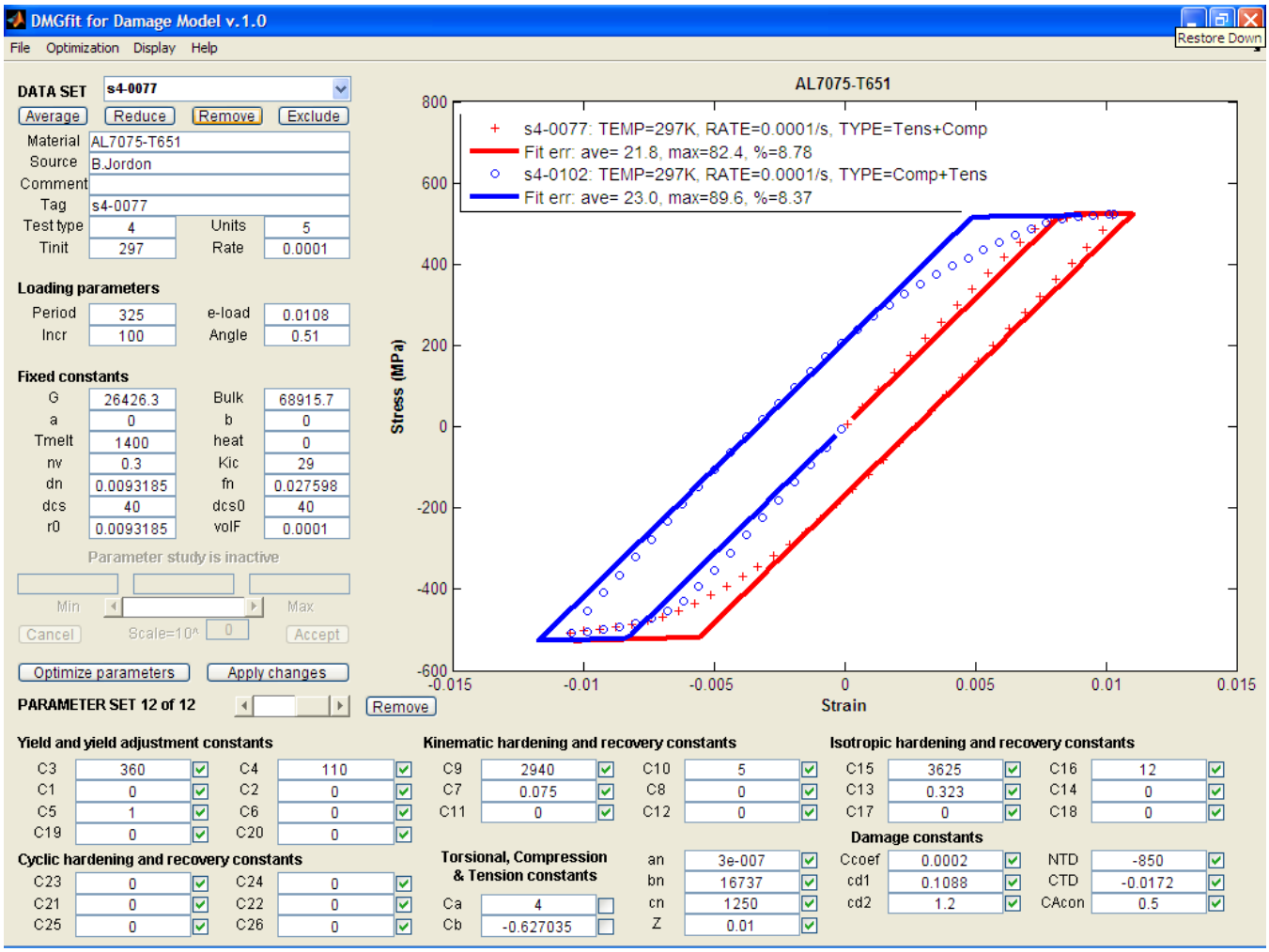

B17-b. Al 7075-T651 alloy: model correlation showing the Bauschinger effect

Reference: Jordon, J.B., Horstemeyer, M.F., Solanki, K., Xue, Y., “Damage and stress state influence on the Bauschinger effect in aluminum alloys”, *Mechanics of Material*, Vol. 39, pp. 920-931, 2007.

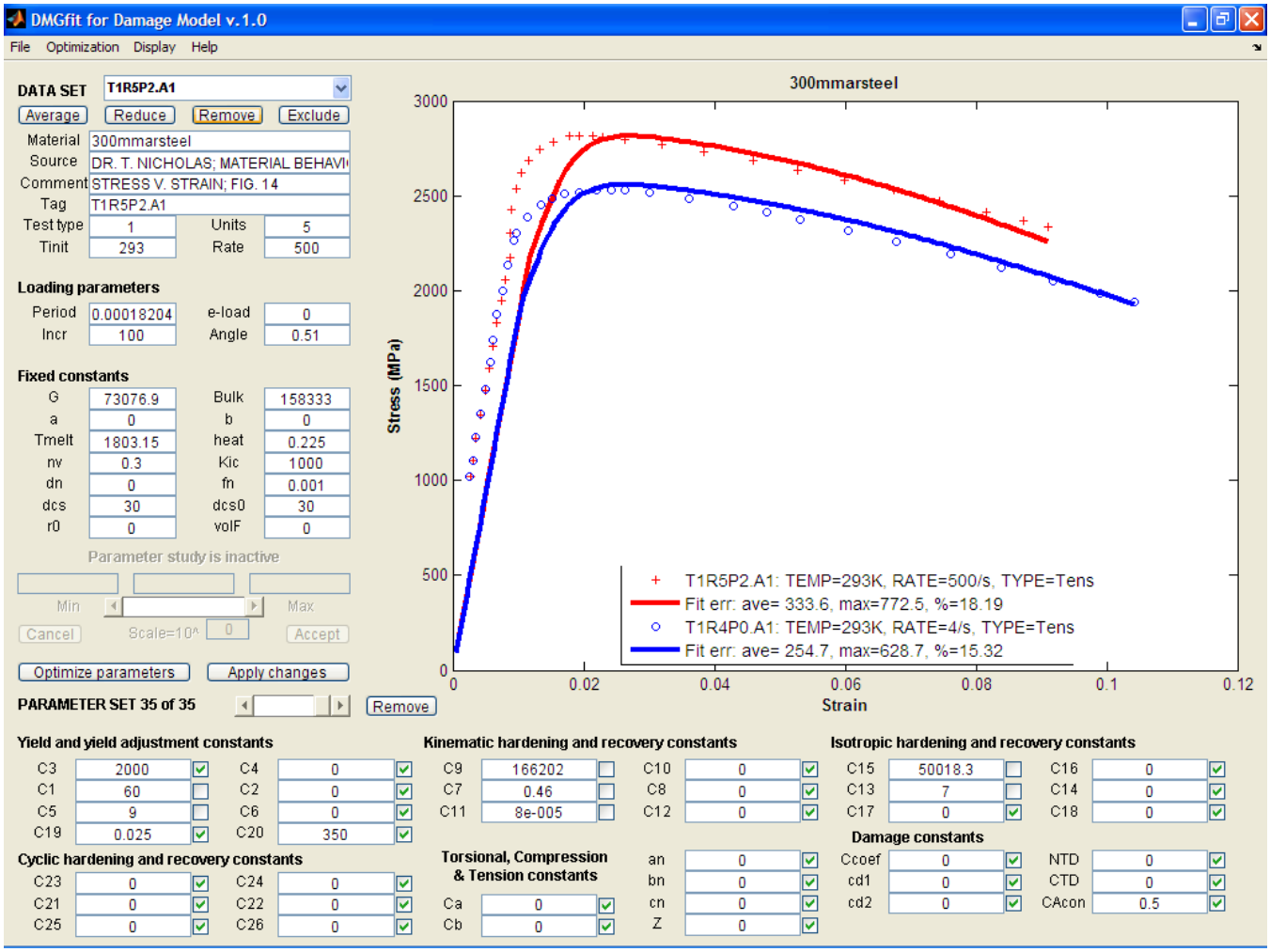

B18. 300 Maraging steel alloy: model correlation with two strain rates

Reference: Nicholas, T., Material behavior at high strain rates, Report AFWAL-TR-80-4053, USAF Wright Aeronautical Laboratories, Wright-Patterson Air Force Base, OH, USA, 1980.

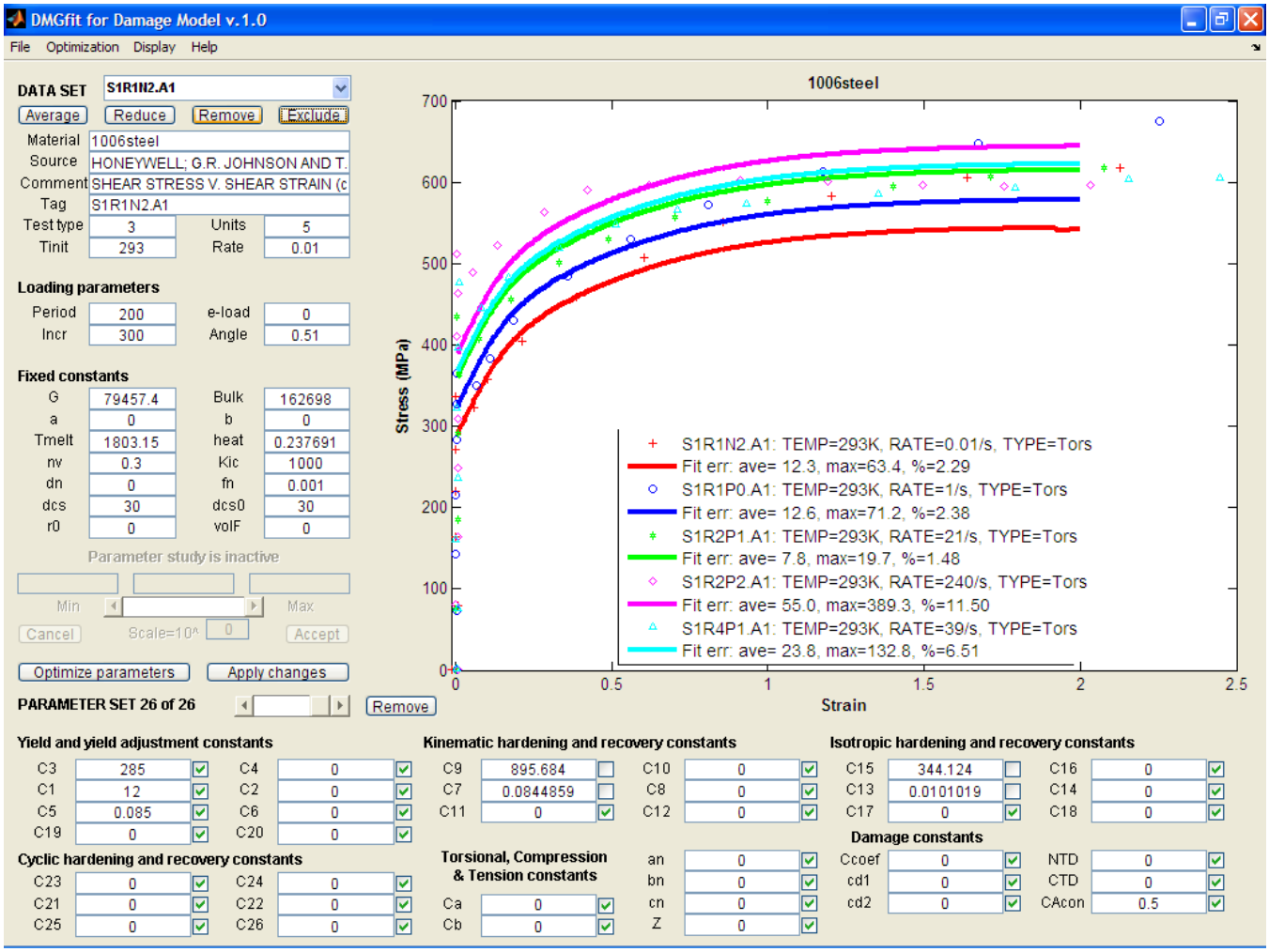

B19. 1006 steel alloy: model correlation at different strain rates

Reference: Johnson, G.R. and Holmquist, T.J., Test data and computational strength and fracture model constants for 23 materials subjected to large strains, high strain rates, and high temperatures, LA-11463-MS, Los Alamos National Laboratory, 1989.

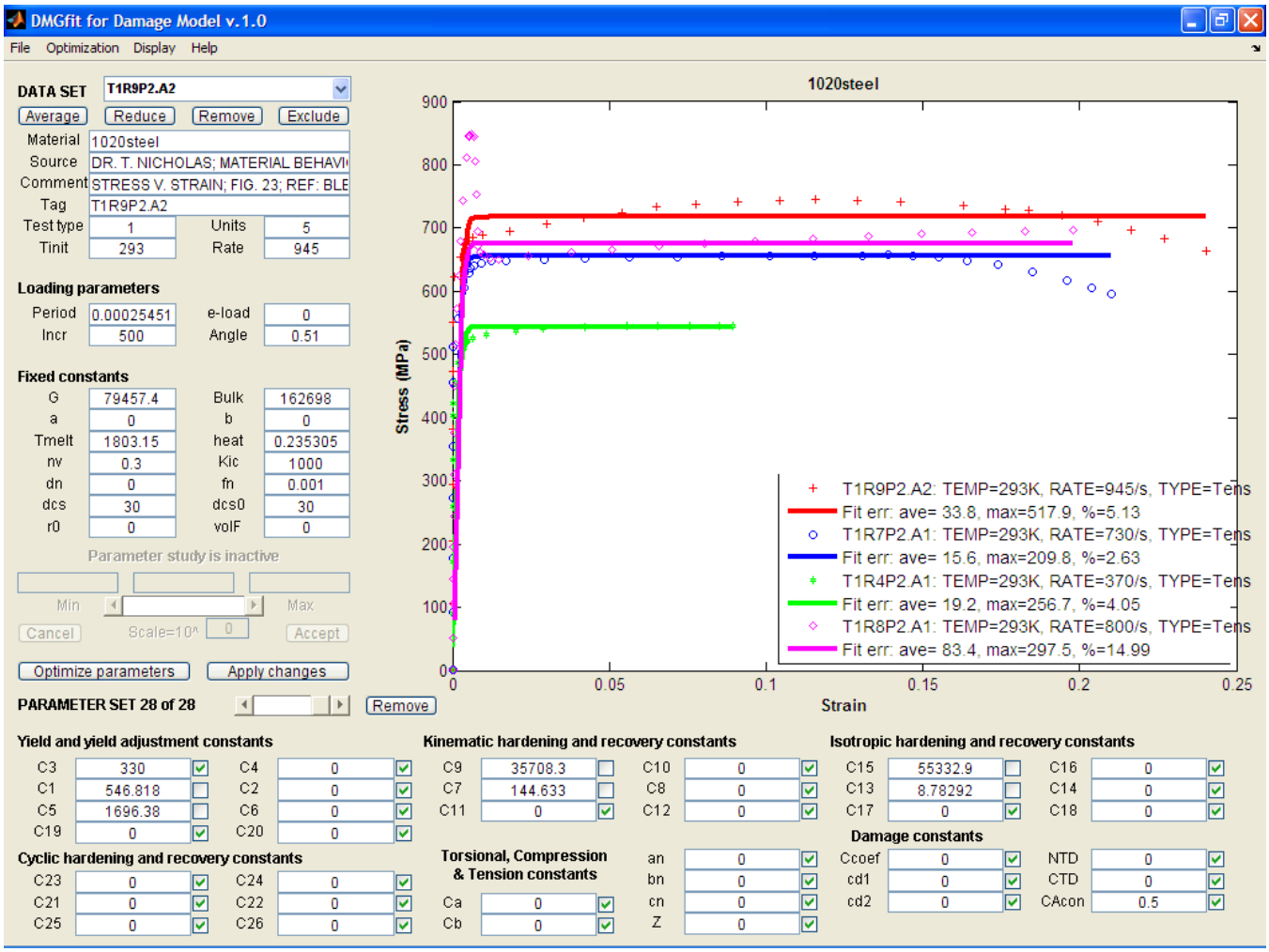

B20. 1020 steel alloy: model correlation with different strain rates.

References:

1. Nicholas, T., Material behavior at high strain rates, Report AFWAL-TR-80-4053, USAF Wright Aeronautical Laboratories, Wright-Patterson Air Force Base, OH, USA, 1980.

2. Bless, UDRI, 1984.

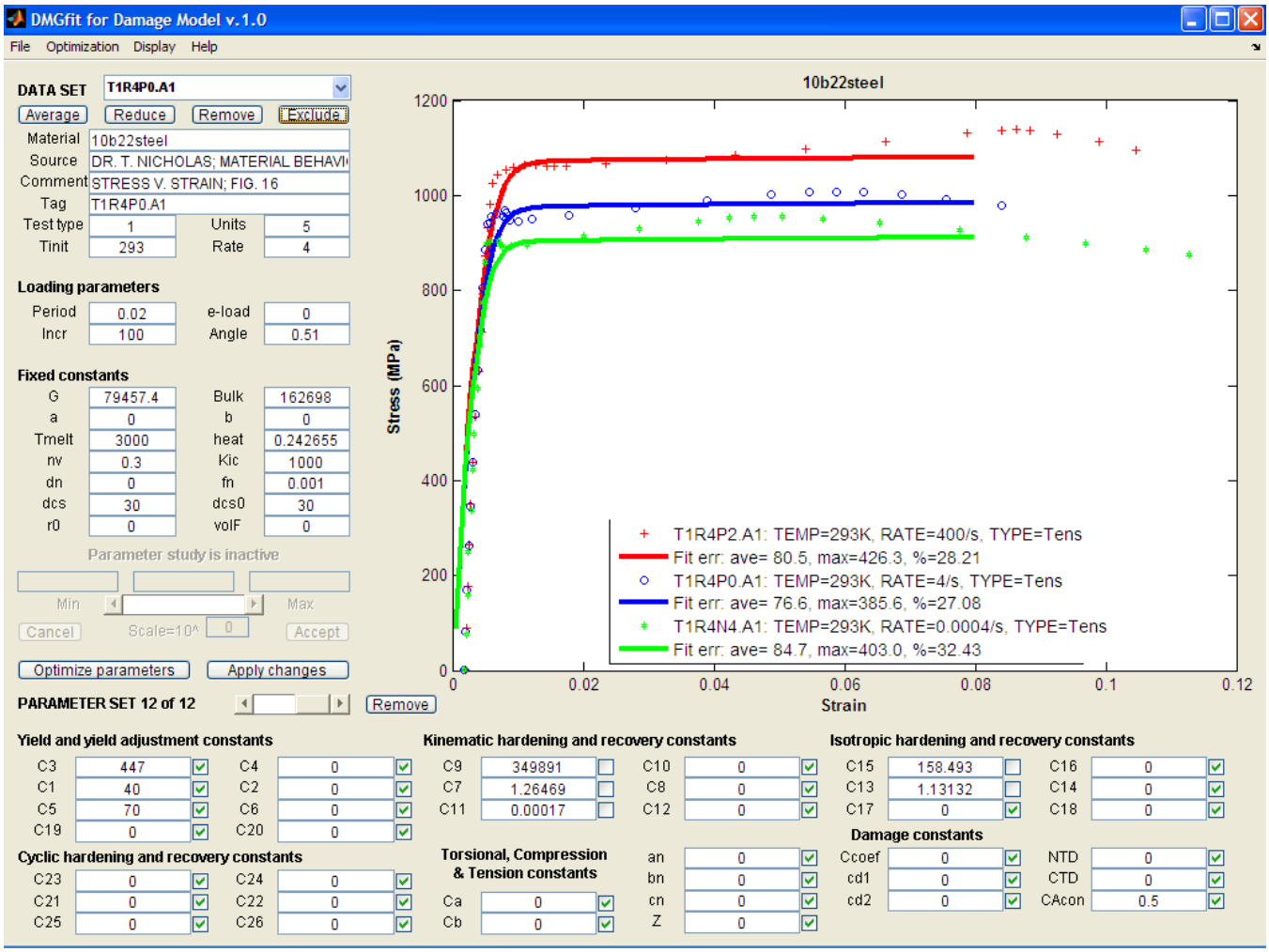

B21. 10b22 steel alloy: model correlation with different strain rates.

Reference: Nicholas, T., Material behavior at high strain rates, Report AFWAL-TR-80-4053, USAF Wright Aeronautical Laboratories, Wright-Patterson Air Force Base, OH, USA, 1980.

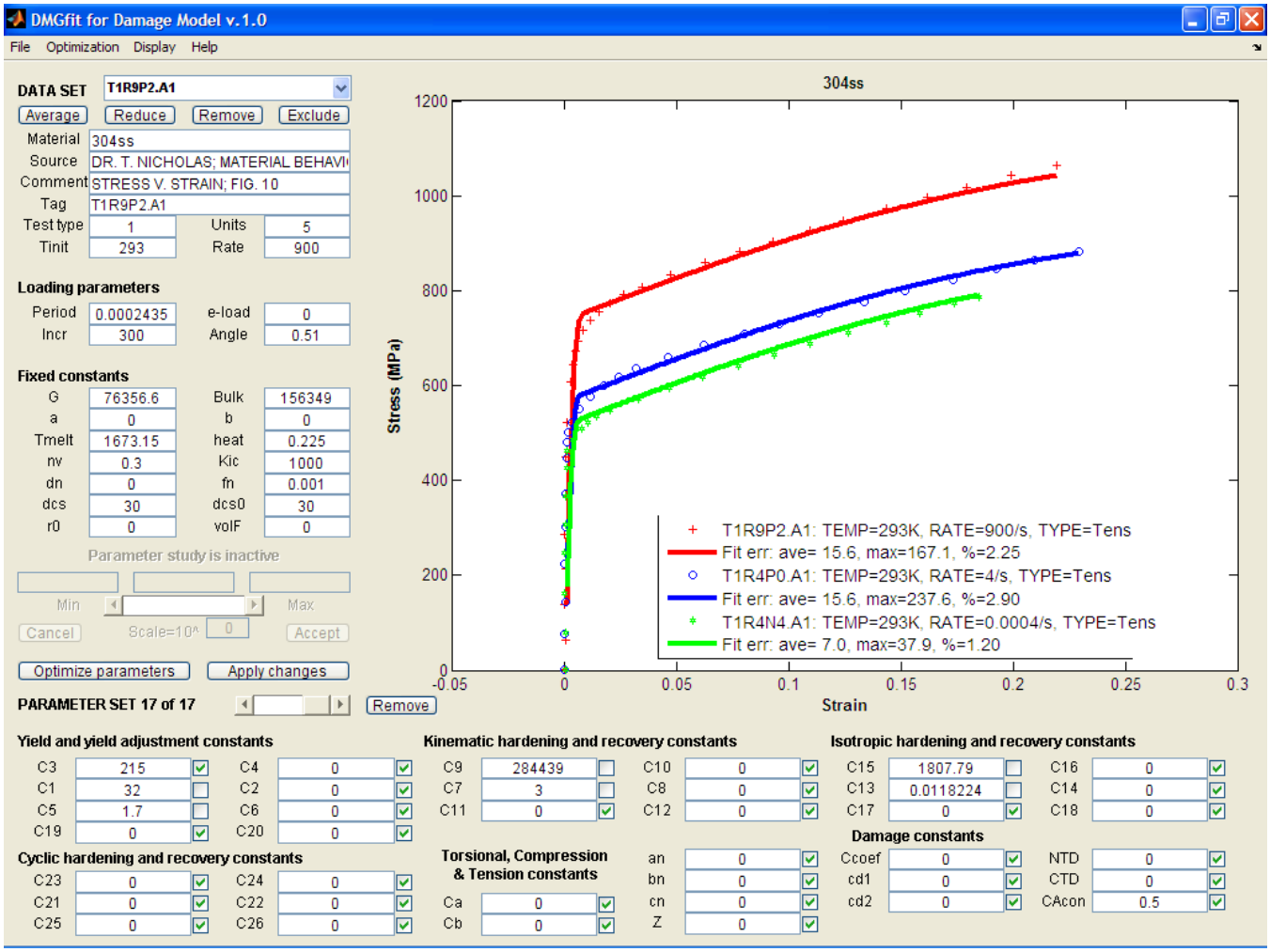

B22. 304L SS alloy: model correlation with different temperatures and strain rates

References:

1. Department of Defense. Aerospace Structural Metals Handbook, Volume 1. West Lafayette: CINDAS/Purdue, 1993.

2. Horstemeyer, M.F., Matalanis, M.M., Sieber, A.M., and Botos, M.L., "Micromechanical Finite Element Calculations of Temperature and Void Configuration Effects on Void Growth and Coalescence," Int J. Plasticity, Vol. 16, 2000.

3. Lu, W. Y., Horstemeyer, M. F., Korellis, J., Grishibar, R., and Mosher, D., “High Temperature Effects in 304L Stainless Steel Notch Tests,” *Theoretical and Applied Fracture Mechanics*, Vol. 30, pp. 139-152, 1998.

4. Nicholas, T., Material behavior at high strain rates, Report AFWAL-TR-80-4053, USAF Wright Aeronautical Laboratories, Wright-Patterson Air Force Base, OH, USA, 1980.

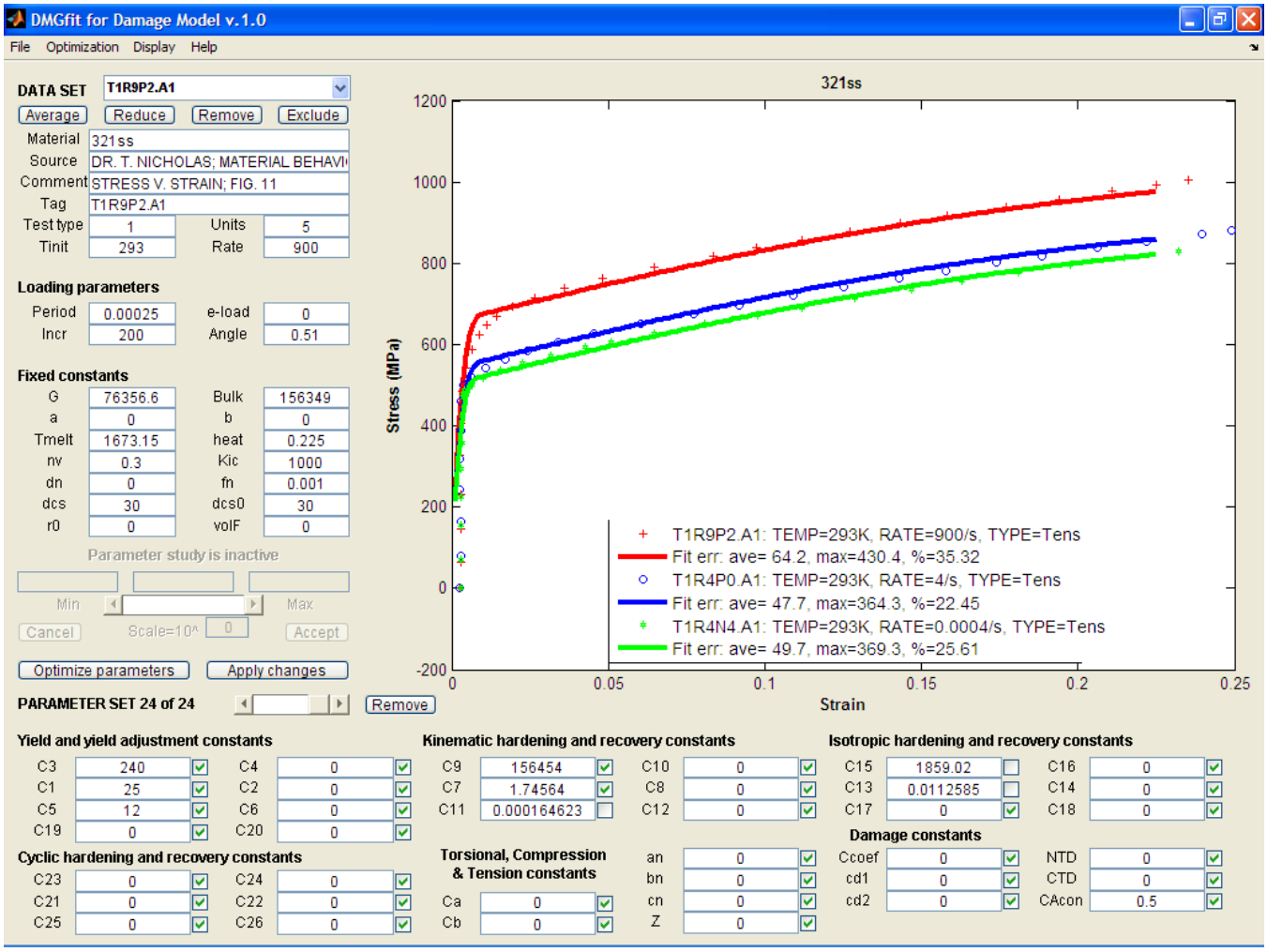

B23. 321 SS alloy: model correlation with different strain rates.

Reference: Nicholas, T., Material behavior at high strain rates, Report AFWAL-TR-80-4053, USAF Wright Aeronautical Laboratories, Wright-Patterson Air Force Base, OH, USA, 1980.

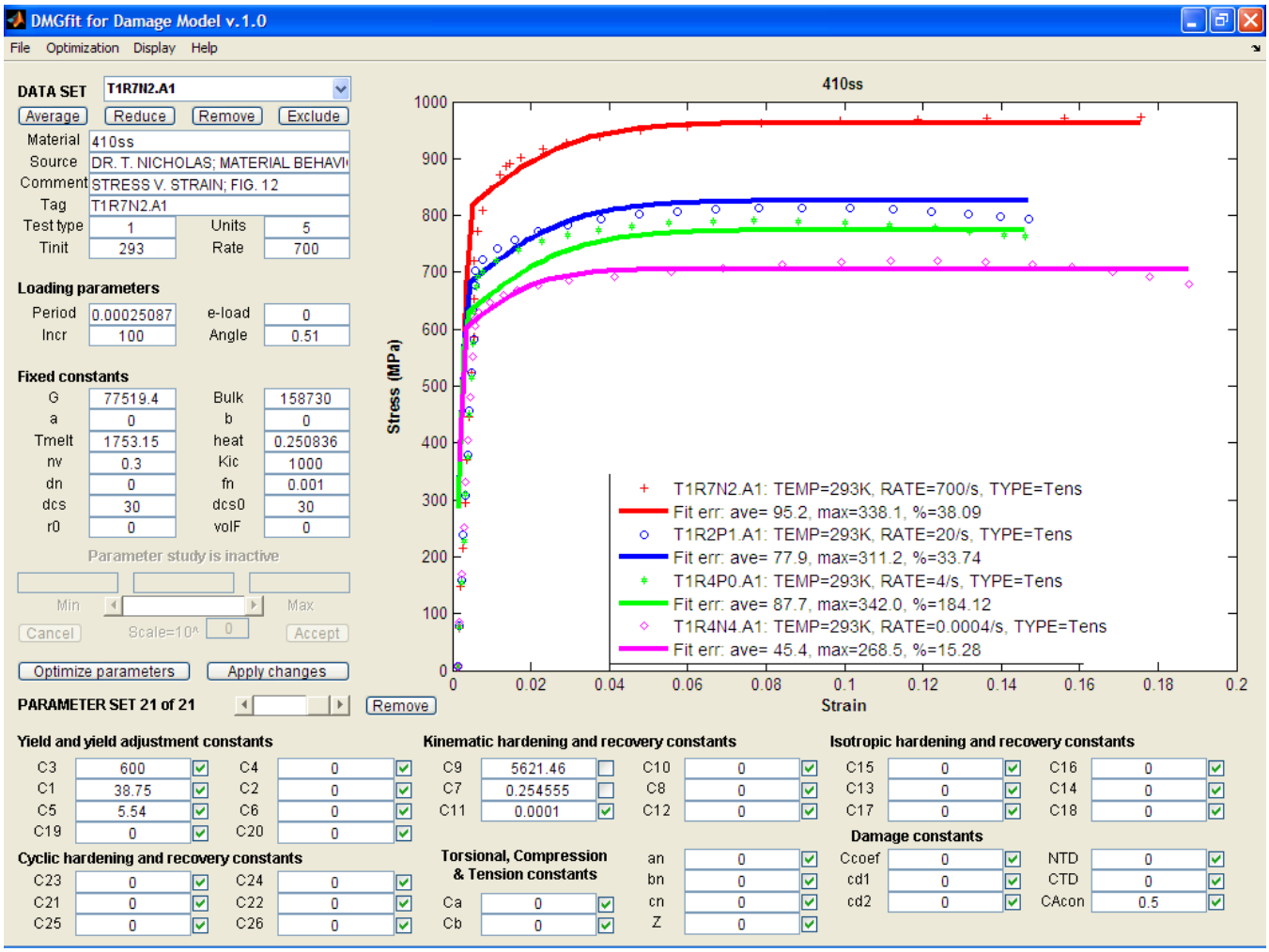

B24. 410 SS alloy: model correlation with different strain rates

Reference: Nicholas, T., Material behavior at high strain rates, Report AFWAL-TR-80-4053, USAF Wright Aeronautical Laboratories, Wright-Patterson Air Force Base, OH, USA, 1980.

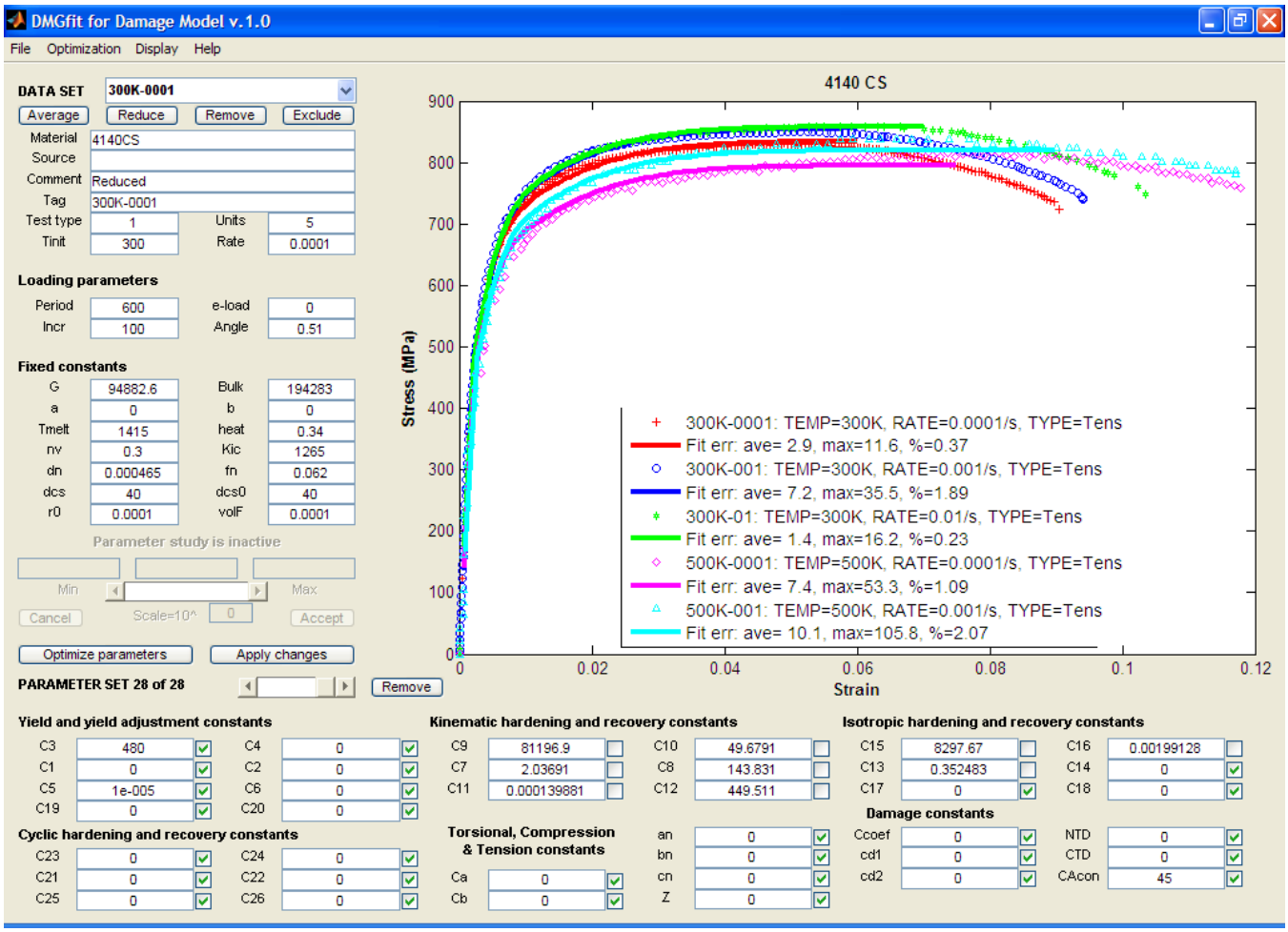

B25. 4140 commercial steel alloy model correlation with different strain rates and temperatures

Reference: Gomez, R.A., Monotonic Plasticity-Damage and Fatigue Life Model Correlations on AISI 4140 Steel, MSc. Thesis, Dept. of Mechanical Engineering, Mississippi State University, 2007.

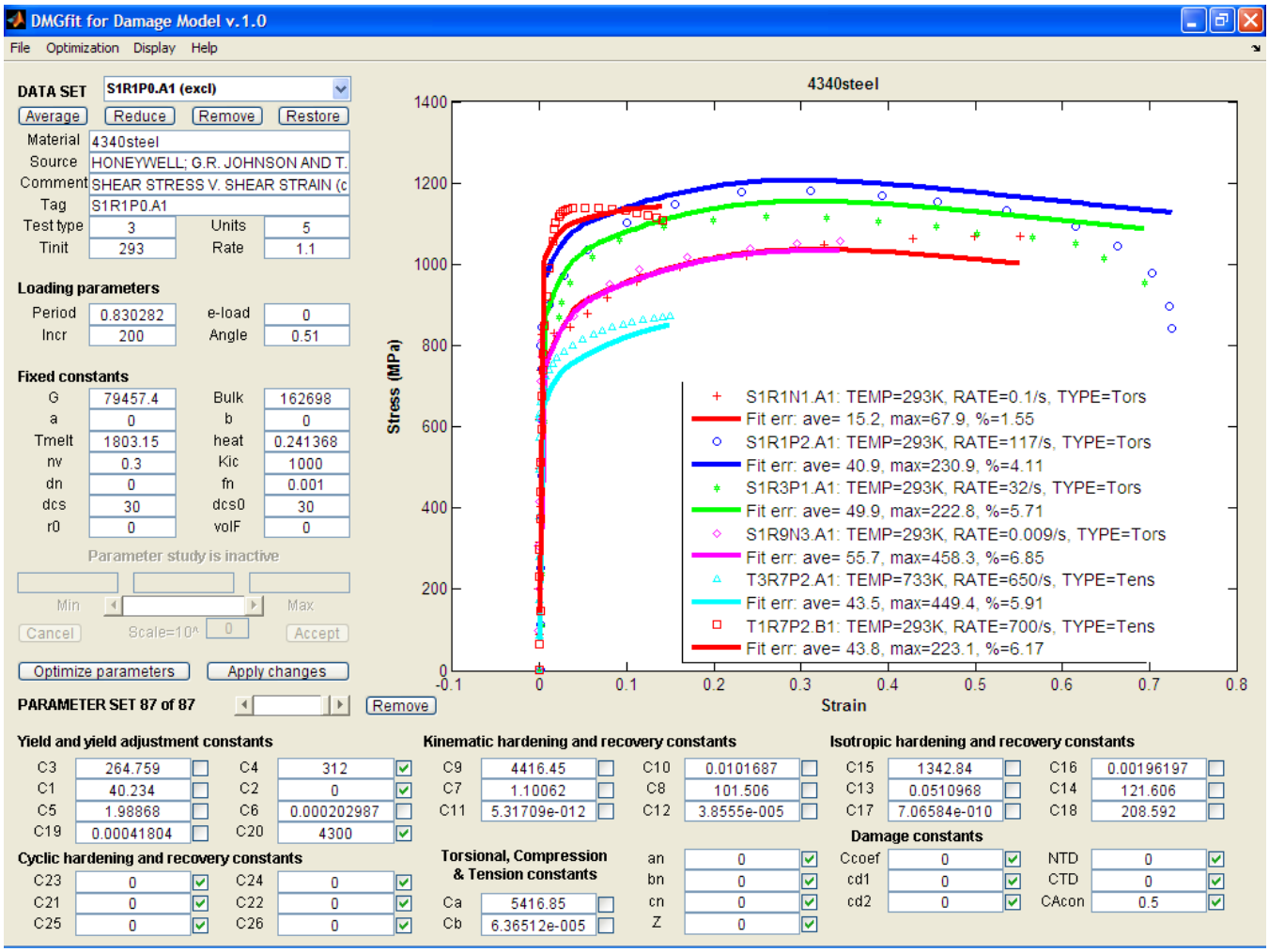

B26. 4340 steel alloy: model correlation with different strain rates

References:

1. Johnson, G.R. and Holmquist, T.J., Test data and computational strength and fracture model constants for 23 materials subjected to large strains, high strain rates, and high temperatures, LA-11463-MS, Los Alamos National Laboratory, 1989.

2. Nicholas, T., Material behavior at high strain rates, Report AFWAL-TR-80-4053, USAF Wright Aeronautical Laboratories, Wright-Patterson Air Force Base, OH, USA, 1980.

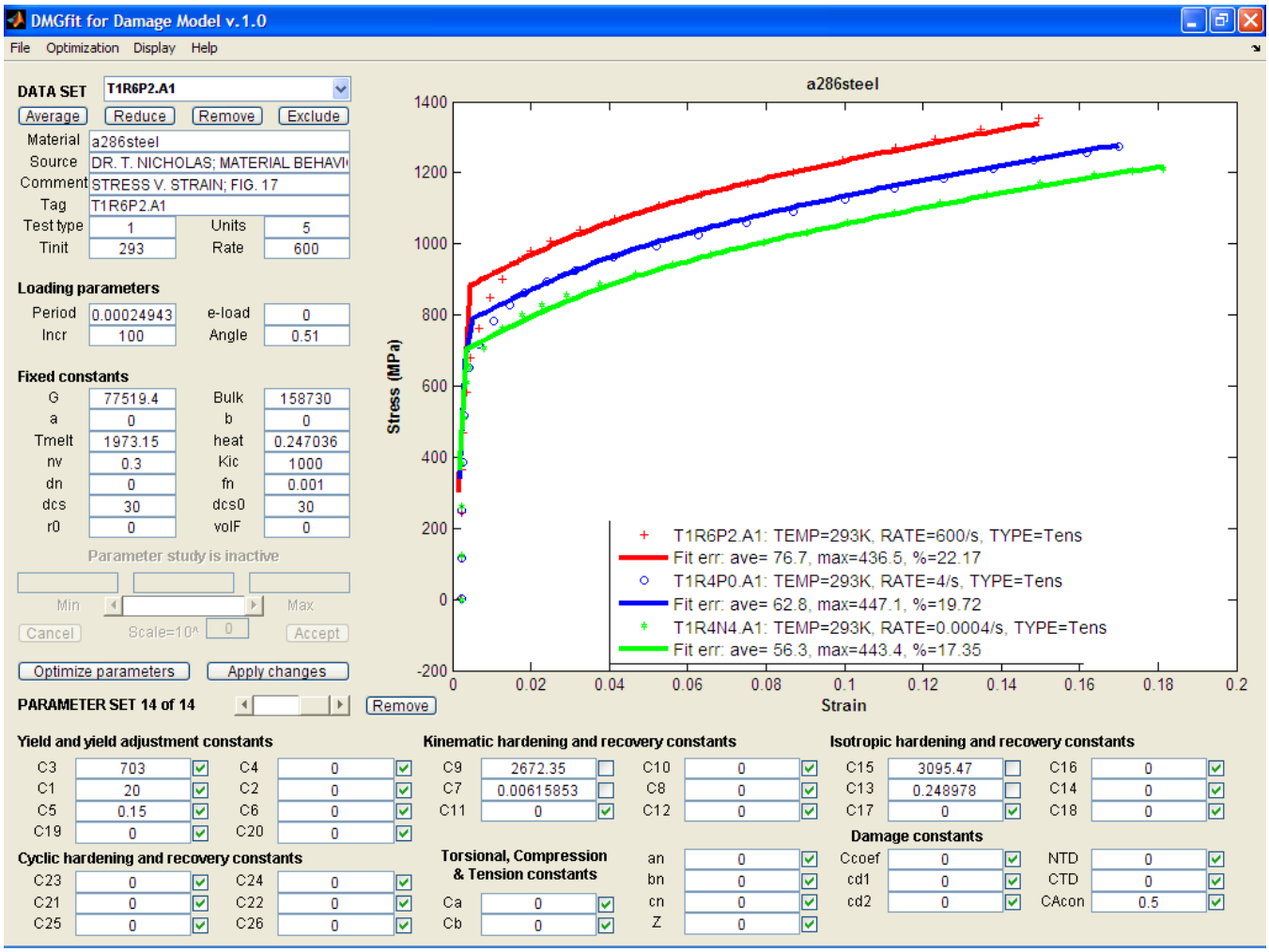

B27. A286 steel alloy: model correlation with different strain rates

Reference: Nicholas, T., Material behavior at high strain rates, Report AFWAL-TR-80-4053, USAF Wright Aeronautical Laboratories, Wright-Patterson Air Force Base, OH, USA, 1980.

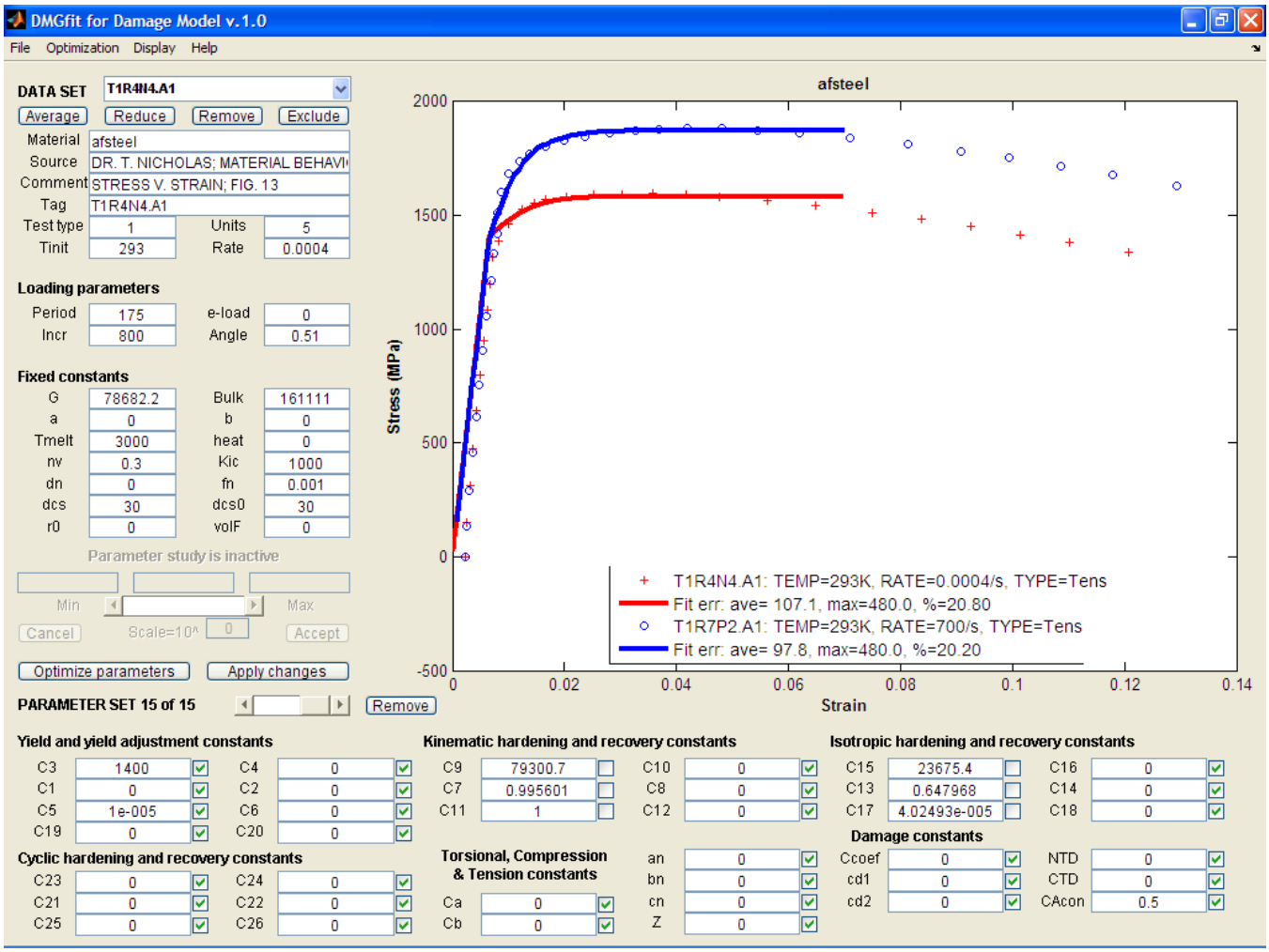

B28. AF steel alloy: model correlation with different strain rates

Reference: Nicholas, T., Material behavior at high strain rates, Report AFWAL-TR-80-4053, USAF Wright Aeronautical Laboratories, Wright-Patterson Air Force Base, OH, USA, 1980.

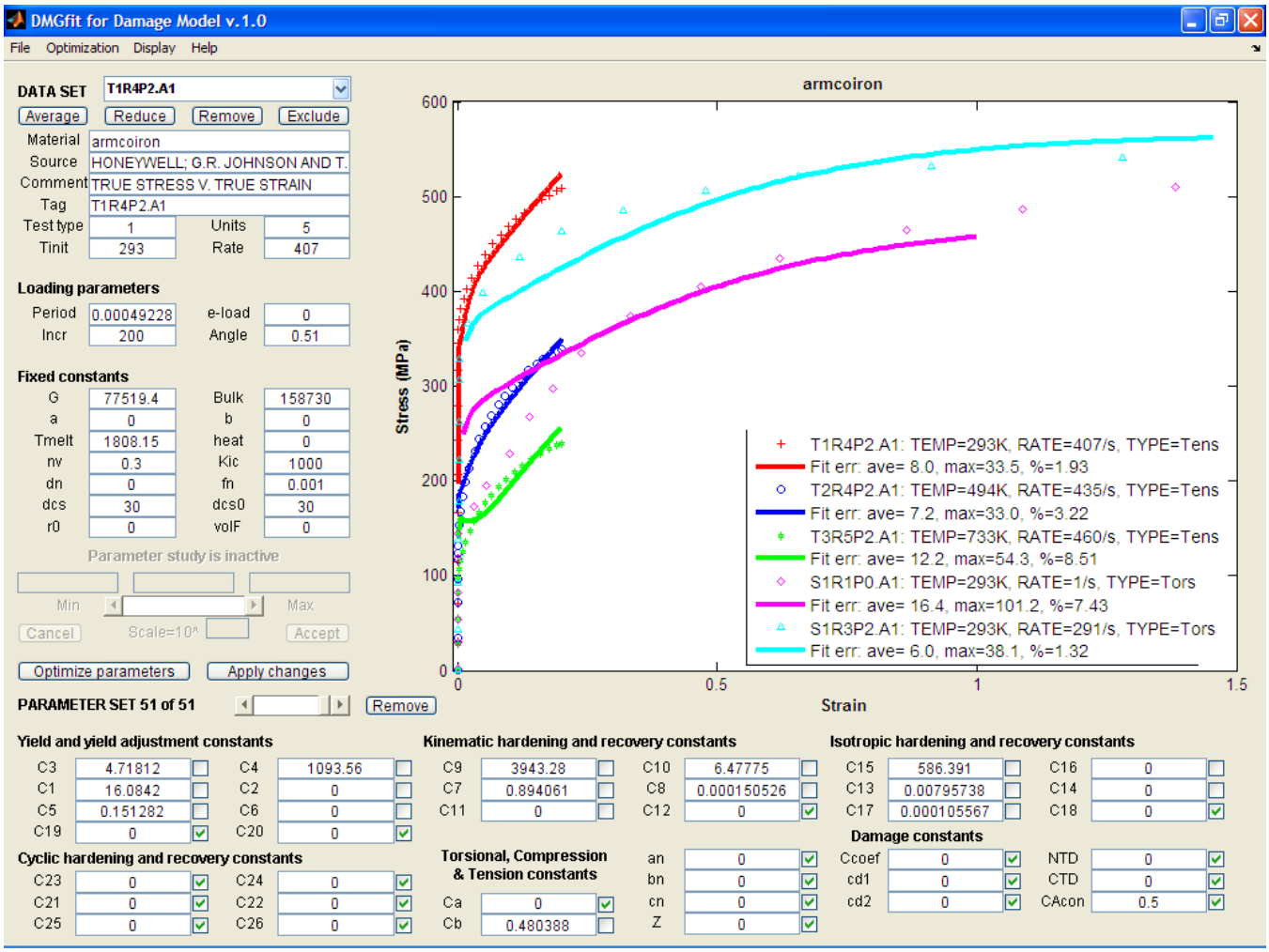

B29. Armco Iron : model correlation with different temperatures and strain rates

Reference: Johnson, G.R. and Holmquist, T.J., Test data and computational strength and fracture model constants for 23 materials subjected to large strains, high strain rates, and high temperatures, LA-11463-MS, Los Alamos National Laboratory, 1989.

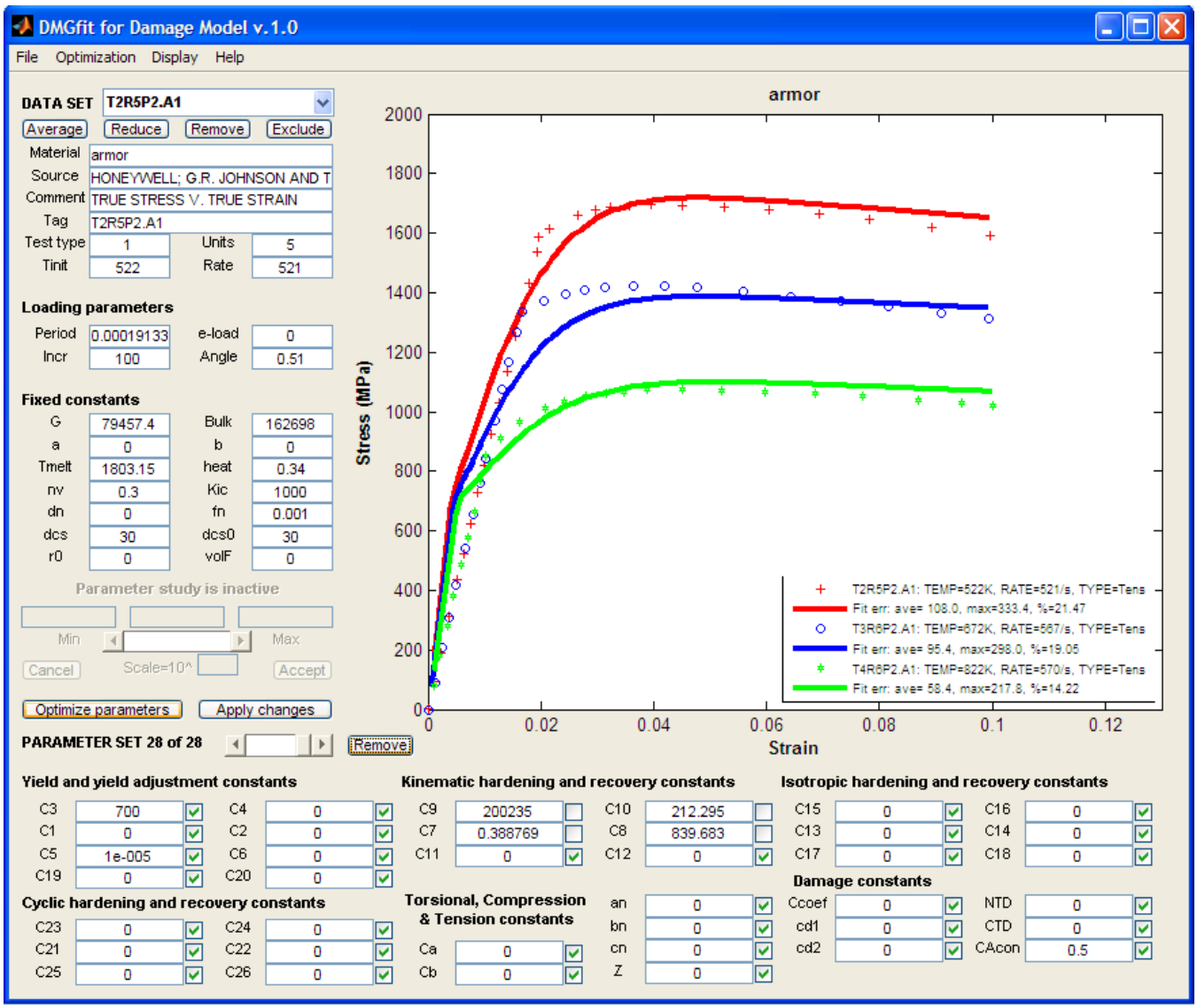

B30. Armor Steel: model correlation with different temperatures

Reference: Johnson, G.R. and Holmquist, T.J., Test data and computational strength and fracture model constants for 23 materials subjected to large strains, high strain rates, and high temperatures, LA-11463-MS, Los Alamos National Laboratory, 1989.

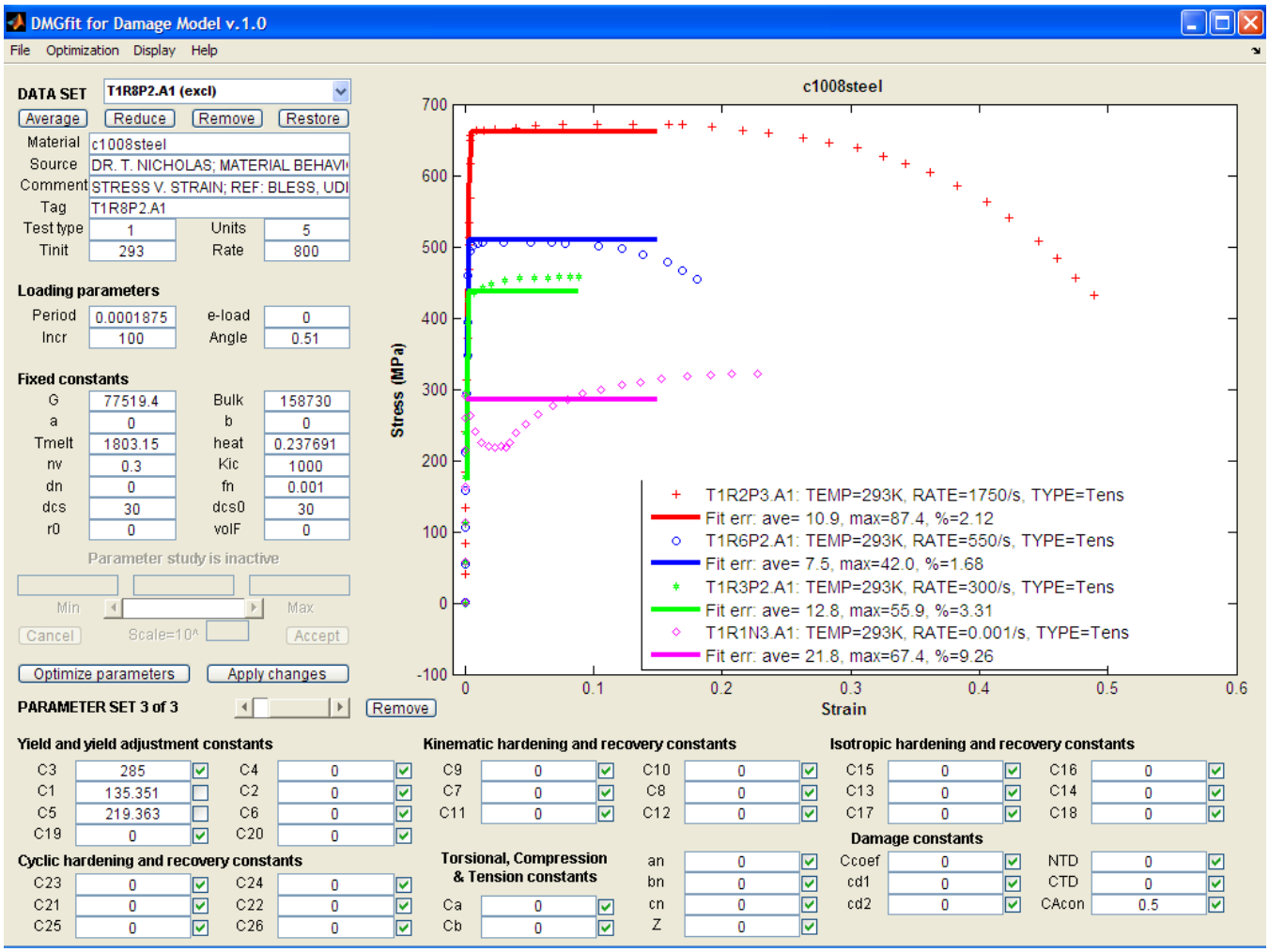

B31. C1008 Steel : model correlation with different strain rates

References:

1. Nicholas, T., Material behavior at high strain rates, Report AFWAL-TR-80-4053, USAF Wright Aeronautical Laboratories, Wright-Patterson Air Force Base, OH, USA, 1980.

2. Bless, UDRI, 1984.

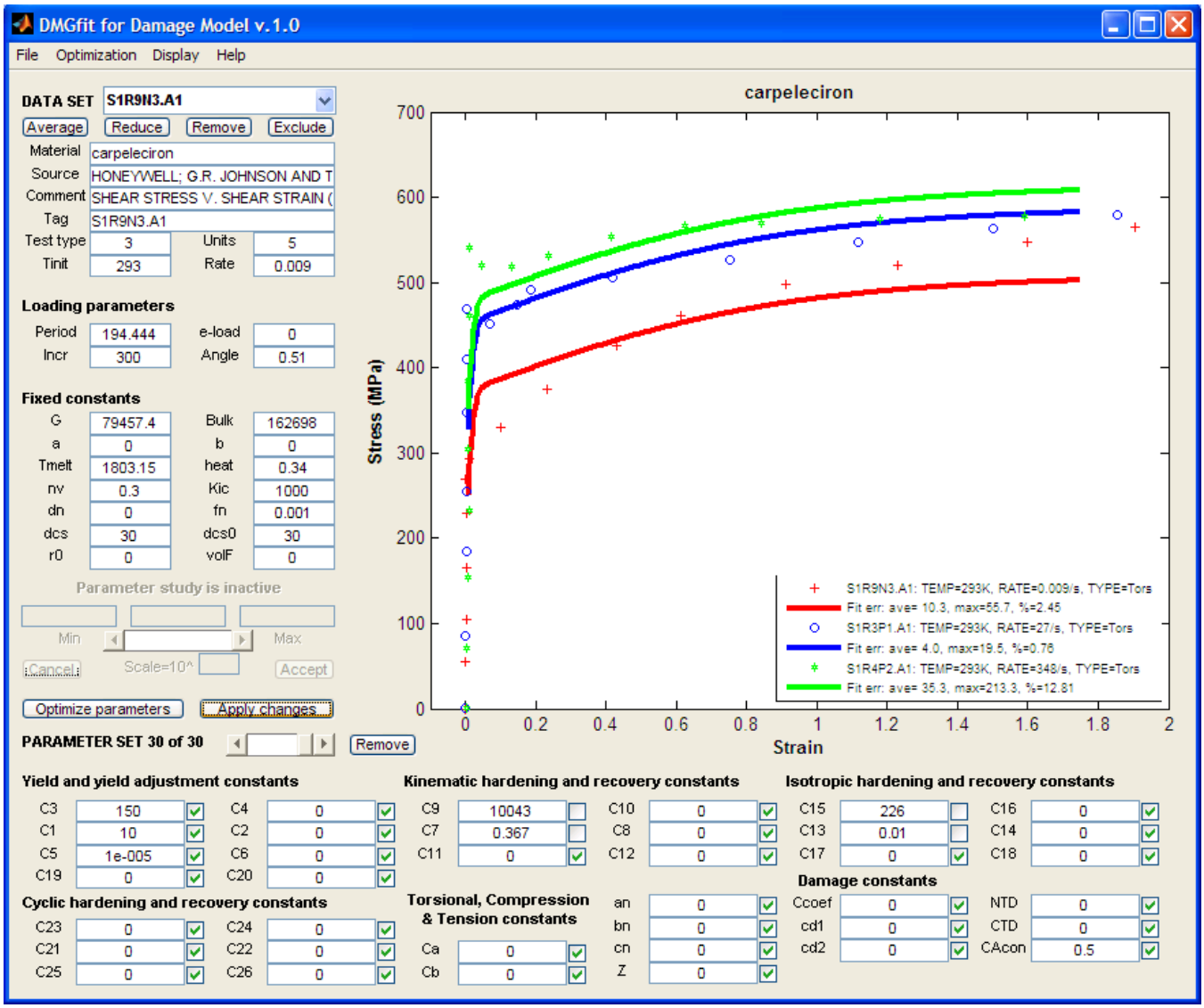

B32. Carpeleciron: model correlation with different strain rates

Reference: Johnson, G.R. and Holmquist, T.J., Test data and computational strength and fracture model constants for 23 materials subjected to large strains, high strain rates, and high temperatures, LA-11463-MS, Los Alamos National Laboratory, 1989.

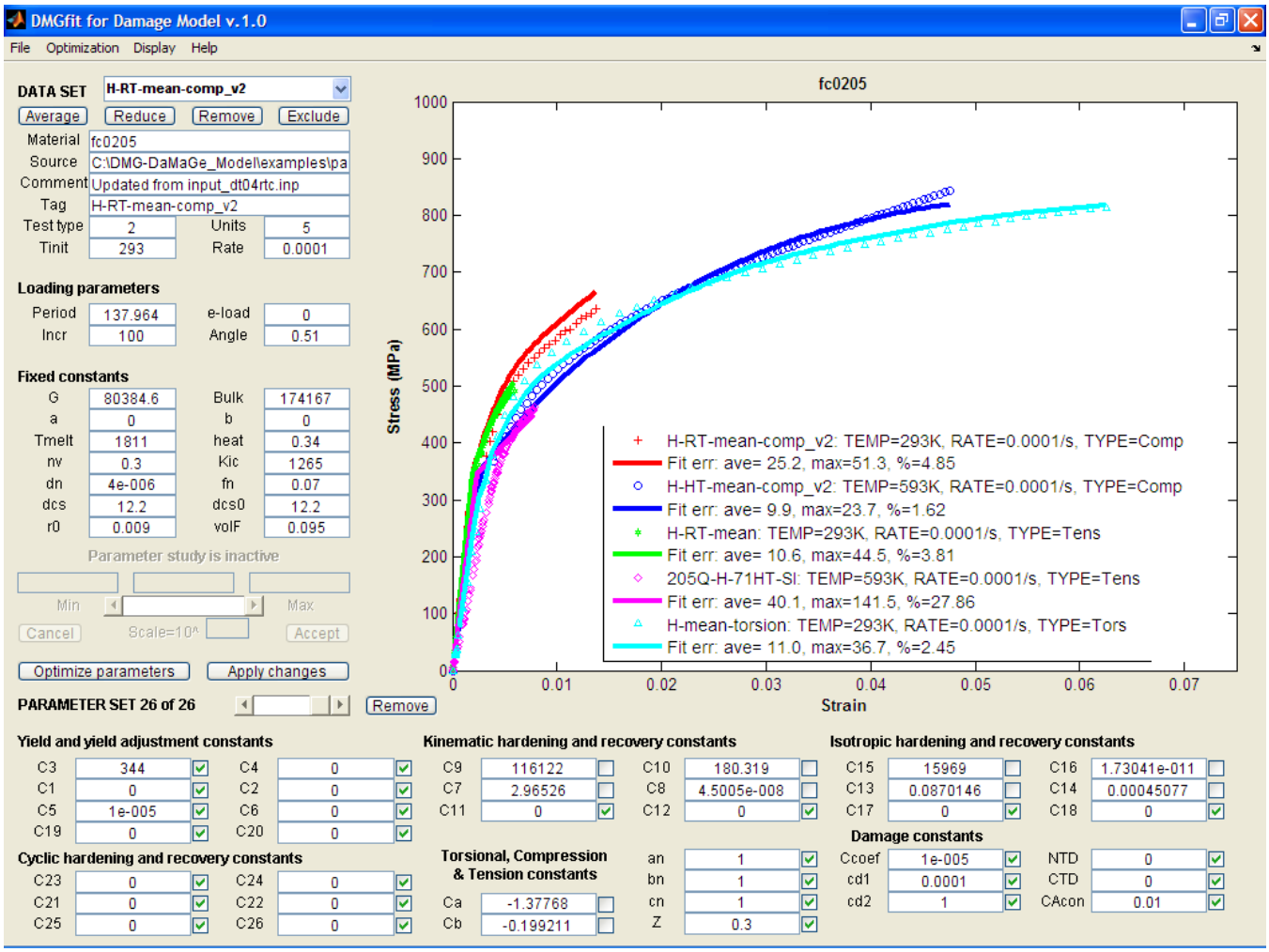

B33. FC0205 steel alloy: model correlation with different temperatures

Reference: Allison, P. G., et al., Microstructure-property relations of a powder metallurgy steel (FC-0205) under various loading conditions, (In preparation), 2009.

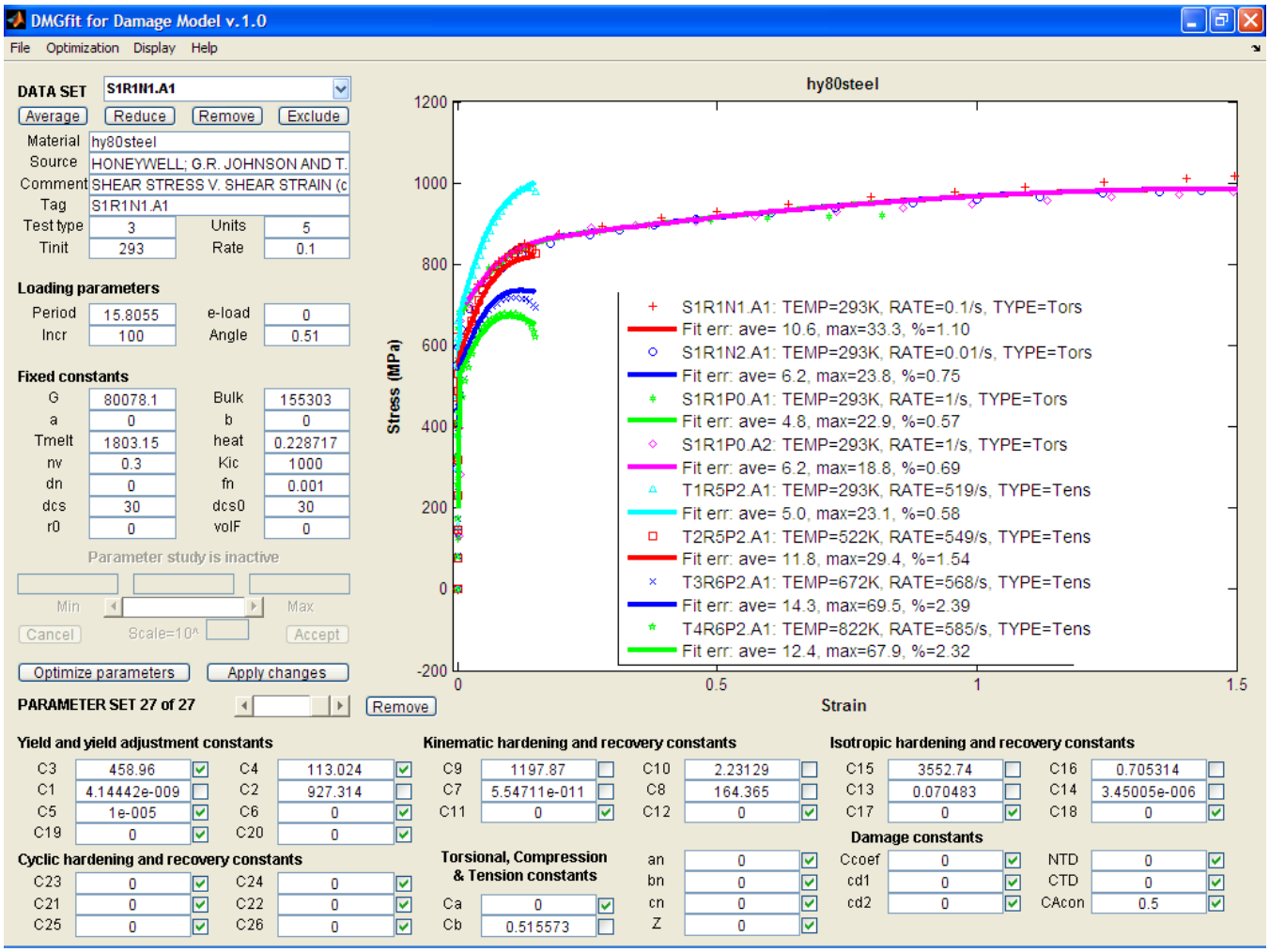

B34. HY80 steel alloy: model correlation with different temperatures and strain rates

Reference: Johnson, G.R. and Holmquist, T.J., Test data and computational strength and fracture model constants for 23 materials subjected to large strains, high strain rates, and high temperatures, LA-11463-MS, Los Alamos National Laboratory, 1989.

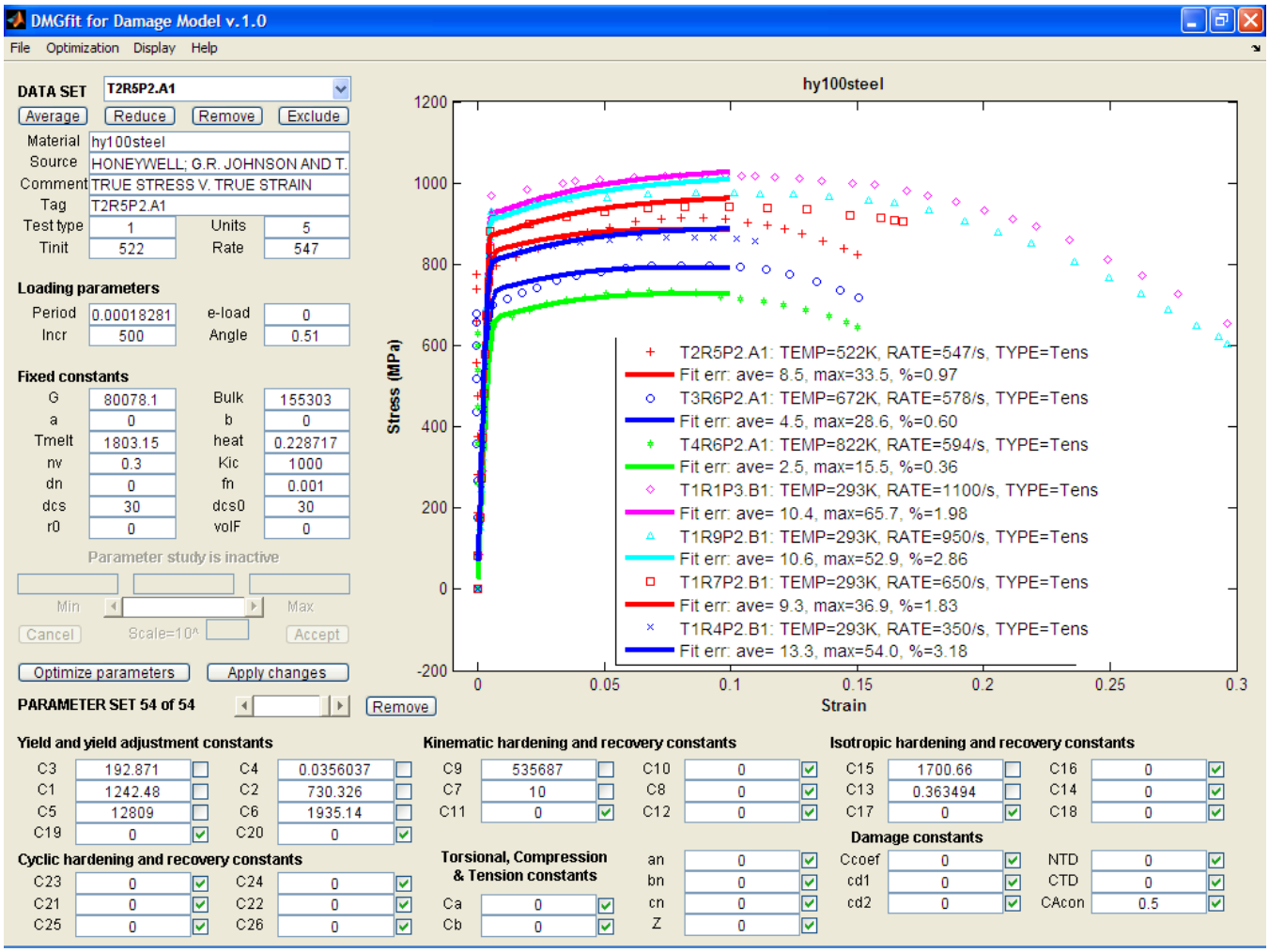

B35. HY100 steel alloy: model correlation with different temperatures and strain rates

References:

1. Johnson, G.R. and Holmquist, T.J., Test data and computational strength and fracture model constants for 23 materials subjected to large strains, high strain rates, and high temperatures, LA-11463-MS, Los Alamos National Laboratory, 1989.

2. Nicholas, T., Material behavior at high strain rates, Report AFWAL-TR-80-4053, USAF Wright Aeronautical Laboratories, Wright-Patterson Air Force Base, OH, USA, 1980.

3. Bless, UDRI, 1984.

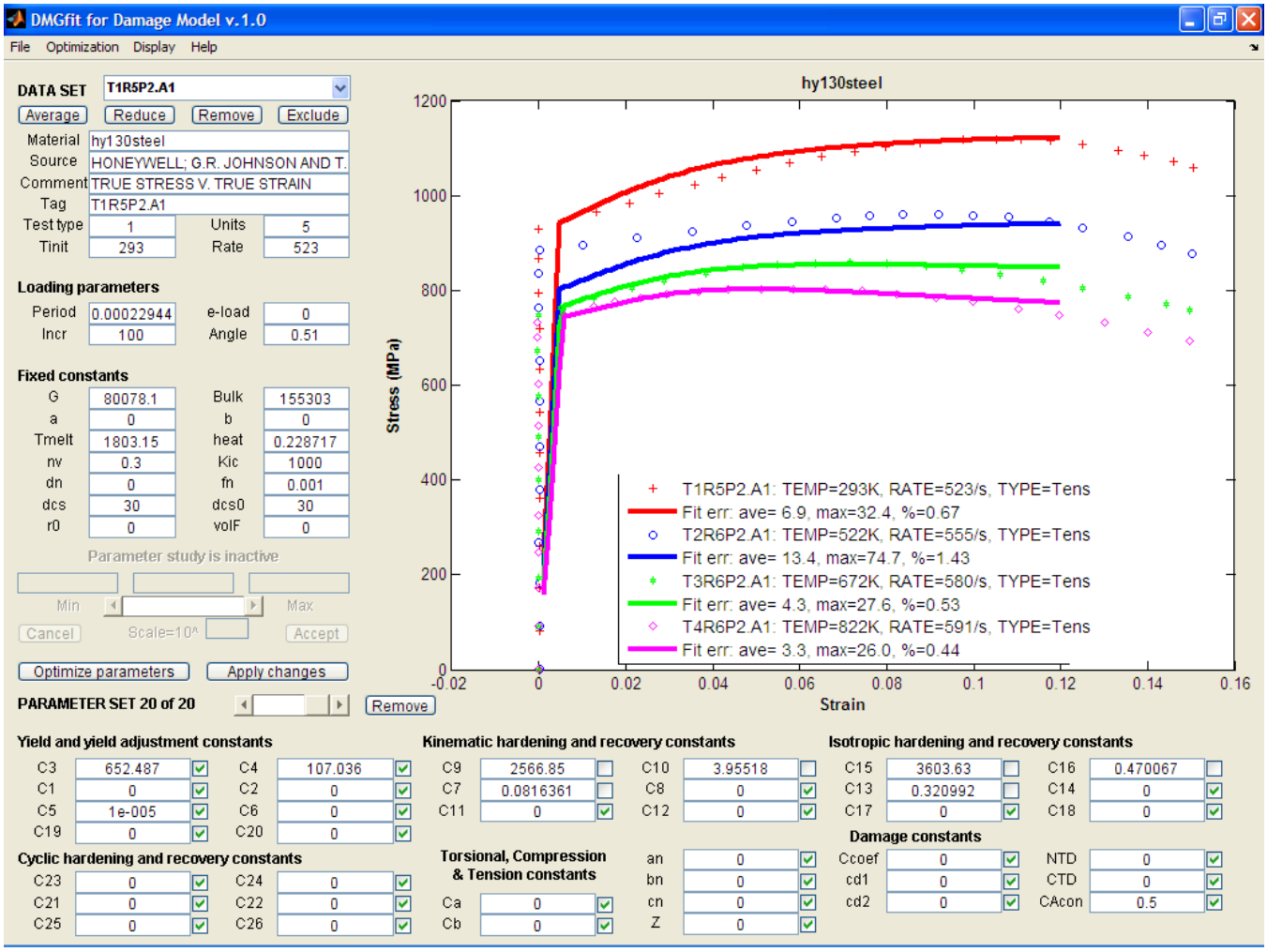

B36. HY130 steel alloy: temperature model correlation

Reference: Johnson, G.R. and Holmquist, T.J., Test data and computational strength and fracture model constants for 23 materials subjected to large strains, high strain rates, and high temperatures, LA-11463-MS, Los Alamos National Laboratory, 1989.

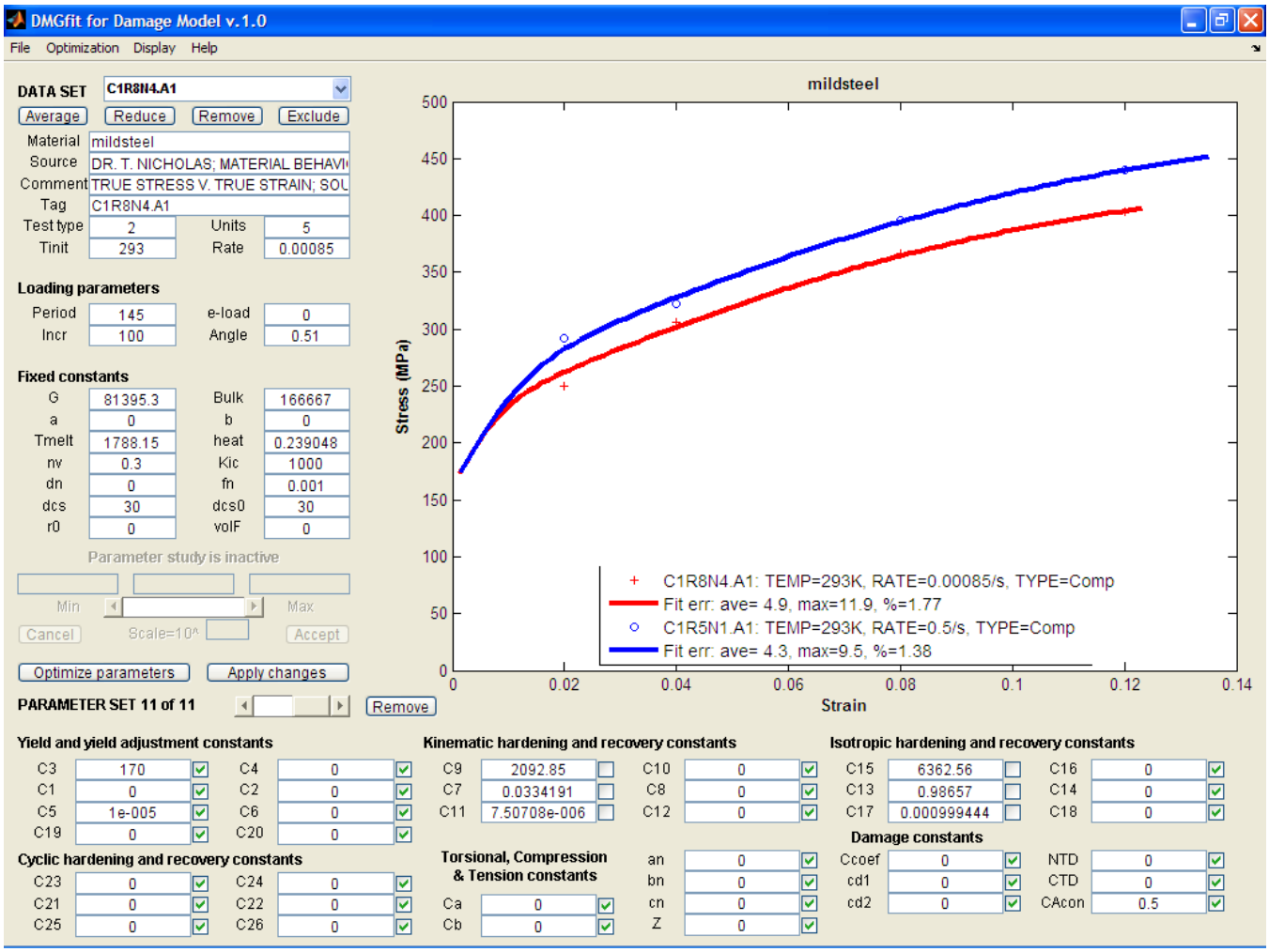

B37. Mild Steel: strain rate model correlation

References:

1. Nicholas, T., Material behavior at high strain rates, Report AFWAL-TR-80-4053, USAF Wright Aeronautical Laboratories, Wright-Patterson Air Force Base, OH, USA, 1980.

2. M.J. Manjoine.

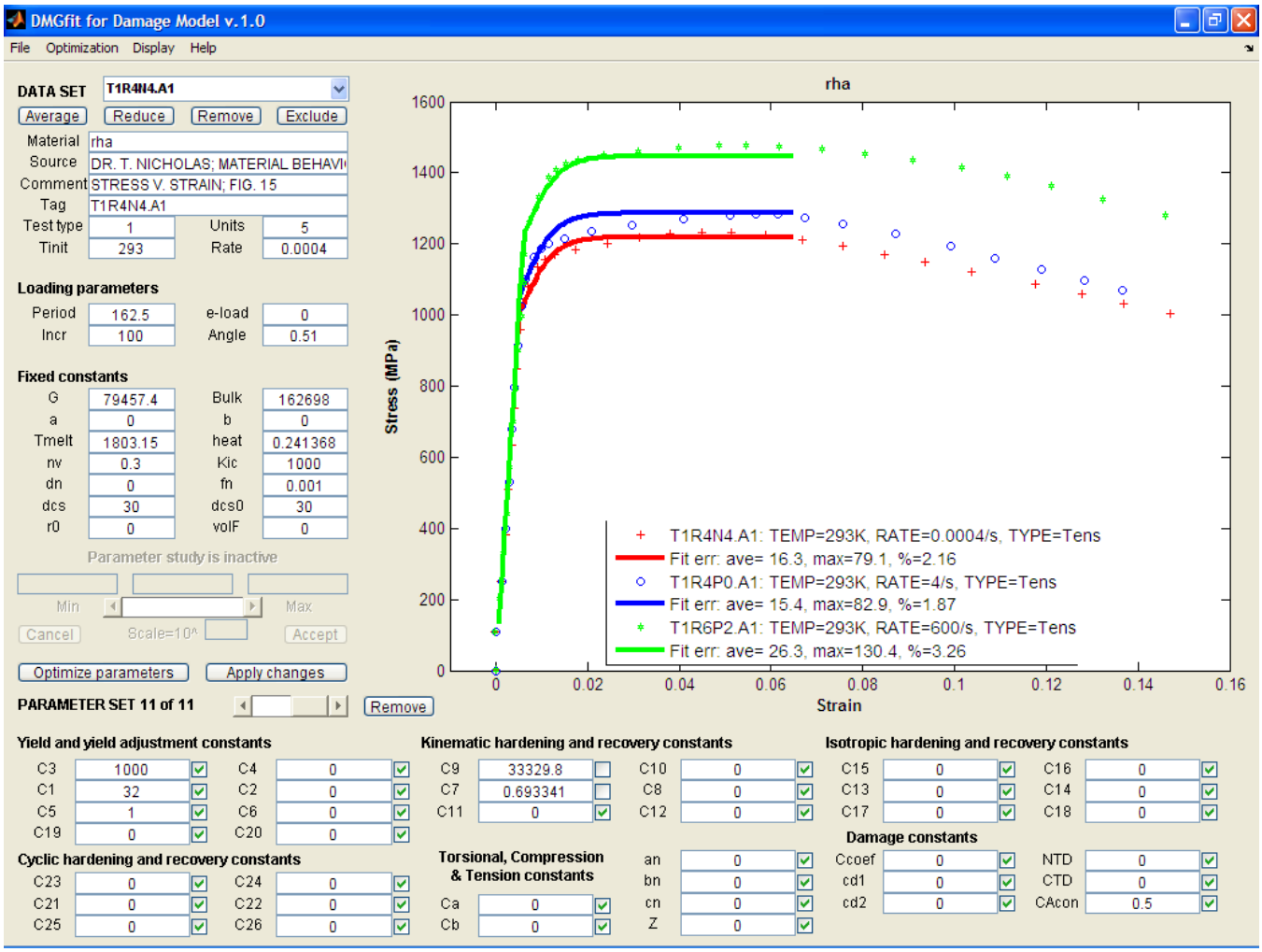

B38. RHA Steel: strain rate model correlation

Reference: Nicholas, T., Material behavior at high strain rates, Report AFWAL-TR-80-4053, USAF Wright Aeronautical Laboratories, Wright-Patterson Air Force Base, OH, USA, 1980.

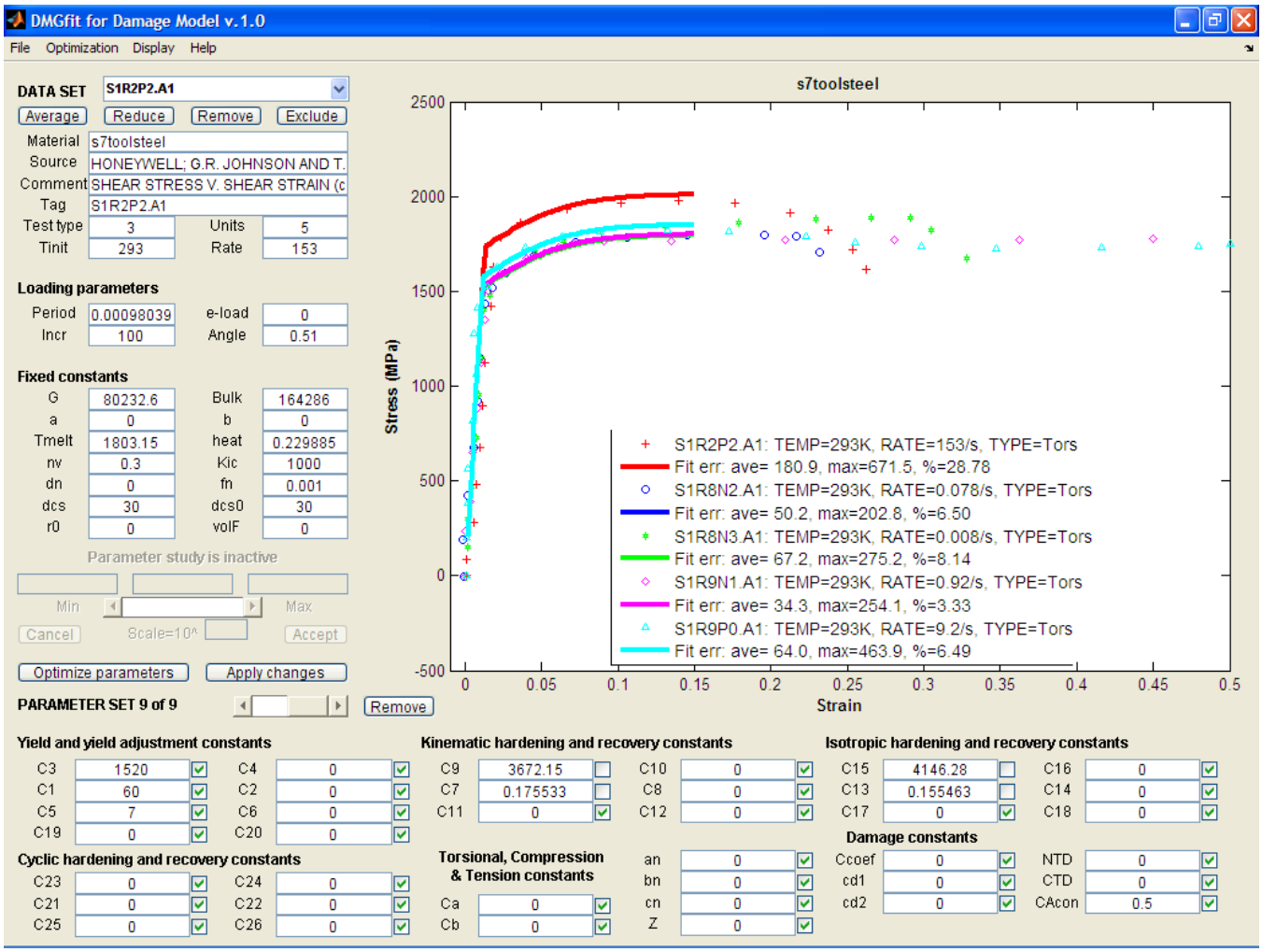

B39. S7tool steel alloy: strain rate model correlation

Reference: Johnson, G.R. and Holmquist, T.J., Test data and computational strength and fracture model constants for 23 materials subjected to large strains, high strain rates, and high temperatures, LA-11463-MS, Los Alamos National Laboratory, 1989.

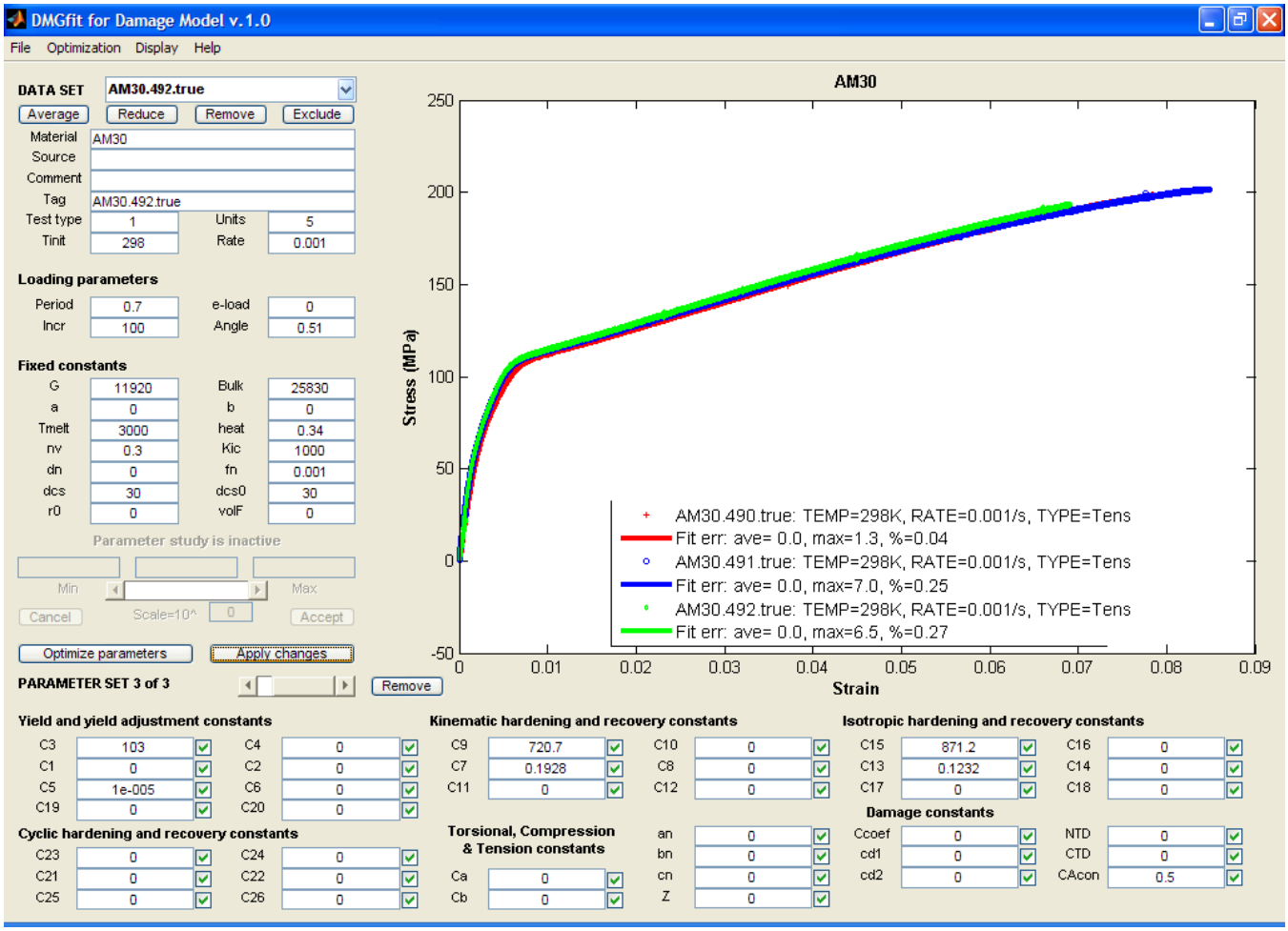

B40. AM30 Mg alloy model correlation

Reference: M.F. Horstemeyer, D. Oglesby, J. Fan, P.M. Gullett, H. El Kadiri, Y. Xue, C. Burton, K. Gall, B. Jelinek, M.K. Jones, S. G. Kim, E.B. Marin, D.L. McDowell, A. Oppedal, N. Yang, "From Atoms to Autos: Designing a Mg Alloy Corvette Cradle by Employing Hierarchical Multiscale Microstructure-Property Models for Monotonic and Cyclic Loads," MSU.CAVS.CMD.2007-R0001.

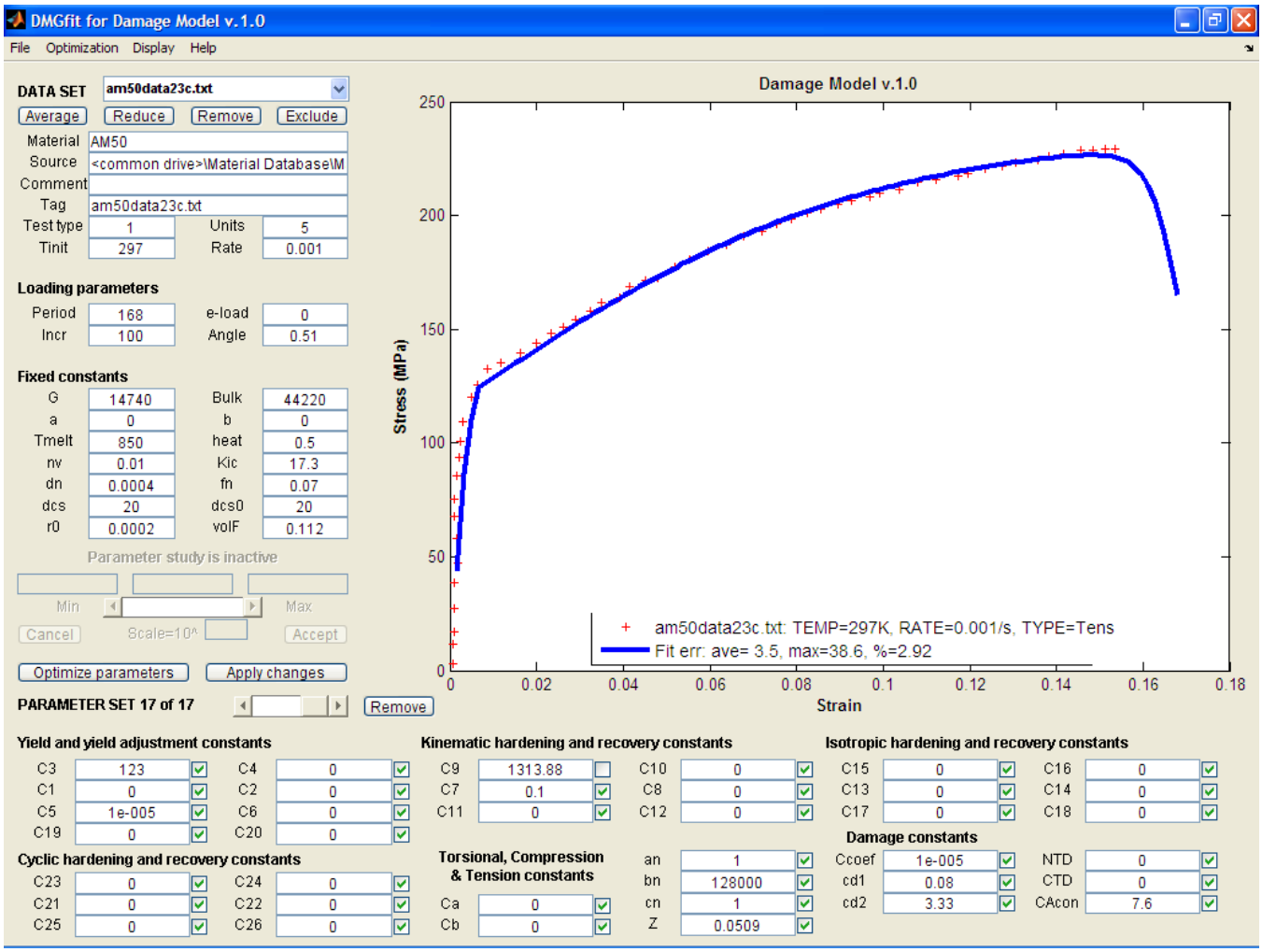

B41. AM50 Mg alloy model correlation

Reference: M.F. Horstemeyer, D. Oglesby, J. Fan, P.M. Gullett, H. El Kadiri, Y. Xue, C. Burton, K. Gall, B. Jelinek, M.K. Jones, S. G. Kim, E.B. Marin, D.L. McDowell, A. Oppedal, N. Yang, "From Atoms to Autos: Designing a Mg Alloy Corvette Cradle by Employing Hierarchical Multiscale Microstructure-Property Models for Monotonic and Cyclic Loads," MSU.CAVS.CMD.2007-R0001

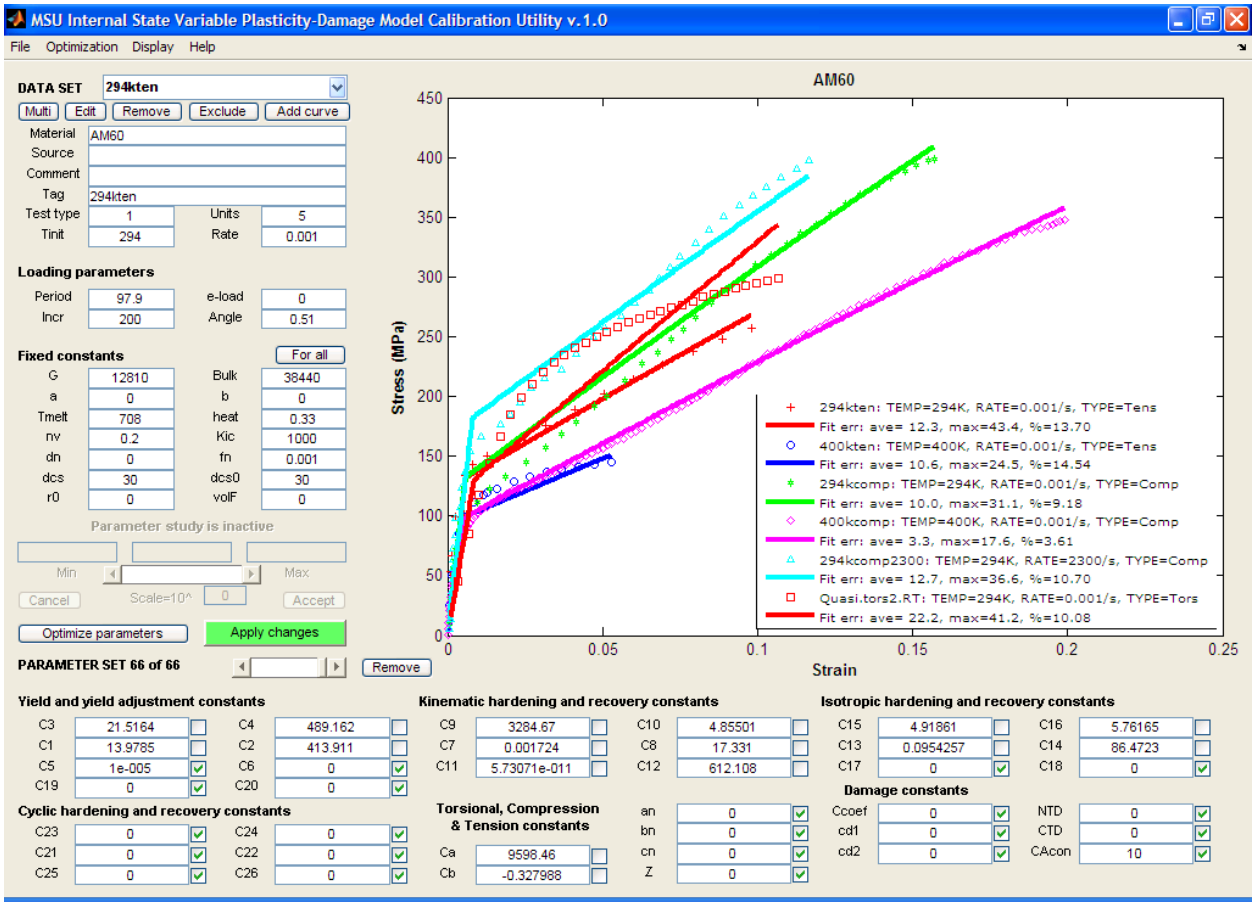

B42. AM60 Mg alloy: temperature model correlation

Reference: M.F. Horstemeyer, D. Oglesby, J. Fan, P.M. Gullett, H. El Kadiri, Y. Xue, C. Burton, K. Gall, B. Jelinek, M.K. Jones, S. G. Kim, E.B. Marin, D.L. McDowell, A. Oppedal, N. Yang, "From Atoms to Autos: Designing a Mg Alloy Corvette Cradle by Employing Hierarchical Multiscale Microstructure-Property Models for Monotonic and Cyclic Loads," MSU.CAVS.CMD.2007-R0001

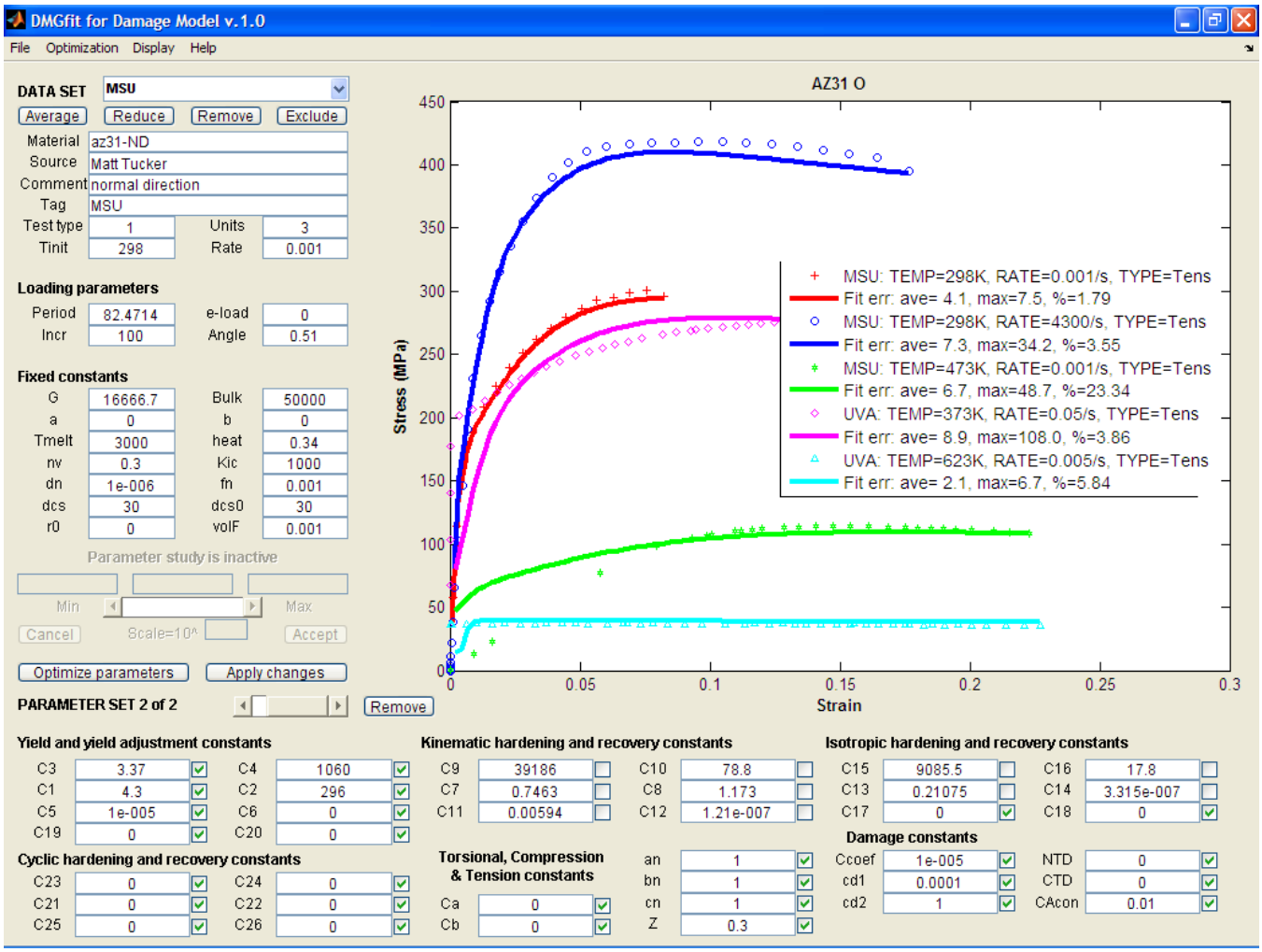

B43. AZ31 Mg alloy: temperature and strain rate model correlation

Reference: F.J. Polesak, III, C.E. Dreyer, T.J. Shultz, and S.R. Agnew, "Blind Study of the Effect of Processing History on the Constitutive Behavior of Alloy AZ31B," Magnesium Technology 2009, Eds. E.A. Nyberg, S.R. Agnew, M.O. Pekguleryuz, and N.R. Neelameggham (TMS-AIME: Warrendale, PA: 2009) 491-496.

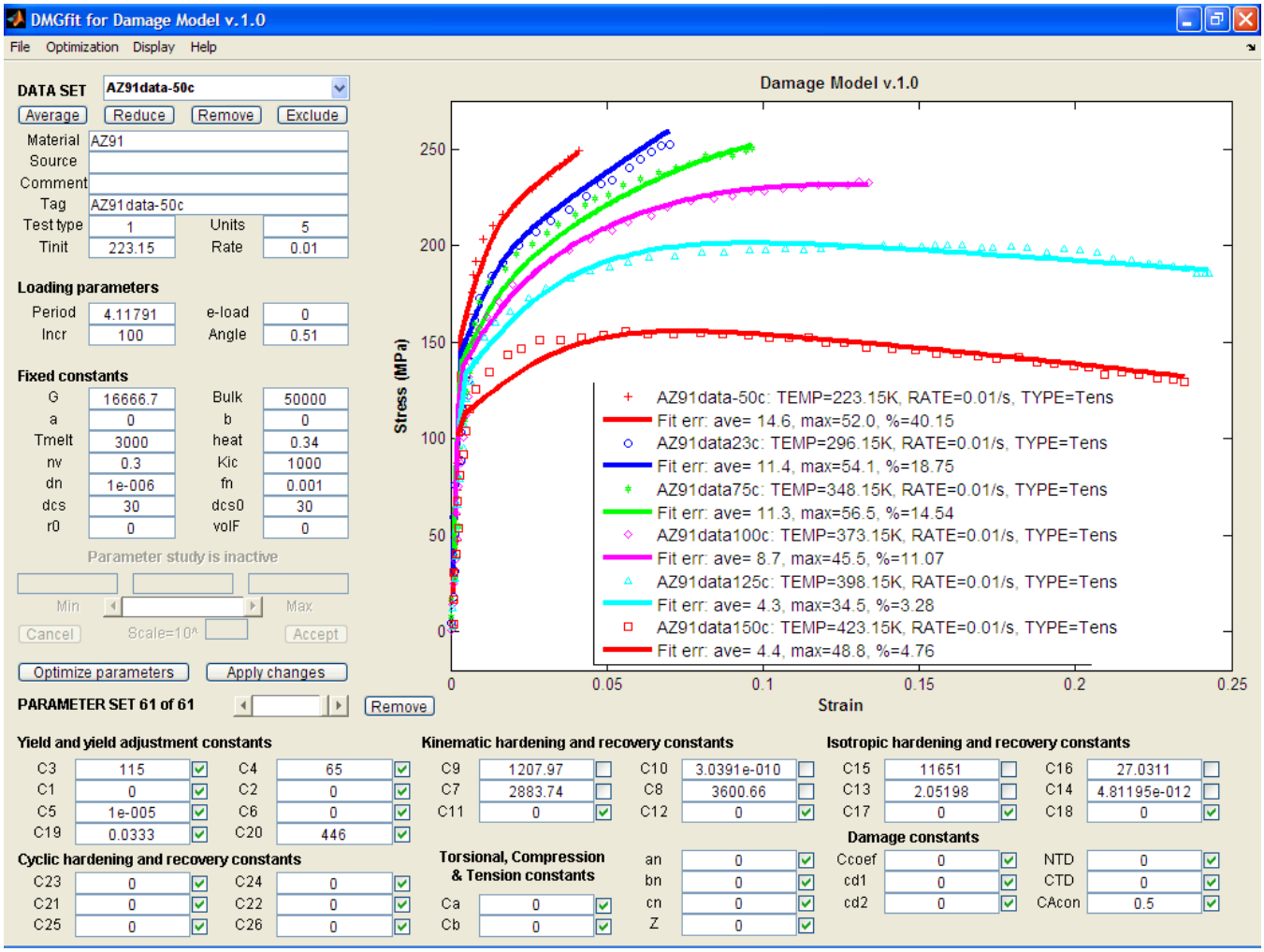

B44. AZ91 Mg alloy: temperature model correlation

Reference: M.F. Horstemeyer, D. Oglesby, J. Fan, P.M. Gullett, H. El Kadiri, Y. Xue, C. Burton, K. Gall, B. Jelinek, M.K. Jones, S. G. Kim, E.B. Marin, D.L. McDowell, A. Oppedal, N. Yang, "From Atoms to Autos: Designing a Mg Alloy Corvette Cradle by Employing Hierarchical Multiscale Microstructure-Property Models for Monotonic and Cyclic Loads," MSU.CAVS.CMD.2007-R0001

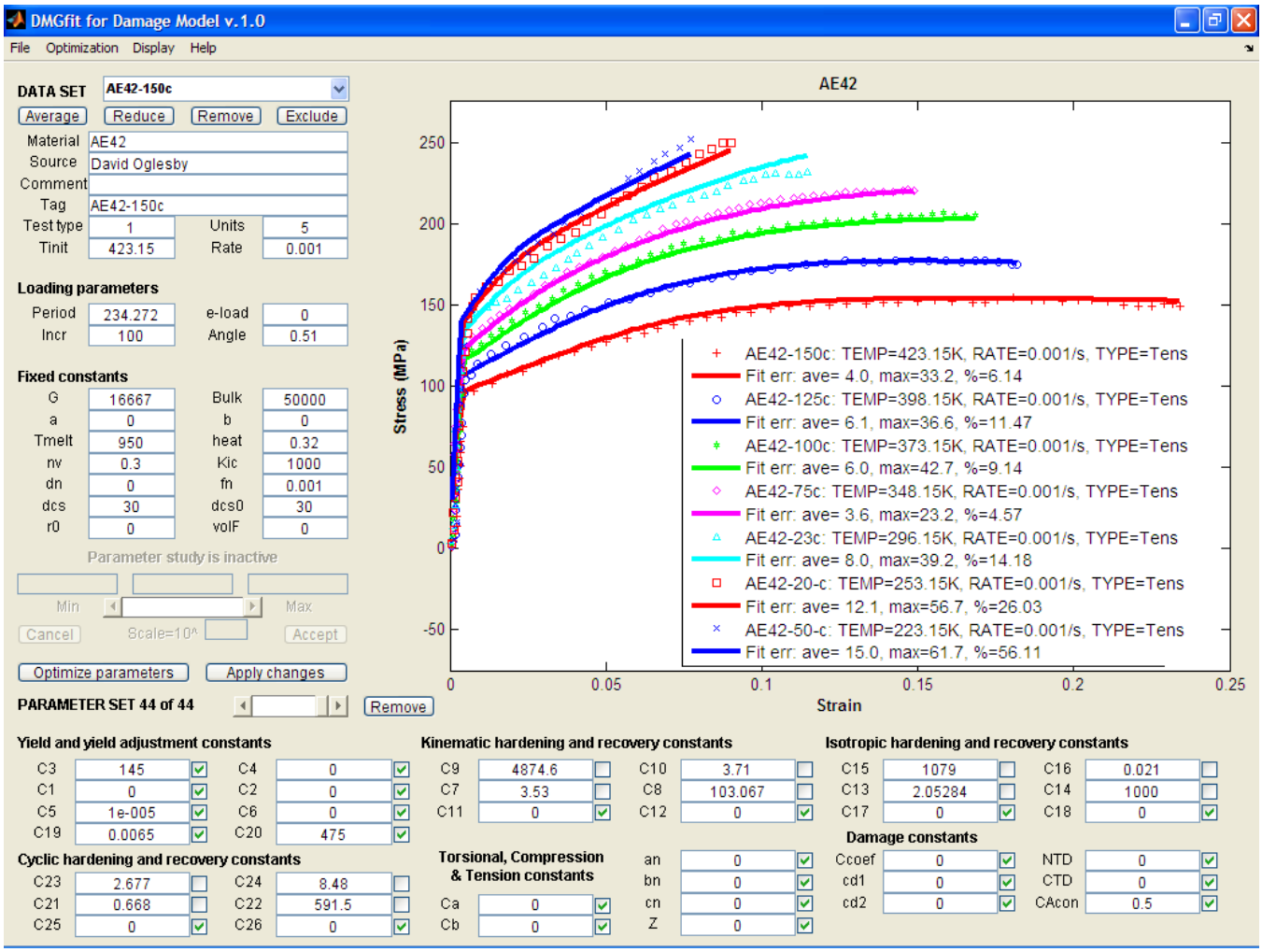

B45. AE42 Mg alloy: temperature and strain rate model correlation

Reference: M.F. Horstemeyer, D. Oglesby, J. Fan, P.M. Gullett, H. El Kadiri, Y. Xue, C. Burton, K. Gall, B. Jelinek, M.K. Jones, S. G. Kim, E.B. Marin, D.L. McDowell, A. Oppedal, N. Yang, "From Atoms to Autos: Designing a Mg Alloy Corvette Cradle by Employing Hierarchical Multiscale Microstructure-Property Models for Monotonic and Cyclic Loads," MSU.CAVS.CMD.2007-R0001

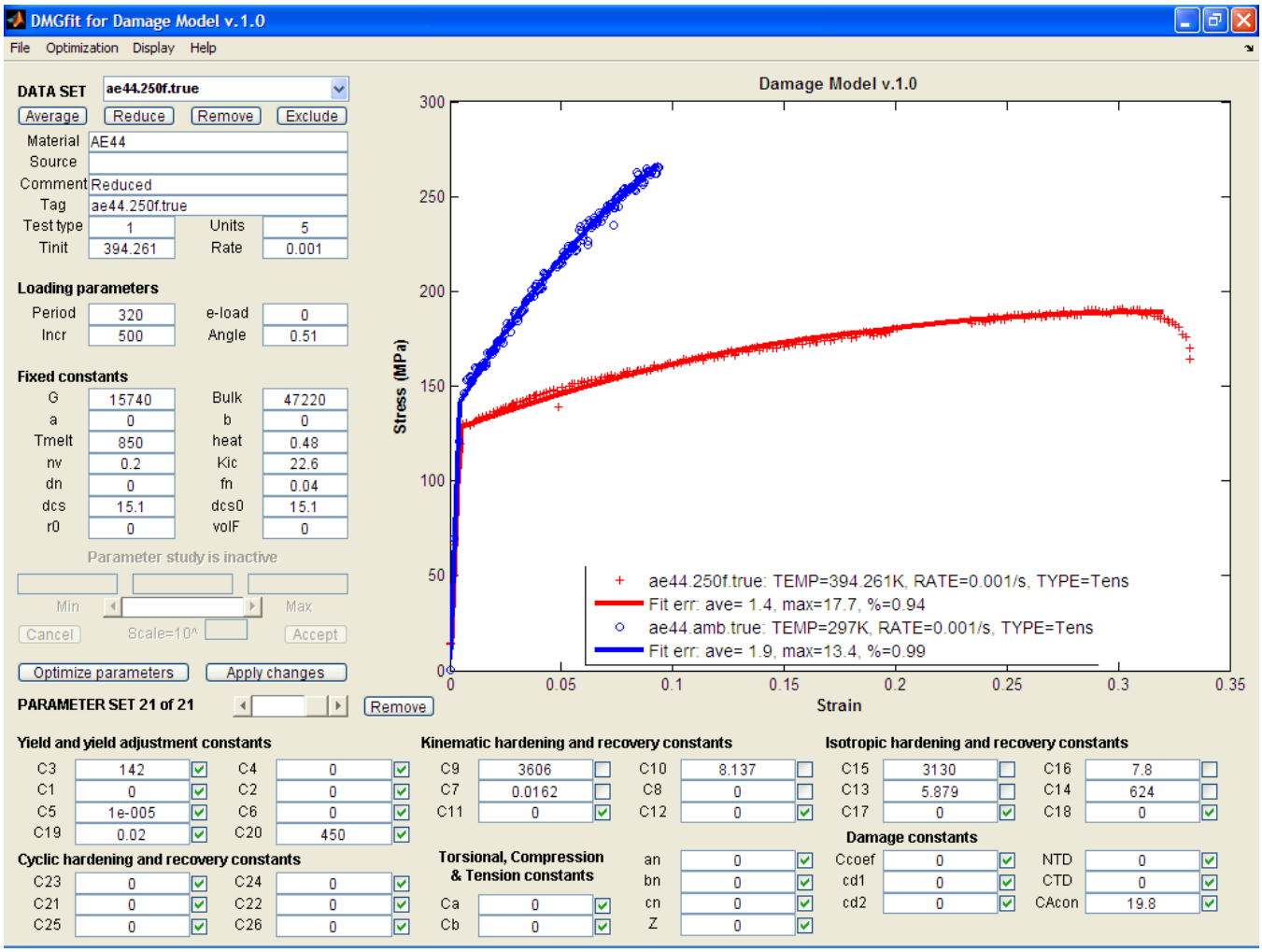

B46. AE44 Mg alloy: temperature model correlation

Reference: M.F. Horstemeyer, D. Oglesby, J. Fan, P.M. Gullett, H. El Kadiri, Y. Xue, C. Burton, K. Gall, B. Jelinek, M.K. Jones, S. G. Kim, E.B. Marin, D.L. McDowell, A. Oppedal, N. Yang, "From Atoms to Autos: Designing a Mg Alloy Corvette Cradle by Employing Hierarchical Multiscale Microstructure-Property Models for Monotonic and Cyclic Loads," MSU.CAVS.CMD.2007-R0001

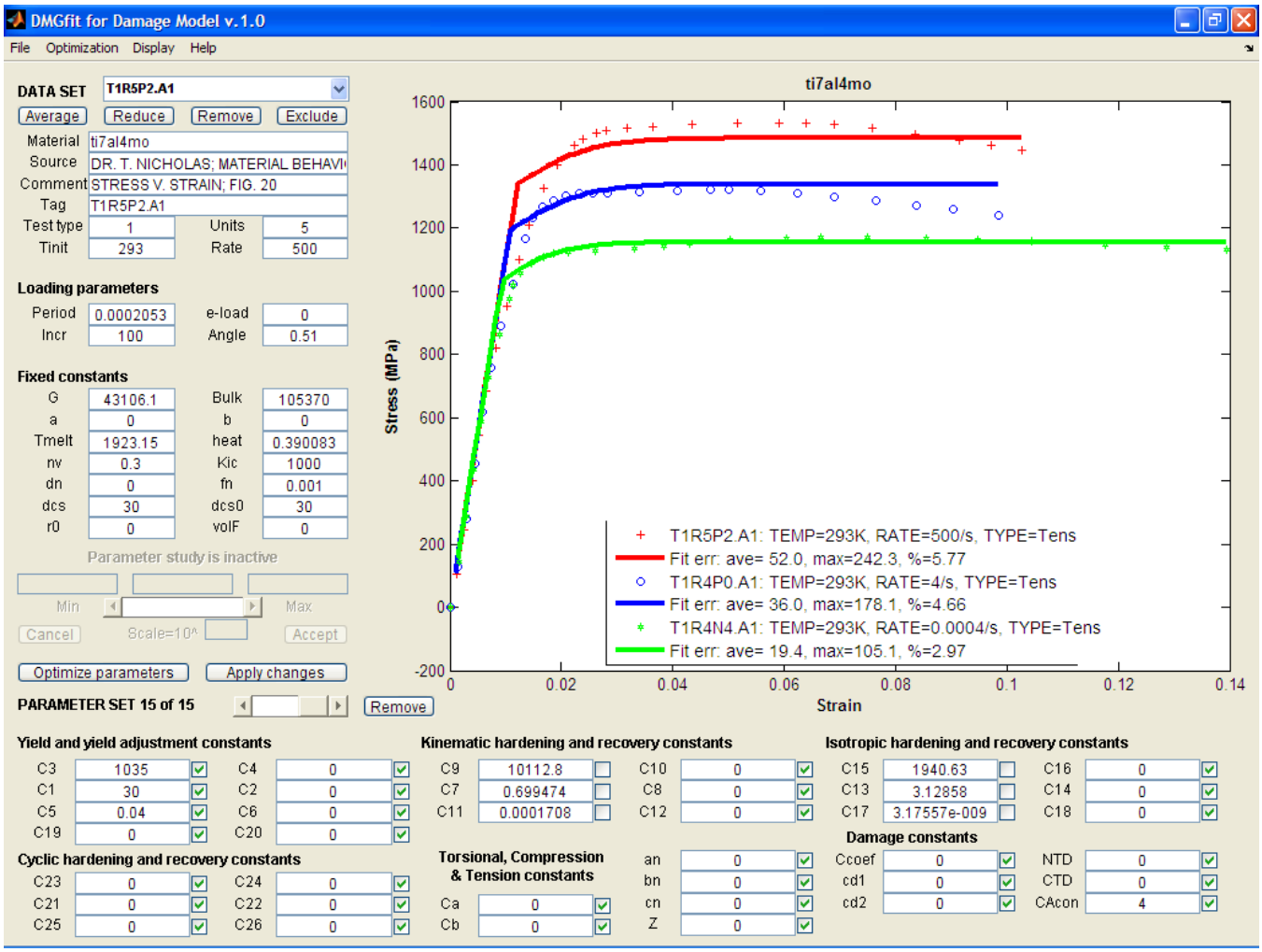

B47. Ti7Al4Mo alloy: strain rate model correlation

Reference: Nicholas, T., Material behavior at high strain rates, Report AFWAL-TR-80-4053, USAF Wright Aeronautical Laboratories, Wright-Patterson Air Force Base, OH, USA, 1980.

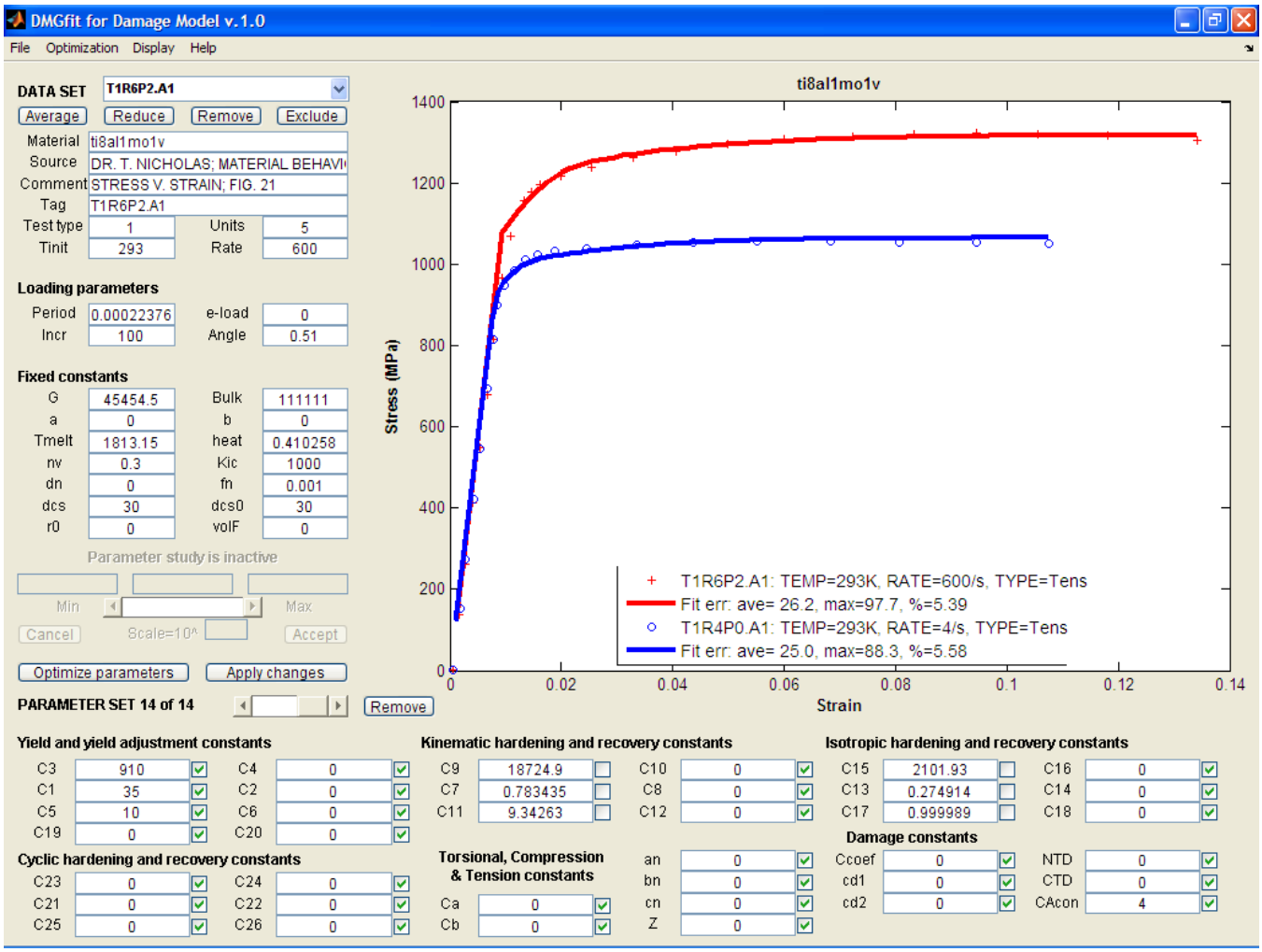

B48. Ti8Al1Mo1V alloy: strain rate model correlation

Reference: Nicholas, T., Material behavior at high strain rates, Report AFWAL-TR-80-4053, USAF Wright Aeronautical Laboratories, Wright-Patterson Air Force Base, OH, USA, 1980.

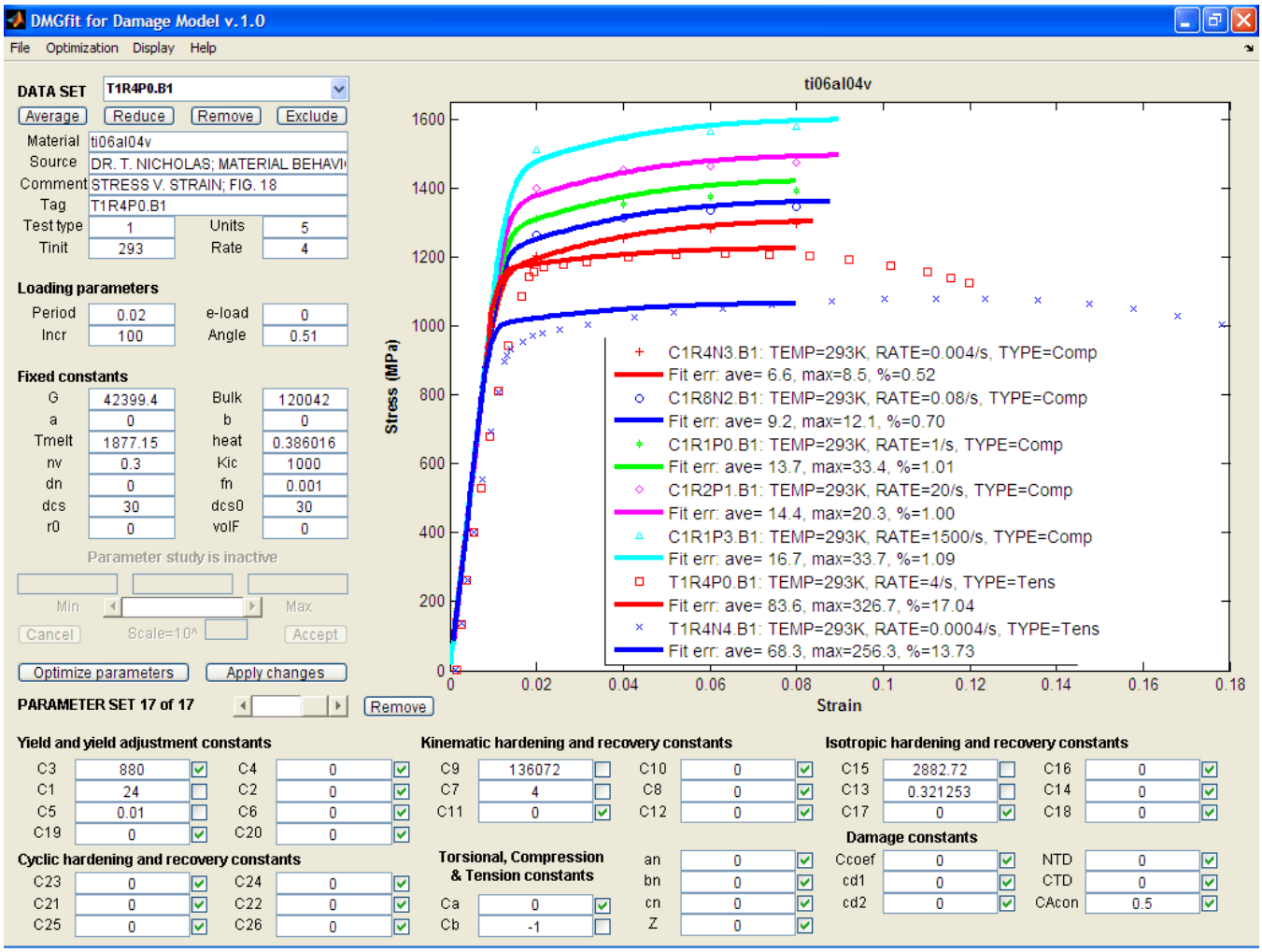

B49. Ti0Al6V4 alloy: strain rate model correlation

References:

1. Department of Defense. Military Standardization Handbook: Metallic Materials and Elements for Aerospace Vehicle Structures MIL-HDBK-5E, Volume 2. June 1987.

2. Johnson, G.R. and Holmquist, T.J., Test data and computational strength and fracture model constants for 23 materials subjected to large strains, high strain rates, and high temperatures, LA-11463-MS, Los Alamos National Laboratory, 1989.

3. Nicholas, T., Material behavior at high strain rates, Report AFWAL-TR-80-4053, USAF Wright Aeronautical Laboratories, Wright-Patterson Air Force Base, OH, USA, 1980.

4. Maiden and Green

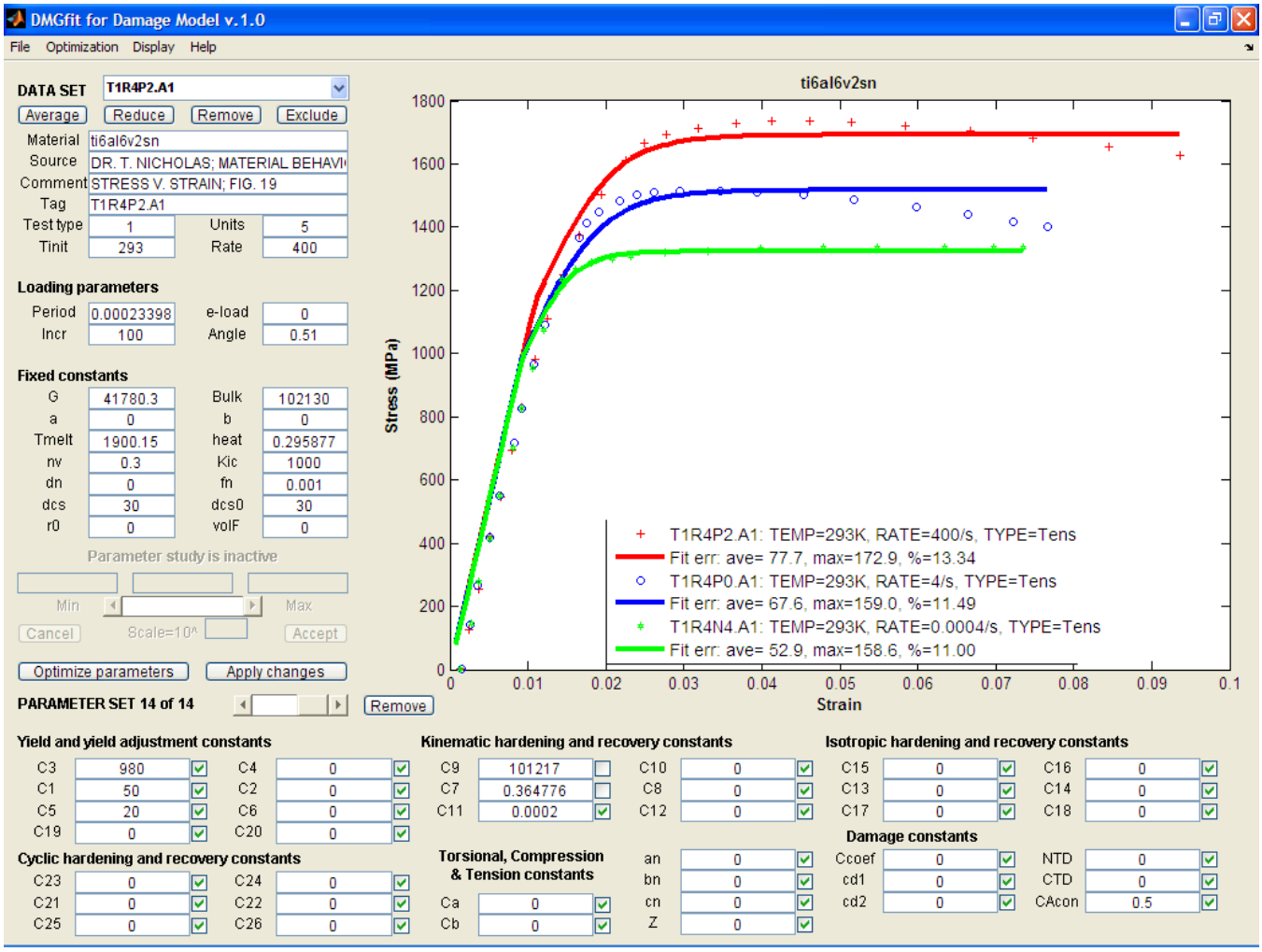

B50. Ti6Al6V2Sn alloy: strain rate model correlation

References:

1. Department of Defense. Military Standardization Handbook: Metallic Materials and Elements for Aerospace Vehicle Structures MIL-HDBK-5E, Volume 2. June 1987.

2. Nicholas, T., Material behavior at high strain rates, Report AFWAL-TR-80-4053, USAF Wright Aeronautical Laboratories, Wright-Patterson Air Force Base, OH, USA, 1980.

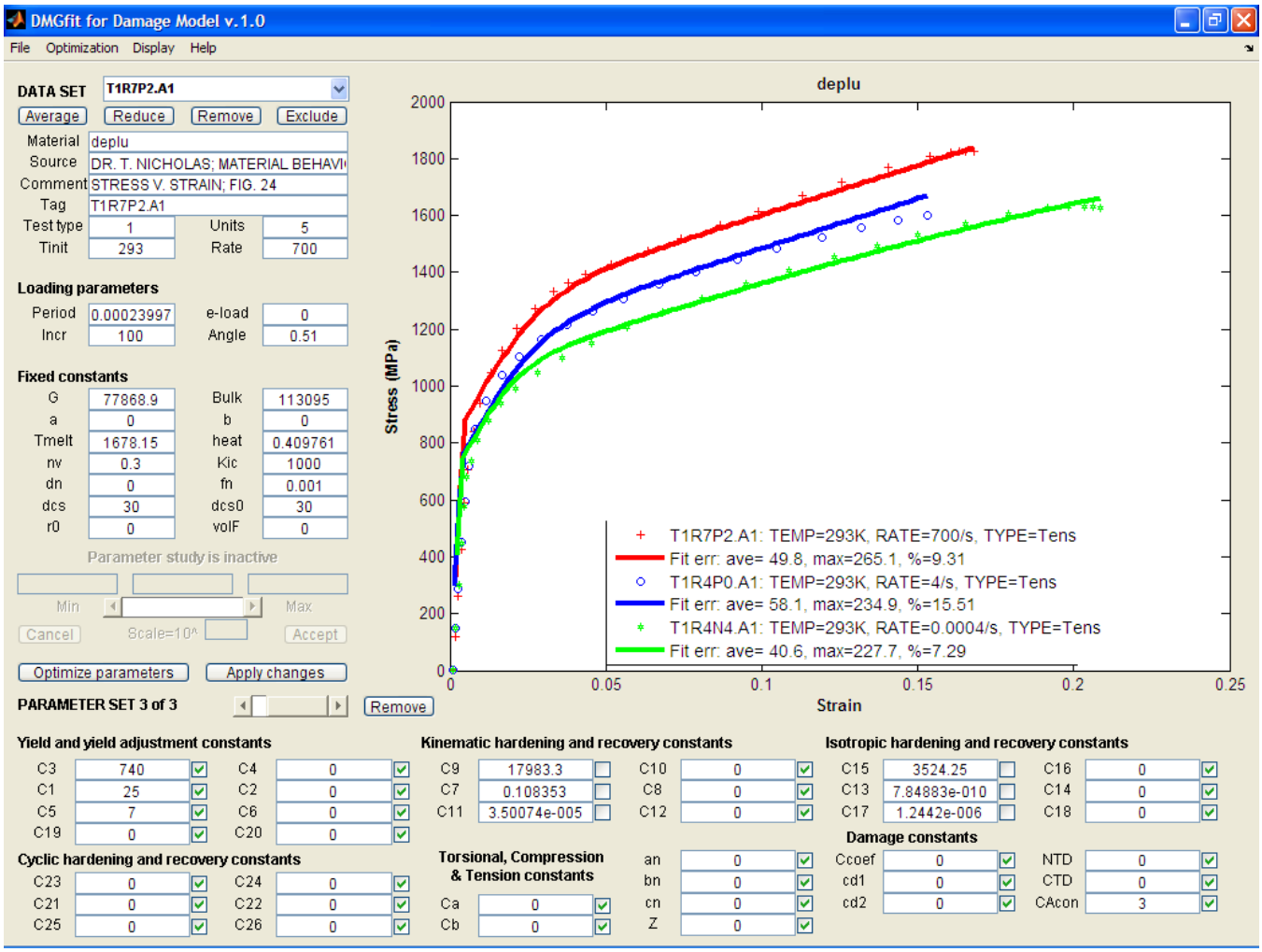

B51. D38 Uranium: strain rate model correlation

Reference: Nicholas, T., Material behavior at high strain rates, Report AFWAL-TR-80-4053, USAF Wright Aeronautical Laboratories, Wright-Patterson Air Force Base, OH, USA, 1980.

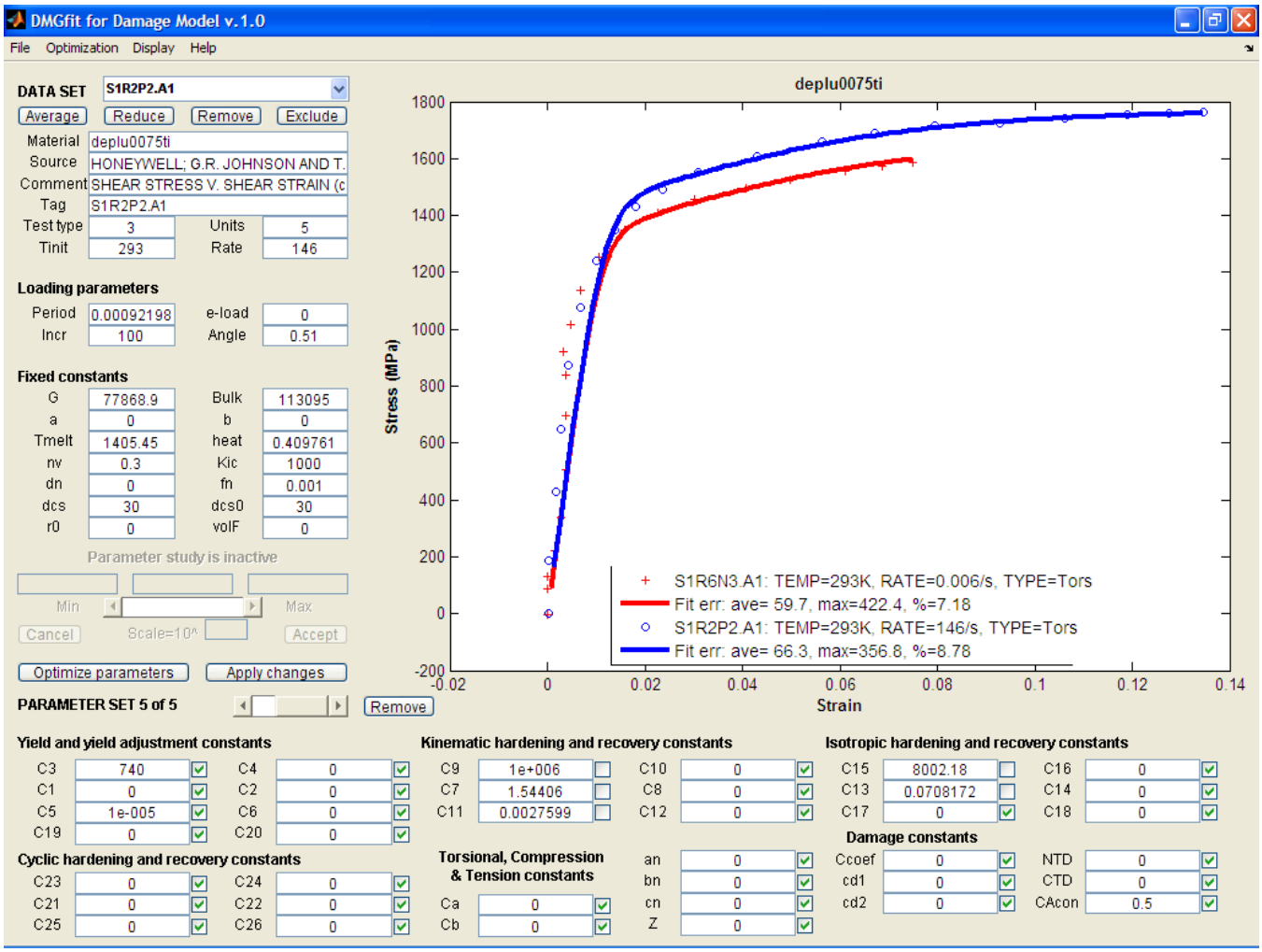

B52. D380075Ti Uranium: strain rate model correlation

Reference: Johnson, G.R. and Holmquist, T.J., Test data and computational strength and fracture model constants for 23 materials subjected to large strains, high strain rates, and high temperatures, LA-11463-MS, Los Alamos National Laboratory, 1989.

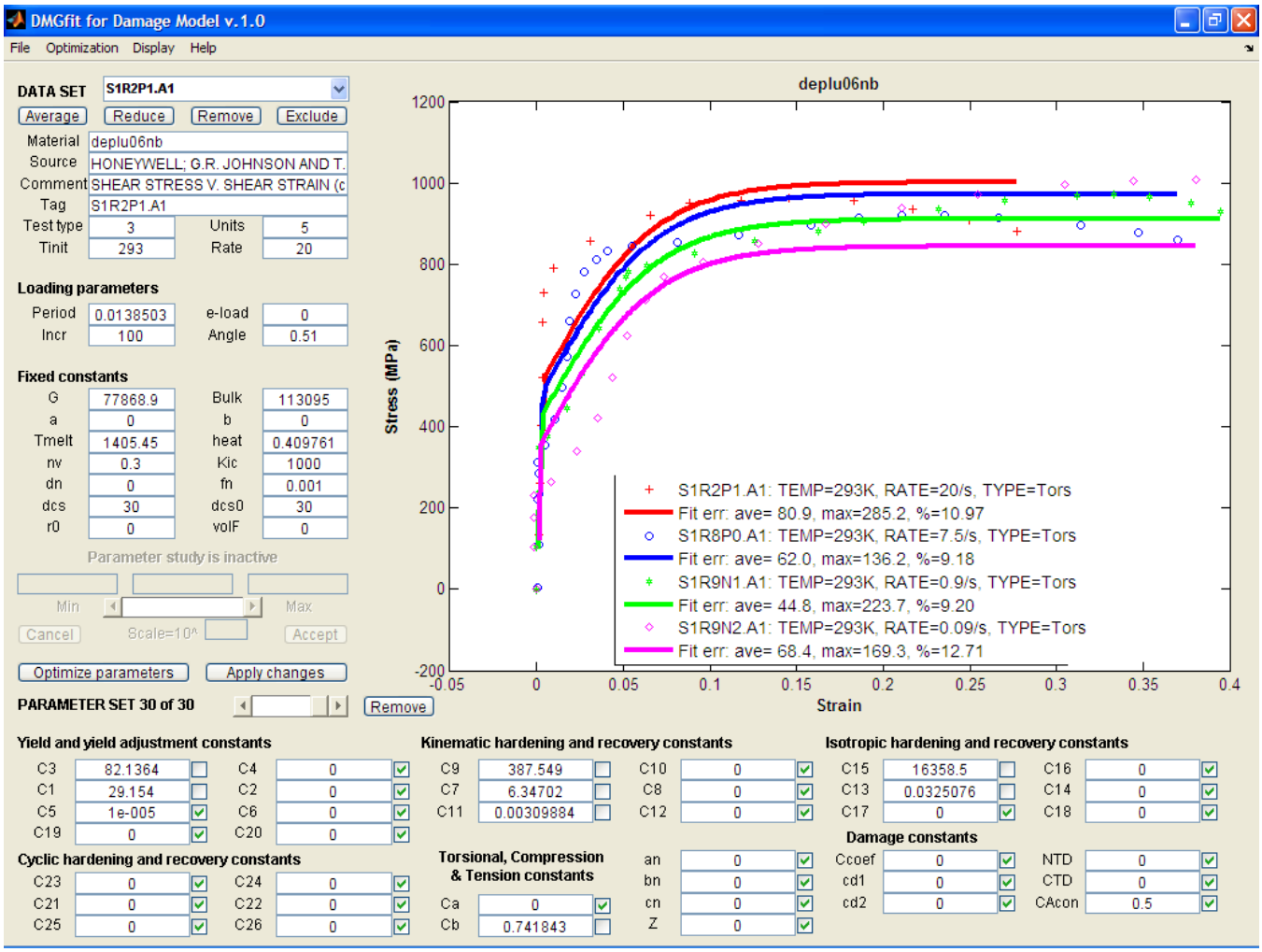

B53. D38006 Nb Uranium: strain rate model correlation

Reference: Johnson, G.R. and Holmquist, T.J., Test data and computational strength and fracture model constants for 23 materials subjected to large strains, high strain rates, and high temperatures, LA-11463-MS, Los Alamos National Laboratory, 1989.

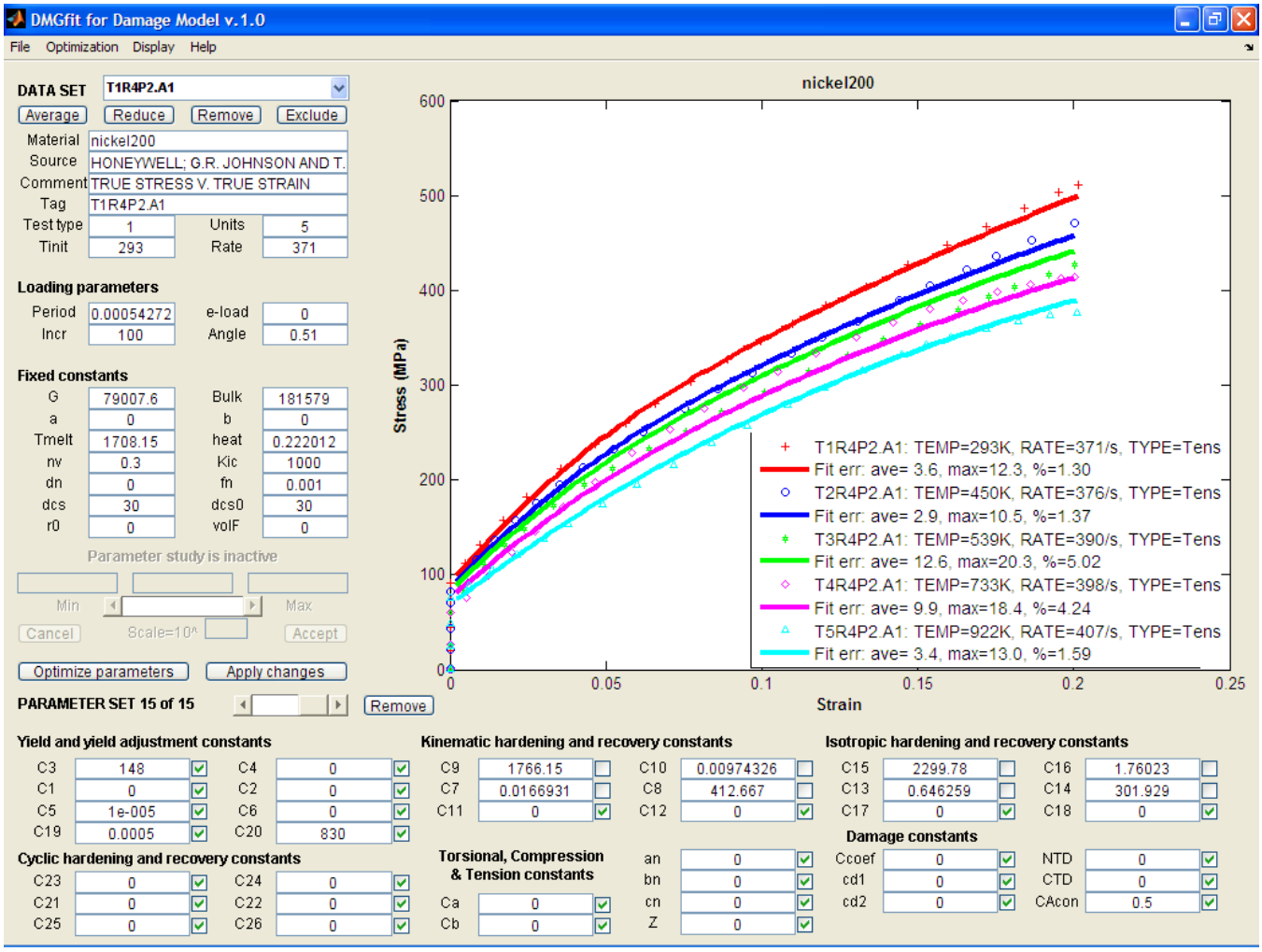

B54. 200 Nickel: temperature model correlation

Reference: Johnson, G.R. and Holmquist, T.J., Test data and computational strength and fracture model constants for 23 materials subjected to large strains, high strain rates, and high temperatures, LA-11463-MS, Los Alamos National Laboratory, 1989.

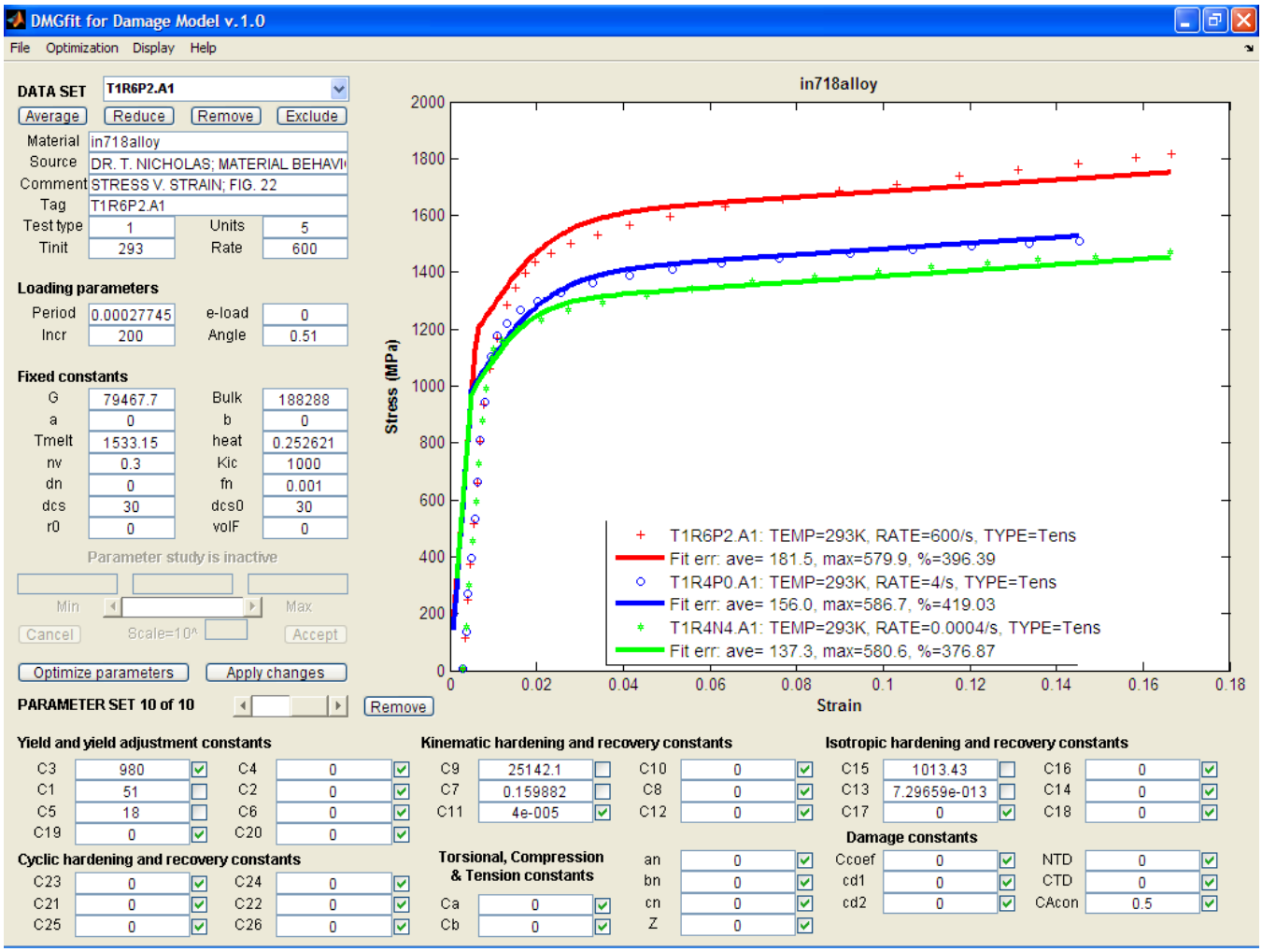

B55. In718 alloy: strain rate model correlation

Reference: Nicholas, T., Material behavior at high strain rates, Report AFWAL-TR-80-4053, USAF Wright Aeronautical Laboratories, Wright-Patterson Air Force Base, OH, USA, 1980.

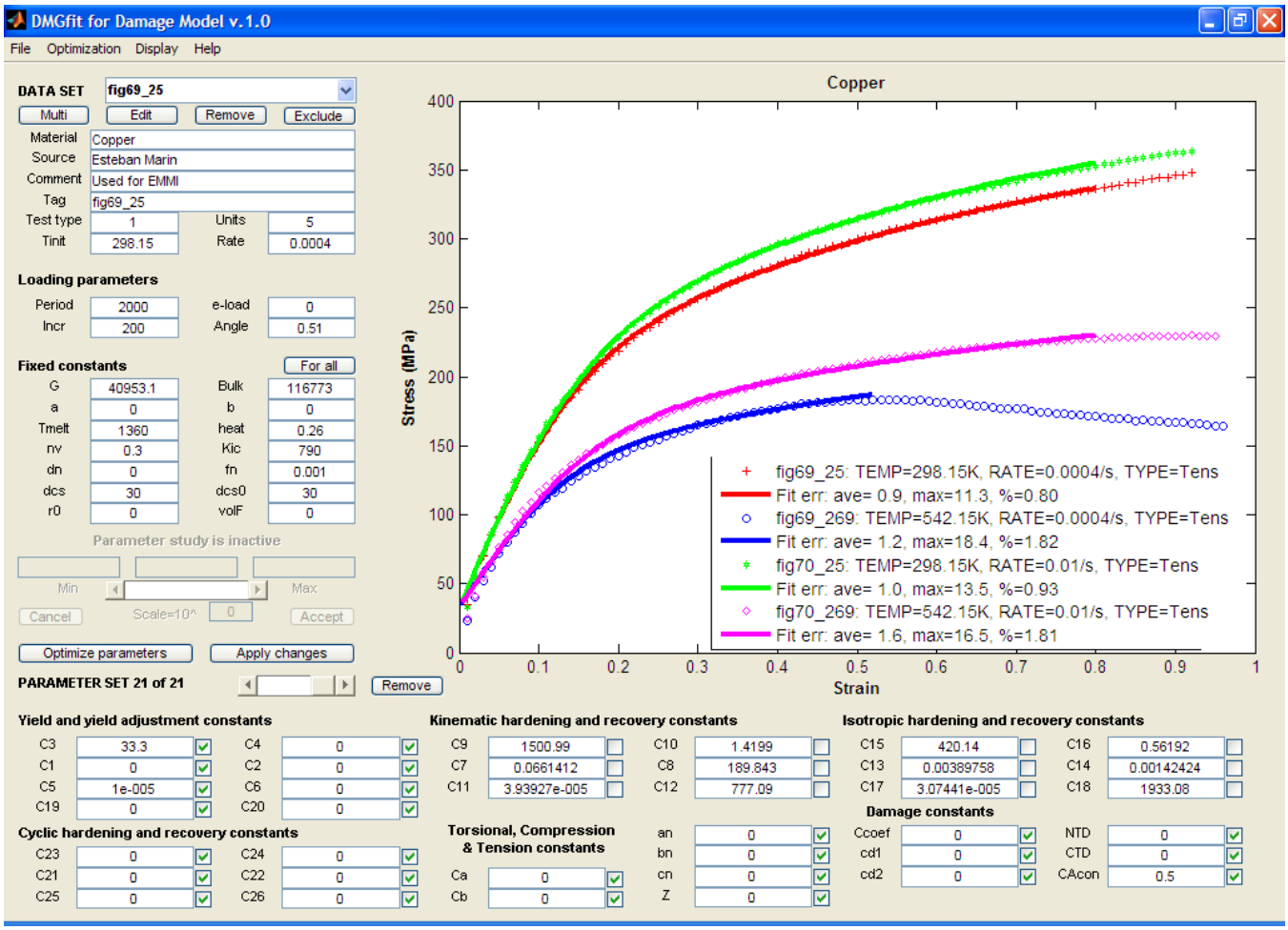

B56. Copper: strain rate and temperature model correlation.

Reference: Tanner A.B., McGinty R.D. and McDowell D.L., Modeling temperature and strain rate history effects in OFHC Cu, Int. Journal of Plasticity, 1999.

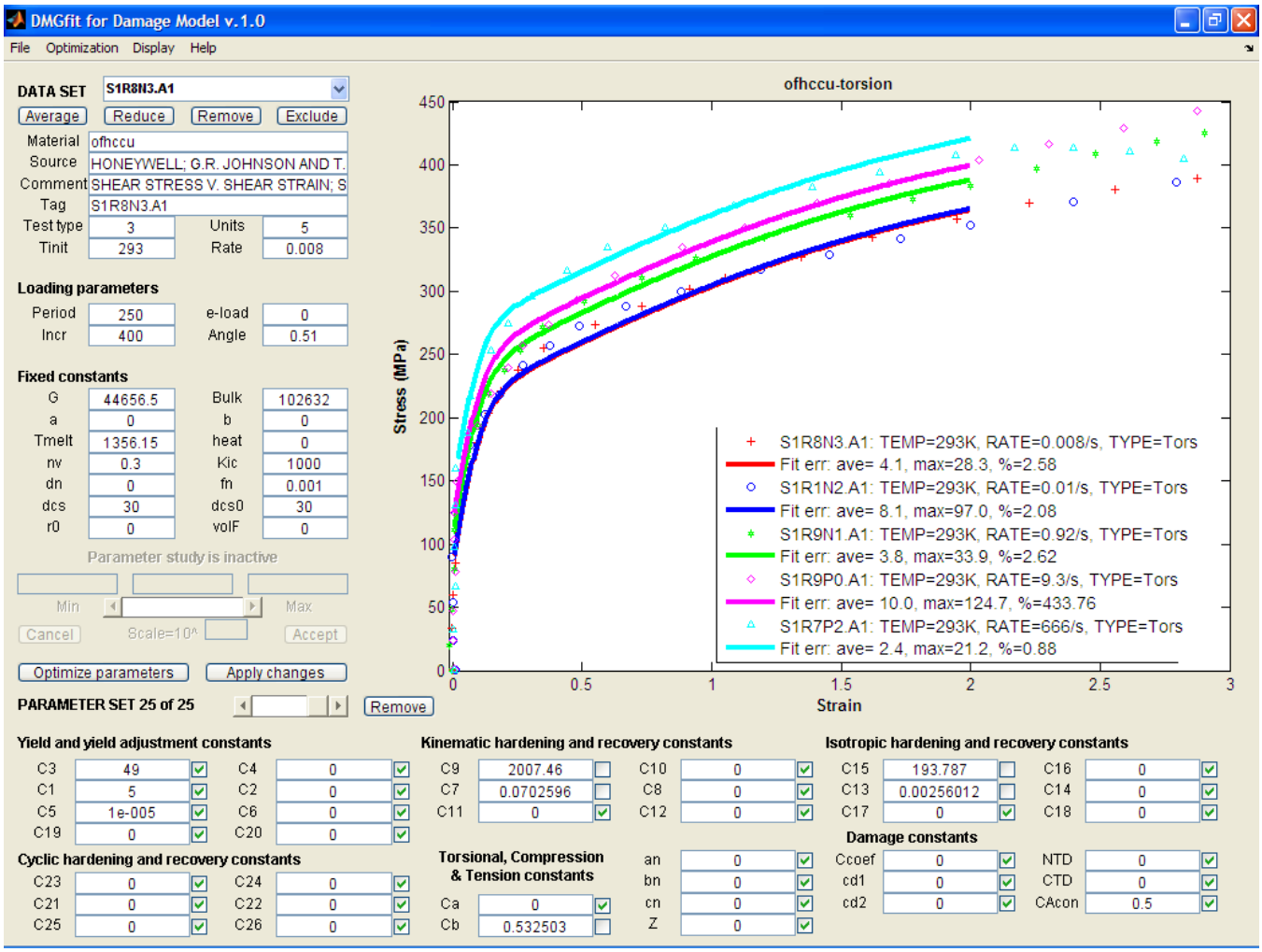

B57. OFHC Copper: strain rate model correlation

References:

1. Johnson, G.R. and Holmquist, T.J., Test data and computational strength and fracture model constants for 23 materials subjected to large strains, high strain rates, and high temperatures, LA-11463-MS, Los Alamos National Laboratory, 1989.

2. Nicholas, T., Material behavior at high strain rates, Report AFWAL-TR-80-4053, USAF Wright Aeronautical Laboratories, Wright-Patterson Air Force Base, OH, USA, 1980.

3. U.S. Lindholm

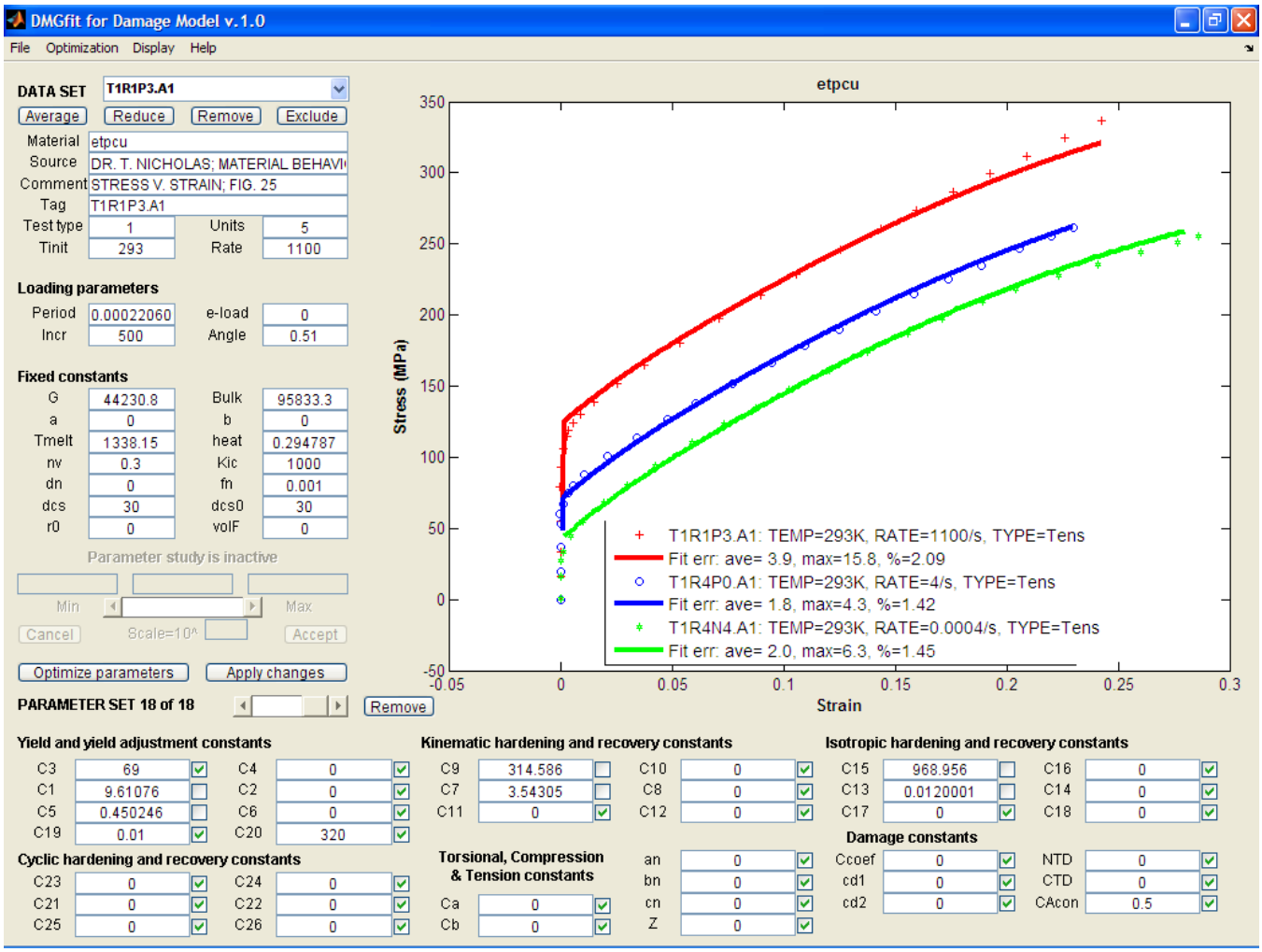

B58. ETP Copper: strain rate model correlation

Reference: Nicholas, T., Material behavior at high strain rates, Report AFWAL-TR-80-4053, USAF Wright Aeronautical Laboratories, Wright-Patterson Air Force Base, OH, USA, 1980.

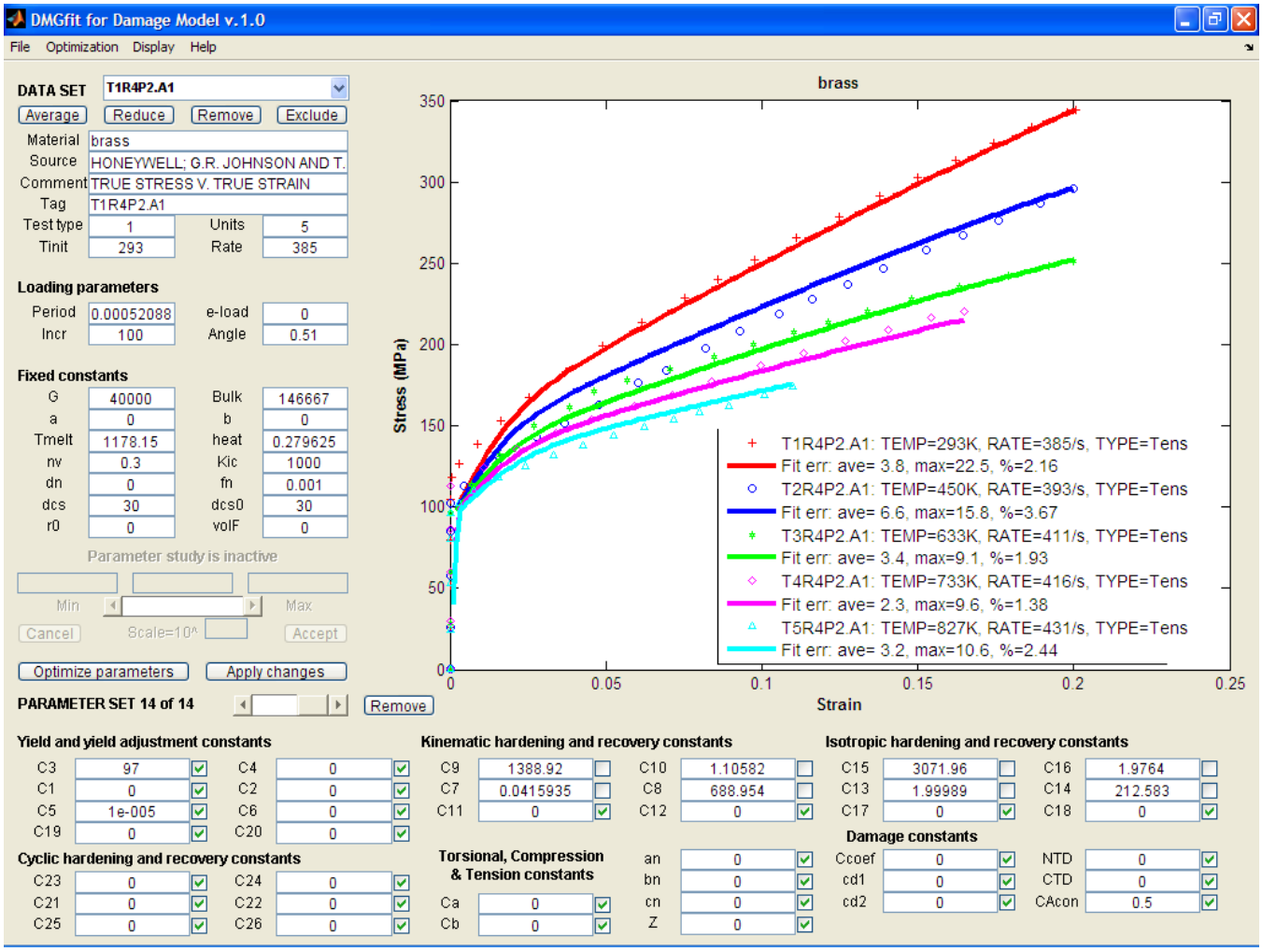

B59. 99% Brass: temperature and strain rate model correlation

Reference: Johnson, G.R. and Holmquist, T.J., Test data and computational strength and fracture model constants for 23 materials subjected to large strains, high strain rates, and high temperatures, LA-11463-MS, Los Alamos National Laboratory, 1989.

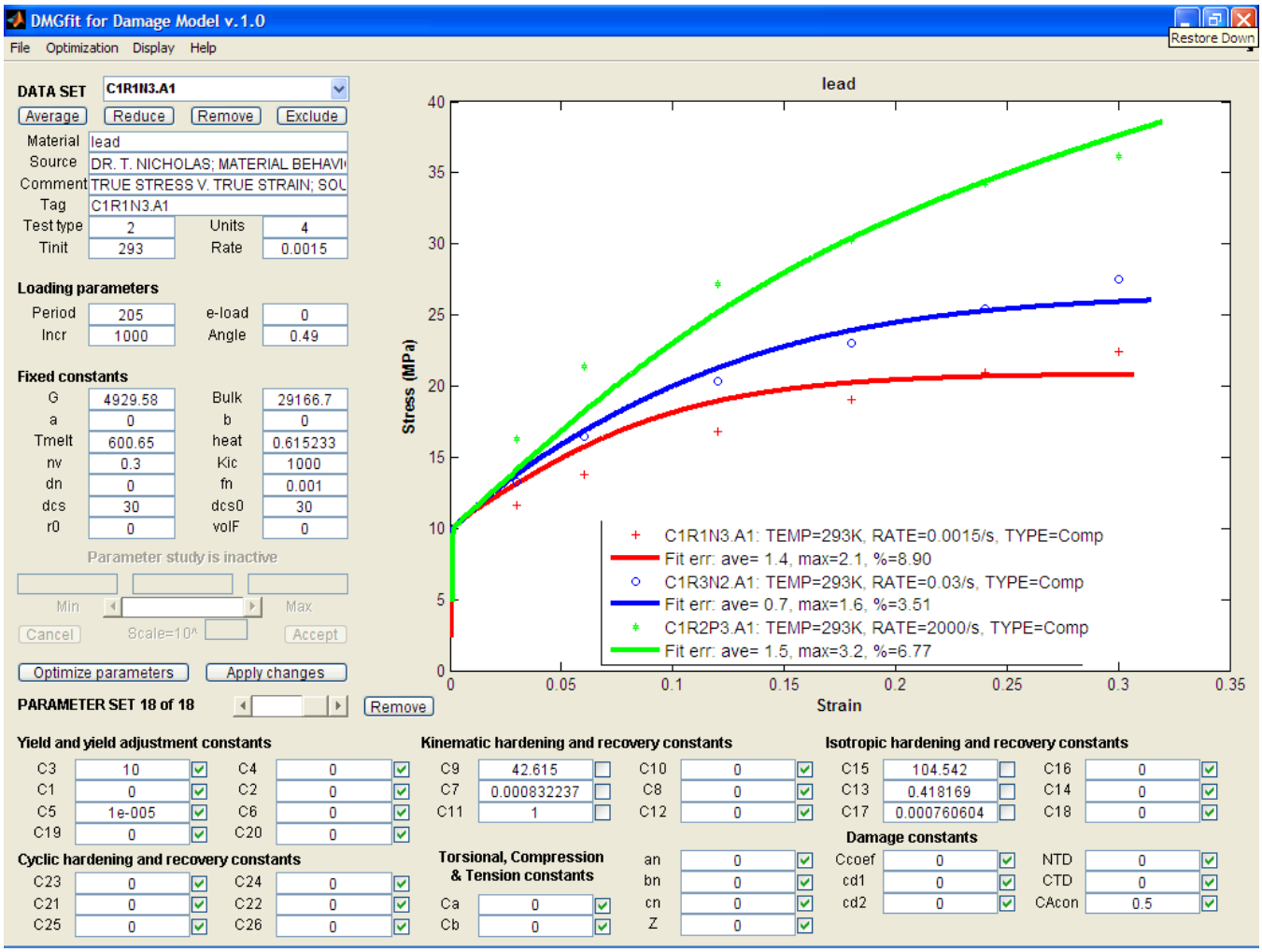

B60. Lead: strain rate model correlation

References:

1. Nicholas, T., Material behavior at high strain rates, Report AFWAL-TR-80-4053, USAF Wright Aeronautical Laboratories, Wright-Patterson Air Force Base, OH, USA, 1980.

2. U.S. Lindholm

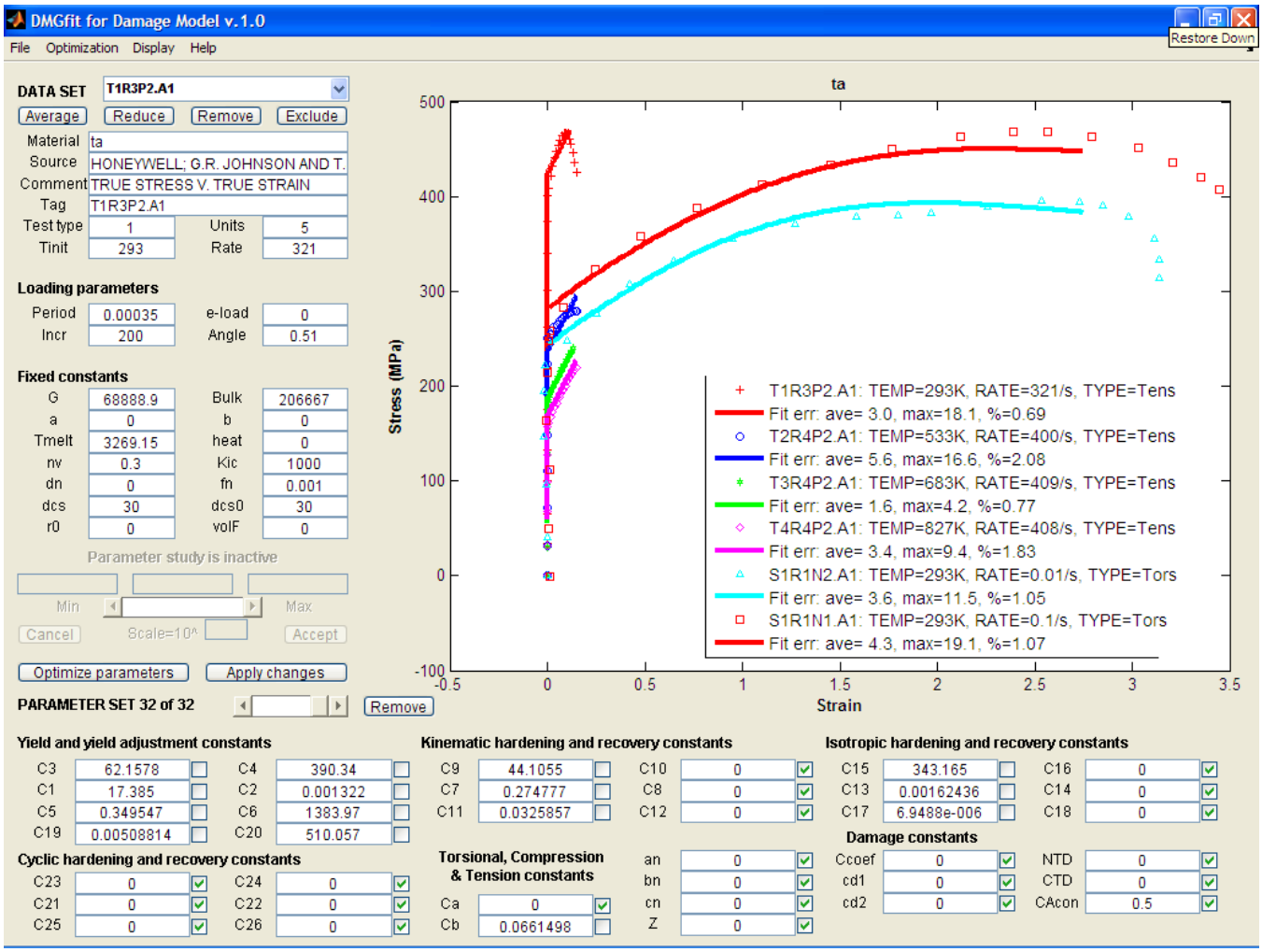

B61. Tantalum: temperature and strain rate model correlation

Reference: Johnson, G.R. and Holmquist, T.J., Test data and computational strength and fracture model constants for 23 materials subjected to large strains, high strain rates, and high temperatures, LA-11463-MS, Los Alamos National Laboratory, 1989.